VEHICLE CONDITION MONITORING: ANOMALOUS VIBRATION DETECTION WITH ACCELEROMETERS

JONAS FREDERIC SCHMIDT

SUPERVISORS:
Prof. Dr. Kai-Uwe Kühnberger

Vehicle Condition Monitoring: Anomalous Vibration Detection with Accelerometers

Dissertation

zur Erlangung des Grades eines Doktors der Naturwissenschaften
eingereicht am Fachbereich Humanwissenschaften
der Universität Osnabrück

vorgelegt von

Jonas Frederic Schmidt

Osnabrück, August 2023

Education is the most powerful weapon
which you can use to change the world.

— Nelson Mandela

Dedicated to all first-generation students

ABSTRACT

Alongside electrification, autonomous driving is the primary factor of the ongoing transformation in the automotive industry. The success of this technology is closely linked to its safety and the trust users have in it. To enhance the safety of future autonomous vehicles, they must not only be able to perceive their external environment but also be capable of monitoring the condition of their internal parts, components, and functions for faults or failures. This task is performed by condition monitoring systems (CMSs), which extend autonomy from mere driving to the level of vehicle diagnostics.

This work deals with computationally efficient and advanced anomaly detection methods for vibration-based CMSs focusing on automotive applications. In individual publications, the detection of low tire pressure, gearbox damage, and loose wheel bolts as anomalies were investigated using vibration data recorded with accelerometers. The proposed anomaly detection algorithms using features from the time, frequency, time-frequency, and graph domain were able to detect the anomalies reliably.

To enhance the accuracy of the anomaly detection algorithms, domain knowledge and a careful selection of feature extraction hyperparameters were combined. The evaluations showed that small neural network architectures executable on microcontrollers and classical anomaly detection algorithms are sufficient to detect anomalies in vibration data accurately.

Computational efficiency is decisive in guaranteeing low-latency predictions of CMSs on vehicle microcontrollers with limited computation capacity. For this purpose, an optimized algorithm for faster computation of horizontal visibility graphs that works efficiently on streamed data was introduced. This algorithm was applied for feature extraction in low tire pressure detection and is particularly suitable for processing data with a high sample rate, such as that from accelerometers.

Furthermore, a method was developed and patented for faster inference of convolutional neural networks on microcontrollers that process streamed data with overlapping successive inputs. This is typically the case when dealing with spectrogram representations from streamed vibration or acoustic data. The method allows larger neural networks to be computed with low latency on microcontrollers so that the driver is quickly warned of condition changes.

PUBLICATIONS

Paper I

Juhnke-Kubitzke, Martina, Daniel Köhne, and Jonas Schmidt (2021). *Counting Horizontal Visibility Graphs*. DOI: https://doi.org/10.48550/arXiv.2111.02723.

Paper II

Bernhard, Johannes, Jonas Schmidt, and Mark Schutera (2022). "Density based Anomaly Detection for Wind Turbine Condition Monitoring." In: *Proceedings of the 1st International Joint Conference on Energy and Environmental Engineering - CoEEE*, INSTICC. SciTePress, pp. 87–93. ISBN: 978-989-758-599-9. DOI: https://doi.org/10.5220/0011358600003355.

Paper III

Schmidt, Jonas (2022). "Tire Pressure Monitoring using Weighted Horizontal Visibility Graphs." In: *2022 International Conference on Control, Automation and Diagnosis (ICCAD)*, pp. 1–6. DOI: https://doi.org/10.1109/ICCAD55197.2022.9853892.

Paper IV

Schmidt, Jonas, Kai-Uwe Kühnberger, Dennis Pape, and Tobias Pobandt (2023). "Detecting Loose Wheel Bolts of a Vehicle Using Accelerometers in the Chassis." In: *Pattern Recognition and Image Analysis*. Cham: Springer Nature Switzerland, pp. 665–679. ISBN: 978-3-031-36616-1. DOI: https://doi.org/10.1007/978-3-031-36616-1_53.

Paper V

Schmidt, Jonas and Daniel Köhne (2023). "A simple scalable linear time algorithm for horizontal visibility graphs." In: *Physica A: Statistical Mechanics and its Applications* 616, p. 128601. ISSN: 0378-4371. DOI: https://doi.org/10.1016/j.physa.2023.128601.

Patent I

Schmidt, Jonas, Michael Hertkorn, and Martin Damian Trochowski (2021). "Computer-implemented method for the calculation of convolutional networks." Pat. DE 10 2020 202 871 A1.

ACKNOWLEDGMENTS

First of all, I would like to thank my supervisor Kai-Uwe Kühnberger, who always supported me with advice during my doctoral studies. You helped me maintain a scientific perspective and keep the big picture in mind during my thesis, combining industry and university research.

I would like to express my gratitude towards Michael Klank, my supervisor at ZF Friedrichshafen AG. You always gave me your trust, freedom, and support to work on topics for this thesis. I also want to highlight the unwavering support and assistance of my colleagues Dennis Pape and Tobias Pobandt. Your expertise in mechanics and physics has greatly aided my understanding of various phenomena in vehicles. I would also like to thank my employer, ZF Friedrichshafen AG, for the scholarship program that supports employees in their further education and research projects.

I am grateful for the countless meetings, discussions, and exchanges with Daniel Köhne. Working with you was a great experience, and tackling a complex problem together always made twice as much fun. Thanks to Martina Juhnke-Kubitzke for her feedback and comments, which significantly improved the mathematical quality of our publications.

Thanks also to Jan-Jakob Völlering, for being there for me throughout my entire academic journey. You have been my go-to person for both personal and scientific matters, and I am fortunate to have you as my friend and confidant.

But most of all, I thank my wife, Kira. Without you, this work would not have been possible. You did everything to give me the time and freedom to write this dissertation. You showed me the right moment to take a break when I was once stuck. You cushioned all the ups and downs that come with a dissertation and cheered me up when I pondered for hours about a problem at my desk and couldn't find a solution. Thank you for all the love and support you give me.

CONTENTS

I INTRODUCTION AND METHODOLOGY 1

1 INTRODUCTION 3
- 1.1 Background 3
- 1.2 Objectives 5
- 1.3 Thesis Outline 8

2 CONDITION MONITORING 9
- 2.1 Maintenance and Failures 9
- 2.2 From Corrective Maintenance to Predictive Maintenance 11
- 2.3 Condition Monitoring Systems 13
- 2.4 Condition Monitoring in the Automotive Sector 16
  - 2.4.1 Applications in Production Vehicles 16
  - 2.4.2 Applications in Research 17
- 2.5 Condition Monitoring in other Industries 22
- 2.6 Outlook 24

3 VEHICLE VIBRATIONS AND ACCELEROMETERS 27
- 3.1 Fundamentals of Mechanical Vibrations 27
  - 3.1.1 Basic Terms of Mechanics 27
  - 3.1.2 Vibration Systems 29
- 3.2 Vehicle Vibrations 33
  - 3.2.1 Causes 33
  - 3.2.2 Effects 34
  - 3.2.3 Mitigations 36
- 3.3 Accelerometers 38
- 3.4 Vibration-based Monitoring 40
- 3.5 Outlook 41

4 VIBRATION SIGNAL ANALYSIS 43
- 4.1 Signals 43
  - 4.1.1 Continuous and Discrete Signals 44
  - 4.1.2 Sinusoids and Complex Exponentials 44
  - 4.1.3 Further Classes of Signals 46
- 4.2 Time Domain Analysis 46
  - 4.2.1 Statistical Features 47
  - 4.2.2 Correlations 48
- 4.3 Frequency Domain Analysis 49
  - 4.3.1 Fourier Series 49
  - 4.3.2 Discrete-Time Fourier Transform 51
  - 4.3.3 Fourier Transform 53
  - 4.3.4 Discrete Fourier Transform 54
- 4.4 Time-Frequency Domain Analysis 56
- 4.5 Graph Domain Analysis 58

4.5.1 Visibility Graphs 59
4.5.2 Graph Features 60
4.6 Outlook 62
5 TIME SERIES ANOMALY DETECTION 63
5.1 Basics of Time Series Anomaly Detection 63
5.1.1 Terminology 63
5.1.2 Anomaly Detection Approaches 65
5.1.3 Evaluation Metrics 66
5.2 Statistical Models 68
5.2.1 Parametric Models 68
5.2.2 Nonparametric Models 69
5.3 Classical Machine Learning Models 70
5.3.1 Neighbor-based Models 70
5.3.2 Autoregressive Models 72
5.3.3 One-class Support Vector Machine 73
5.4 Deep Learning Models 75
5.4.1 Autoencoders 75
5.4.2 Recurrent Neural Networks 76
5.4.3 Convolutional Neural Networks 77
5.4.4 Graph Neural Networks 79
5.5 Outlook 80

II RESEARCH 81
6 COUNTING HORIZONTAL VISIBILITY GRAPHS 83
7 DENSITY BASED ANOMALY DETECTION FOR WIND TURBINE CONDITION MONITORING 85
8 TIRE PRESSURE MONITORING USING WEIGHTED HORIZONTAL VISIBILITY GRAPHS 87
9 DETECTING LOOSE WHEEL BOLTS OF A VEHICLE USING ACCELEROMETERS IN THE CHASSIS 89
10 A SIMPLE SCALABLE LINEAR TIME ALGORITHM FOR HORIZONTAL VISIBILITY GRAPHS 91
11 PATENT: COMPUTER-IMPLEMENTED METHOD FOR THE CALCULATION OF CONVOLUTIONAL NETWORKS 93
12 DISCUSSION 95
13 CONCLUSION 99

III APPENDIX 101
A RUNTIME DATA OF HORIZONTAL VISIBILITY ALGORITHMS FOR SYNTHETIC AND EMPIRICAL TIME SERIES 103

BIBLIOGRAPHY 105

LIST OF FIGURES

Figure 1 Data flow diagram of a CMS - Comprehensive overview of the general case and the research focusing on developing advanced anomaly detection algorithms for vibration-based CMSs with automotive applications. 6

Figure 2 The observed failure rate over the lifetime of a technical system with the three main causes of failure (Maisonnier, 2018). 10

Figure 3 Degradation curve of the wear reserve with the basic maintenance measures (Preusche, 2018). 11

Figure 4 Schematic structure of a condition monitoring system (Ryll and Götze, 2010). 13

Figure 5 Model for the vibration of an elastic medium (Obst, Hardt, and Fuhrmann, 2018). 29

Figure 6 SDOF spring-mass system (Rao, 2018). 30

Figure 7 Graphical visualization of the equation of motion of a harmonic oscillator (Rao, 2018). 31

Figure 8 The vehicle coordinate system. 34

Figure 9 Transmission paths within the vehicle from the excitation to the passenger (Wallentowitz, 2005). 35

Figure 10 Influence of sampling on the frequency domain: In (a), the FT of the original signal is presented, where (b) and (c) show the continued DTFT for the cases $\Omega_s > 2\Omega_B$ and $\Omega_s < 2\Omega_B$ (Oppenheim, Willsky, and Nawab, 1996). 54

Figure 11 Spectrogram a) has a high frequency resolution, whereas b) has a high time resolution. 57

Figure 12 Illustration of a Mel filter bank. As the frequency increases, more frequency bins are utilized to calculate the corresponding Mel bin. 58

Figure 13 Transformation of a time series into its HVG and VG, respectively. 59

Figure 14 Invariance of HVG under additive noise. 60

Figure 15 Illustration of a ROC curve and precision-recall curve. The anomaly scoring 1 was generated by an algorithm with high precision and low sensitivity, and the anomaly scoring 2 by an algorithm with low precision and high sensitivity. 67
Figure 16 Data set with two clusters and varying local densities (Chandola, Banerjee, and Kumar, 2009). 71

LIST OF TABLES

Table 1 Vibration phenomena in the vehicle (Wallentowitz, 2005). 37
Table 2 Measurement and frequency ranges of commercial accelerometers based on the study by (Elies and Ebenhöch, 2015). 39

ABBREVIATIONS

ABS Anti-lock braking system

ACC Adaptive cruise control

AD Anomaly detection

AE Autoencoder

ANC Active noise cancellation

ANN Artificial neural network

AR Autoregressive

ARIMA Autoregressive integrated moving average

ARMA Autoregressive moving average

AUC Area under curve

CM Condition monitoring

CMS Condition monitoring system

COF	Connectivity-based outlier factor
DFT	Discrete Fourier transform
DTFS	Discrete-time Fourier series
DTFT	Discrete-time Fourier transform
ECU	Electronic control unit
ESC	Electronic stability control
EU	European Union
FFT	Fast Fourier transform
FN	False negative
FP	False positive
FT	Fourier transform
GNN	Graph neural network
HVG	Horizontal visibility graph
KNN	K-nearest neighbors
LKA	Lane keeping assist
LOF	Local outlier factor
LSTM	Long short-term memory
MA	Moving average
ML	Machine learning
NVH	Noise, vibration, and harshness
RNN	Recurrent neural network
SDOF	Single-degree-of-freedom
SoH	State-of-health
STFT	Short-time Fourier transform
SVM	Support vector machine
PID	Parameter identifier
TN	True negative
TP	True positive
VG	Visibility graph

Part I

INTRODUCTION AND METHODOLOGY

1 INTRODUCTION

1.1 BACKGROUND

The patent *DRP No. 37435* filed by engineer Carl Benz on January 29, 1886, entitled *Fahrzeug mit Gasmotorenbetrieb* is today considered the birth of the automobile (Kirchberg et al., 1981). Since then, the automotive industry has grown to become the largest industry in Germany in terms of sales of 411 billion Euro in 2021, with over 750,000 direct employees and over 2.2 million, including suppliers and the secondary market (BMWK, 2022a). The automotive industry is currently undergoing one of the most significant transformations since the invention of the automobile. This is due to the parallel transformation of drive technology and vehicle control systems, which fundamentally change the driving experience and human interaction with the vehicle (Fredriksson et al., 2018; Yurtsever et al., 2020).

In drive technology, there is a strong trend toward electrification. According to the Verband der Automobilindustrie e.V.[1], the global annual registrations of electrified vehicles more than tripled from 2018 to 2021 (Fritz, 2022). This number increased from 2 million to more than 6.5 million, corresponding to one of nine registered cars. This is also supported by EU-level political regulations (Reg. (EU) 2023/851, 2023), according to which no new vehicles with combustion engines may be registered from 2035 unless it can be ensured that these can only be fueled with climate-neutral synthetic fuels. At the national level in Germany, the transformation is being driven forward by government subsidies for electric or hybrid vehicles or by tax benefits for electrified company vehicles (BMWK, 2022b). The *Paris agreement* to limit global warming to 1.5 degrees is the background to these efforts (UNEP, 2015). This commits the EU to achieving zero emissions by 2050. The transport sector accounted 2017 for 27% of greenhouse gas emissions in the EU (EEA, 2019), half of which were caused by passenger cars and the automotive industry (Pichler et al., 2021).

The second major transformation is changing vehicle control, particularly by *whom* the vehicle is controlled. Car manufacturers offer customers an increasing number of assistance systems that support the driver in driving situations or independently perform driving maneuvers (Knoll, 2010). According to the Society of Automotive Engineers' definition, the levels of autonomous driving are divided into levels 0 to 5 (ORAD Committee, 2021). As the level increases, the de-

1 *The Verband der Automobilindustrie e.V. (Association of the Automotive Industry) is an umbrella organization representing the German automotive industry's interests.*

gree of automation increases, and the vehicle takes on more tasks and responsibilities (Schönewolf, 2020). At level 0, there is no automation, meaning the driver steers, accelerates, and brakes unassisted. Level 1 includes functions like a lane keeping assist (LKA) or adaptive cruise control (ACC), which assist with steering, acceleration, and braking, but only longitudinally or laterally, not simultaneously. At level 2, assistance systems partially take over lateral and longitudinal control simultaneously, whereby the driver temporarily no longer has to hold the steering wheel. However, he remains solely responsible and liable for the driving behavior and must be alert at all times to be able to intervene. The car manufacturer bears the responsibility and liability at level 3, whereby the system only operates under predefined conditions, such as during the day or at low speed. There is a crucial step between levels 2 and 3, as the driver no longer has to monitor the system constantly but can also use the smartphone or watch a movie. Nevertheless, he must be able to take over driving again when the system reaches its limit and communicates this with a warning tone. At level 4, the driver no longer needs to be ready to intervene. He is also allowed to sleep. However, this is limited to certain driving conditions, routes, or road types, such as highways. This is the difference to level 5, where there are no more restrictions to certain conditions, and the driver becomes a passenger (Wienrich, 2023).

The race between manufacturers to reach the next level has long been on: In January 2023, Google subsidiary *Waymo* became the first to reach 1 million miles traveled with its level 4 robo cab fleet, with no injuries and only two relevant collisions (Victor et al., 2023). However, it is currently difficult to predict when such systems will go into series production.

According to Bertoncello and Wee (2015), autonomous driving is not restricted to changing automobility but will also significantly impact our social life. For example, when autonomous driving becomes widespread, Brown, Gonder, and Repac (2014) see great fuel-saving potential due to higher efficiency, less congestion, and better traffic flow. This also emphasizes the ecological impact of this disruptive technology. Anderson et al. (2016) stated that urban areas would require less parking space, as autonomous vehicles can drop off their passengers in the city and park outside the city. Marletto (2019), on the other hand, argues that autonomous driving could counteract the trend of urbanization, as commuting time to a city becomes less relevant because it can be spent on other activities.

In addition to the technical feasibility challenge, other factors will affect the widespread adoption of autonomous vehicles. Potential passengers must accept and trust this new type of vehicle. A study by Ro and Ha (2019) identified that a decisive factor for this is *safety*, which significantly influenced the attitude and purchase intention of the survey participants.

If, due to the rise of autonomous driving, people become vehicle users rather than vehicle owners, e.g., through mobility-on-demand services like robo cabs, then the sense of responsibility for the vehicle may decrease, as they only use it but no longer own it (Heinrichs, 2016). Even if the passenger remains the vehicle owner, he or she can pursue other activities while driving and may be distracted. Consequently, these distracted passengers become unaware of alterations in the vehicle's handling characteristics or less conscious of potential faults, which decreases road safety.

This gap in the chain of responsibility is closed by condition monitoring systems (CMSs) in the vehicle because they take over automated monitoring of the vehicle's condition and warn the passenger in case of a fault. Whether it is an autonomous or a regular vehicle, CMSs, increase safety and protect other road users from potential accidents. CMSs thus make a decisive contribution to the acceptance of autonomous vehicles. They are one of the many pieces of the puzzle needed to ultimately build a truly autonomous vehicle, in line with ZF Friedrichshafen AG's vision of zero emissions and zero accidents (Stratmann, 2015).

1.2 OBJECTIVES

This work aims to develop computational efficient and advanced methods for anomaly detection in vibration-based CMSs, focusing on automotive applications. It was conducted in cooperation and collaboration with the digitalization department for mechatronic systems at ZF Friedrichshafen AG, my employer and scholarship provider. Therefore, no data collected through test drives related to this work and programming code will be published to comply with confidentiality obligations. This thesis includes three papers dealing with anomaly detection in vibration data for condition monitoring (CM) and one paper and granted patent dealing with the computational efficiency of feature extraction and convolutional neural networks (CNNs) inference. While investigating horizontal visibility graphs (HVGs) used to analyze vibration data, conjectures arose that they have specific combinatorial properties (Luque et al., 2009). These conjectures were proved in a further publication.

An essential application of the developed methods for anomaly detection is in the context of autonomous driving. The research in autonomous driving focuses mainly on developing algorithms to control vehicles on the road without accidents and perceiving the environment outside the car. However, for increased safety, reliability, and social acceptance, the autonomous vehicle should also monitor itself and its components equally. This is where CM comes in, to extend the autonomy from the driving level to the diagnostic level and thus make driving safer for all road users. Figure 1 displays the data flow

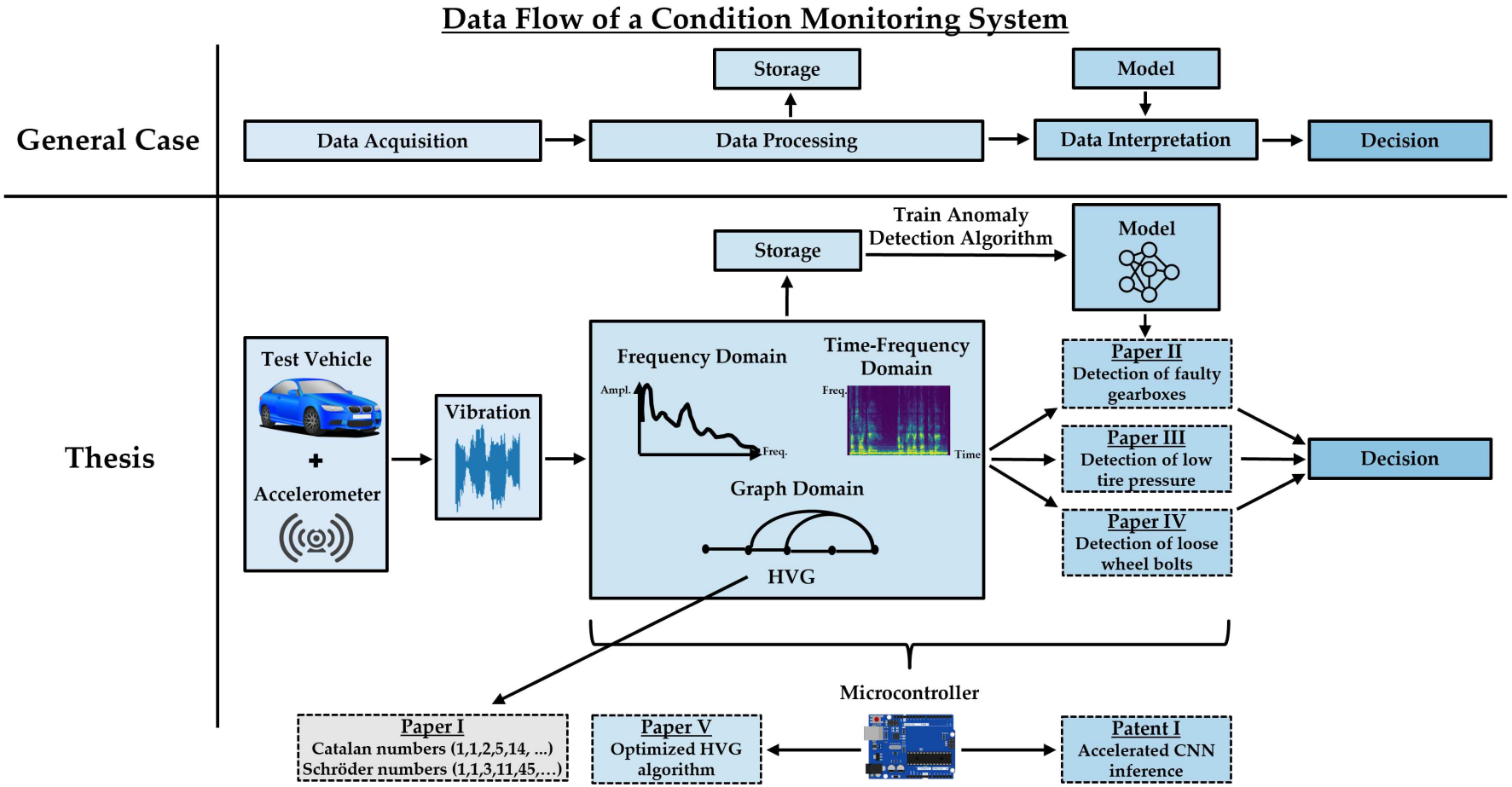

Figure 1: Data flow diagram of a CMS - Comprehensive overview of the general case and the research focusing on developing advanced anomaly detection algorithms for vibration-based CMSs with automotive applications.

in a CMS based on the general case and the specific data flow for this research focusing on detecting anomalous vibration data in the vehicle. In addition, the relations between scientific publications and patents and the processing steps during CM are shown.

In the following, the studies are presented in the order in which their methods are applied in a CMS, and each paper's research contribution is summarized:

(i) Paper V proposes a simple and scalable algorithm for computing HVGs that works efficiently for streamed data, such as vibration signals, recorded in the vehicle. It is particularly well suited for batch-wise data and high sampling rates and provides computational efficiency in the data processing step of a CMS. The algorithm has a worst-case time complexity of $O(n)$. Unlike previous publications, it does not require a tree-based data structure.

(ii) Paper II introduces a density-based k-nearest neighbor algorithm to detect damage to gearboxes that represents the data interpretation step of a CMS. In contrast to deep-learning-based approaches, it provides an explainable anomaly detection that can be traced back to the conspicuous frequency ranges. Since we did not have access to data from faulty vehicle gearboxes, we used data from the gearboxes of wind turbines, which ZF Friedrichshafen AG also produces.

(iii) Paper III also focuses on the data interpretation step of a CMS by demonstrating that low tire pressure can be reliably detected using the vibration data in the chassis, which is converted into HVGs and whose graph properties are used as input for a gradient-boosting algorithm.

(iv) Paper IV deals with detecting loose wheel bolts based on vibration data in the chassis. The investigated semi-supervised anomaly detection algorithms enable reliable detection as soon as three out of five wheel bolts are loose and can thus increase safety on the road by preventing potential accidents due to wheel loss in advance.

(v) Patent I enables faster inference of CNNs on microcontrollers when they process streamed data, such as audio or vibration data, and the inputs overlap. The approach on which the patent is based allows larger neural networks to be computed with low latency on embedded hardware and helps to realize real-time inference during the data interpretation step of a CMS in the vehicle.

(vi) Paper I is purely theoretical since it presents the proofs of several properties of HVGs that have emerged as conjectures

during the thesis. Specifically, the ordered degree sequence uniquely determines them when they arise from a data sequence with no equal entries. In addition, we demonstrate that the HVGs of data sequences with and without equal entries are counted by the Catalan and Schröder numbers, respectively.

1.3 THESIS OUTLINE

The chronology of this thesis is based on the data flow in a CMS, as illustrated in Figure 1. It begins with an overview of CM and maintenance strategies focusing on the automotive sector. Chapter 3 addresses the vibrations occurring in vehicles and the sensor technology, namely accelerometers, to measure the vibrations during the data acquisition step of a CMS. Chapter 4 covers the various methods used for feature extraction of vibration signals in the data processing step, including those from the time, frequency, time-frequency, and graph domains. Chapter 5 focuses on time series anomaly detection as part of the data interpretation step of a CMS, highlighting the particularly suitable algorithms for analyzing vehicle vibration data. Finally, the thesis concludes by discussing the papers, placing them in a broader context, along with future research perspectives.

2 CONDITION MONITORING

The concept of monitoring the condition of technical devices has been around since the earliest development of machines when people used their senses to detect problems. While this traditional method of using our senses of sight, hearing, touch, smell, and taste is still relevant, it has been enhanced by advanced scientific instruments. These instruments enable us to measure the health or condition of machines or machine parts, allowing us to detect and fix problems early before they cause failure (Davies, 1998). A general definition by Kelly (1997, p.234) describes *Condition Monitoring* (CM) as *"The periodic, routine, or continuous measurement and interpretation of data to indicate the condition of an item"*. CM involves the installation of sensor systems on machines, together with data acquisition and analysis methods, as well as diagnostic techniques. This chapter will explain how CM relates to the overall maintenance process and describe the elements and different types of maintenance. Furthermore, applications of CM in the automotive sector and other industrial areas will be introduced.

2.1 MAINTENANCE AND FAILURES

The *failure rate* is a metric that describes the failure occurrence of technical systems. It is defined as the frequency with which a technical system fails. The failure rate is expressed by the number of failures per unit of time. Figure 2 illustrates the observed failure rate and its main causes over the lifetime of a technical system. Because of its shape, this is also called the *bathtub curve* (Maisonnier, 2018). The failures are divided into three categories: *Early failures*, *random failures*, and *wear-out failures*. The first category is due to design, manufacturing, or assembly errors. They usually occur immediately after first use. Increasing the number of quality checks can prevent such failures. Random failures occur independent of the age of the product. They are often caused by operating errors or temporary overloading of the technical system. As the product ages, the probability of age-related failures increases. Regular wear and tear of the system in the form of material fatigue or corrosion cause wear-out failures. They are an unavoidable part of the long-term use of technical systems (Anderson, 1976).

Maintenance is closely related to CM because maintenance measures can be derived from the observed condition. DIN 31501 states that maintenance consists of the *"Kombination aller technischen und administrativen Maßnahmen sowie Maßnahmen des Managements während*

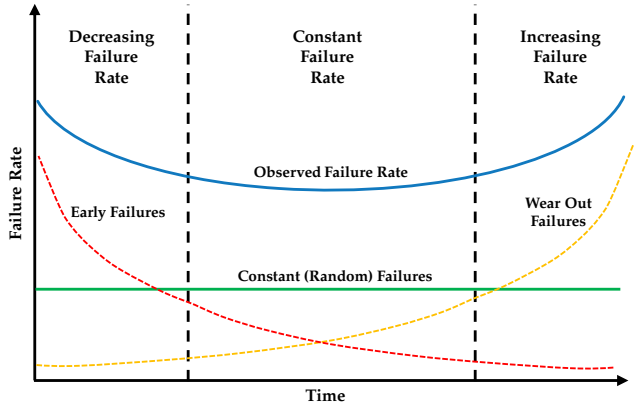

Figure 2: The observed failure rate over the lifetime of a technical system with the three main causes of failure (Maisonnier, 2018).

des Lebenszyklus eines Objekts, die dem Erhalt oder der Wiederherstellung ihres funktionsfähigen Zustands dient, sodass es die geforderte Funktion erfüllen kann[1] (Deutsches Institut für Normung e. V., 2019, p.4). According to Rishel and Canel (2006), plant engineering and maintenance account for 20 to 40 percent of manufacturing costs. Therefore, maintenance, as well as its timing and planning, significantly impact the profitability of industrial production processes. The profitability can be increased if management focuses on maintenance costs and integrates them into the corporate strategy. Increasing profitability is an indirect result of the primary goals of maintenance. Leidinger (2014) defines them as:

(i) Safety

(ii) Availability

(iii) Reliability

(iv) Value preservation.

The goal of safety means that the technical system should not pose any hazards to people or the environment. Availability and reliability refer to the operation of the technical system, which should be permanent and trouble-free. In addition, value preservation should ensure the technical system has a high life expectancy. This is becoming increasingly important due to developments toward an ecological and sustainable economy (Serrat, 2012).

Maintenance includes all countermeasures to reduce the failure rates or to restore failed technical systems to their functional condition. DIN 31501 divides maintenance into four basic measures: service, inspection, repair, and improvement. Figure 3 shows the effects

1 *Author's translation: "Combination of all technical and administrative measures as well as management measures during the life cycle of an object, which serves to maintain or restore its functional condition so that it can fulfill the required function"*

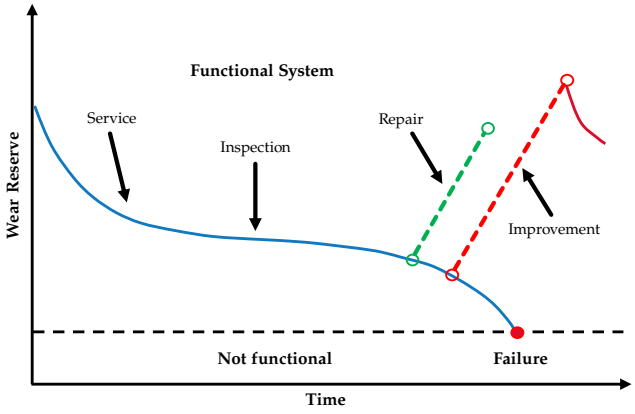

Figure 3: Degradation curve of the wear reserve with the basic maintenance measures (Preusche, 2018).

of the primary measures on the wear reserve of a technical system. The *wear reserve* is defined here as the reserve of possible functional performance of the technical system. If the wear reserve is used up, the technical system loses functionality and must be repaired. The reduction of the wear reserve is slowed down by service. This includes, for example, lubrication or cleaning. Inspection is used to assess the condition of the technical system. Measuring, testing, and diagnostic systems are applied for this purpose. Inspection has no direct effect on the wear reserve. It is required to detect the technical system's condition. If the inspection is done regularly or continuously, this corresponds to CM. Repair includes measures that increase the wear reserve again, for example, by replacing or repairing damaged components. Improvement aims to optimize a technical system to increase the maximum wear reserve compared to the initial condition (Pawellek, 2016).

2.2 FROM CORRECTIVE MAINTENANCE TO PREDICTIVE MAINTENANCE

The maintenance strategies differ in whether the maintenance is applied correctively or preventively. *Corrective maintenance* carries out measures only after a failure has occurred. They are consciously taken into account. The advantage of this method is that the wear reserve is entirely used up. This reduces the inspection effort, resources for spare parts, and assembly effort. The time at which the wear reserve is exhausted is unknown a priori. Therefore, failure can occur at any time, and the company must be able to perform maintenance for critical components also at any time. From a business perspective, this is disadvantageous for optimizing operations and planning human and operational resources (Schröder, 2010).

Preventive maintenance aims to avoid failures and perform maintenance before a failure occurs. The advantage is that maintenance mea-

sures become plannable. In this way, required operational resources for maintenance can be determined in advance, and processes can be optimized. However, for preventive maintenance to be successful, a failure must be avoided, and consequently, maintenance must be performed on a technical system that still has remaining potential for use. The risk is that the replacement time is chosen too early, and the remaining utilization potential is not exploited.

On the other hand, if it is chosen too late, the probability of an unplanned failure increases. The simplest implementation option for preventive maintenance is to perform maintenance tasks at regular intervals according to a *time-based* schedule. Alternatively, this can be based on the number of hours a machine has been operating. In the case of vehicles, it is common to use the kilometers driven by a car as a benchmark. The intervals are determined according to empirical values or manufacturer recommendations. This strategy can be very costly, depending on the choice of intervals.

The subsequent two advanced maintenance strategies both belong to the class of preventive maintenance strategies. *Condition-based maintenance* follows the approach of monitoring the condition of a technical system and planning maintenance measures accordingly. CM makes it possible to renew technical systems only when a predefined wear reserve has been reached. In doing so, the wear reserve can be utilized to the greatest extent. Developing such a strategy requires investments in modern measuring and testing technology, diagnostic algorithm development, and highly qualified employees to perform the evaluation (Strunz, 2012).

Predictive maintenance goes one step further by making predictions about the future state of the technical system and forecasting the expected time of failure. This strategy aims to predict the remaining service life of the technical system and determine the optimal time for maintenance measures. This is done based on information about the condition of the system and past data about maintenance measures. This strategy requires advanced algorithms for making accurate predictions (Theissler et al., 2021). CM is thus an essential component of condition-based and predictive maintenance.

The terms condition-based and predictive maintenance are sometimes used interchangeably in the literature. However, the former focuses on *diagnostic* methods, i.e., determining the actual condition of a technical system. Most diagnostic methods provide a warning or alarm but no information about the remaining life of the system. This is where predictive maintenance comes in, using *prognostic* methods to predict when a failure will occur. One challenge is to validate this methodology. The predicted failure times must be compared to the actual failure times. However, many critical applications have preventive maintenance policies to avoid failure conditions, which reduces the number of observed failures and makes validation difficult. Never-

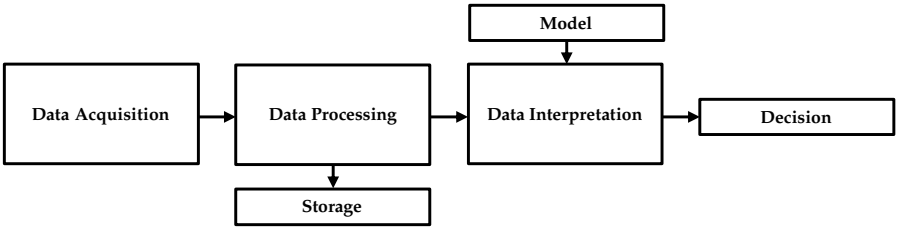

Figure 4: Schematic structure of a condition monitoring system (Ryll and Götze, 2010).

theless, CM increases the amount of degradation data available, making it easier to validate prognostic methods (Tinga and Loendersloot, 2019).

The selection of the optimal maintenance strategy depends on the application. None is universally suitable. Only by combining the strategies can an optimized approach be designed. Corrective maintenance waits until the failure occurs and only then restores technical functionality, which is why it is suitable in cases where the effort of the other strategies is too high or a failure does not lead to a critical operating condition (Leidinger, 2014). Preventive maintenance strategies should be used where there is a threat of high production losses or a potential risk to people and the environment. Here, higher maintenance costs for increased safety are then consciously accepted. Time-based maintenance is favored if failure data is known and there is a low level of variation in the failures. Condition-based or predictive maintenance has the advantage that by inspecting the condition of the technical system, maintenance measures can be planned more intelligently, and the wear reserve can be utilized to a greater extent. However, they are also associated with high investments in measurement equipment, data processing, and data transfer. Therefore, the technical feasibility and economic advantage must be given (Strunz, 2012).

Value-based maintenance optimizes maintenance costs by ideally combining various maintenance strategies. In this strategy, an individual decision is made for each part and component of a technical system regarding which type of maintenance is economically most valuable (Leidinger, 2014).

2.3 CONDITION MONITORING SYSTEMS

Implementing CM requires a system architecture consisting of hardware and software components, which are explained in more detail in the following. Their selection and interaction are crucial for the functionality of a CM application. The system that executes CM is called Condition Monitoring System (CMS) (Hameed, Ahn, and Cho, 2010). Figure 4 visualizes the CMS data process flow. The first step

is *data acquisition*. This step involves gathering data from an object or environment through the use of sensors. These data can be versatile, as the sensor and measured variable choice depend on the application. Standard physical state variables collected include temperature, pressure, weather and environmental parameters, oil analysis, and vibration and acoustic data. Due to the advancement of computer and sensor technology, they are becoming more powerful and less expensive, facilitating the data collection of a CMS and increasing the application possibilities (Jardine, Lin, and Banjevic, 2006).

In addition to this data collected by sensors, additional meta-data can be collected that provides information on whether changes have been made to a machine, e.g., replacement of spare parts or oil changes. This meta-data is just as necessary as the data collected by the sensors because it can be used to validate the CMS. They also provide essential feedback for the developers of the CMS and give helpful information for possible improvements to the system.

The next step is *data processing*. One challenge with CM is that the sensors used for data acquisition are a technical system that can also produce failures and errors. Further processing of sensor data can only be successful if the information provided by the sensors is accurate. The first component of data processing is, therefore, *data cleaning*. For this, a check of the data and its quality is performed. There are different approaches to this. Two or more redundant sensors can be used, but it would be unclear which sensor measures incorrect signals in this case. At least three redundant sensors are needed to determine which sensor is not working. If redundant sensors are not justifiable for economic reasons, the value range of the sensor signals can be checked, and whether they are in a pre-defined range. Additionally, the sensor failure may show up in a characteristic pattern so that the CMS can detect the sensor failure (Grimmelius et al., 1999).

Once the data cleaning and quality checks are finished, the second part of the data processing begins. This part is called *feature extraction*. In this part, the relevant information is extracted from the raw sensor signals to serve as indicators to identify the state of the monitored object. The feature extraction methods used depend on the signal the sensors are measuring. If waveform data are available, such as acoustic or vibration data, methods from the field of *signal processing* are applied (Oppenheim, Willsky, and Nawab, 1996). These can be divided into methods that analyze the sensor signal in the time, frequency, or time-frequency domains (see Chapter 4). If the sensor is an optical sensor, methods from the field of image processing are applied, e.g., digital filters to blur, sharpen, or denoise the image (Jardine, Lin, and Banjevic, 2006). These are stored in databases if required for subsequent processing, data analysis, or for training machine learning (ML) algorithms (Hameed, Ahn, and Cho, 2010).

The *model* takes over the task of sensor signal interpretation. The extracted features are the model's input, and the output is an estimate for the technical system's current condition. Accordingly, the models for condition monitoring can be categorized into four types. One approach is to use a *physical model* of the wear process of the technical system. The performance of this approach depends mainly on the accuracy of the model and usually requires vast domain knowledge of experts implementing the model. An advantage of the approach is that the physical description of the process means that the factors influencing wear and their magnitude are known, and the model and its output become explainable. A disadvantage, however, is that a physical model may use many different physical quantities as parameters, each of which must be measured with sensors. *Knowledge-based models* are another approach. They are designed to simulate the behavior and decision-making of experts. The most common type of these models are *rule-based models*, which experts implement. Their advantage lies in their high interpretability. At the same time, however, they are also error-prone in implementation if very complex conditions have to be expressed or many rules exist.

Data-driven methods create models not based on the knowledge of experts but based on collected data and the features that have been extracted from them. They use approaches from statistics, stochastics, and ML. However, a disadvantage of these methods is that they require a large amount of data, which is only available in some cases or is very expensive to collect. Advantageously, their performance also improves as the amount of data increases, which is more common in the era of Big Data and advanced sensor technology, as well as cheap computing and storage capacity (Arena et al., 2022).

A combination of a physical and data-based model represents a *digital twin* (Santos and Montevechi, 2022). This methodology creates a physical and functional copy of the technical system or individual components to be monitored. The digital twin is a dynamic model of a physical system that is continuously updated throughout the life cycle of a technical system depending on the condition and maintenance actions performed. This creates a link between the digital and physical worlds. This hybrid methodology shares the advantages and disadvantages of physical and data-based methodologies. Nevertheless, maintaining the digital twin in addition to the technical system requires more effort. This is necessary to ensure that the digital twin is up-to-date and does not reflect an outdated state (Arena et al., 2022).

Based on the determined condition of the technical system, maintenance measures and planning can now be initiated in the final *decision* step. This leads to a gain in time for necessary preparations, which prevents unplanned downtimes (Ryll and Götze, 2010).

2.4 CONDITION MONITORING IN THE AUTOMOTIVE SECTOR

With the accelerated development of sensor and network technology, an increasing number of data sources in the car can be used for CM. These include, for example, pressure, vibration, temperature, voltage, and other electrical and mechanical state variables. On the one hand, the numerous data sources offer new possibilities for condition monitoring applications. On the other hand, modern cars increasingly include more complex hardware and software systems, making maintenance challenging (Ahmed and Nandi, 2020). Due to the increased computing capacity of edge computing systems, vehicle parameters can be analyzed directly in the car. Alternatively, they can be sent from telemetry systems to the cloud for evaluation. In both scenarios, the goal is to warn the driver of critical situations and failures. This early warning can prevent more severe damage to the vehicle and increase the safety of those on board (Arena et al., 2022).

Current developments towards autonomous driving increase the need for cost-effective engineering solutions to ensure vehicle safety and reliability over the lifetime of a car. Data-driven evaluation methods for CM based on ML are increasingly becoming the norm. They enable exploiting the richness of the vehicle's data and learning patterns for assessing vehicle health from the collected data (Theissler et al., 2021).

2.4.1 *Applications in Production Vehicles*

Due to technical progress and legal regulations, there are already a large number of condition monitoring systems that are used in series-produced vehicles. The aim is to reduce accidents in road traffic and increase driving comfort. CM applications in cars determine the condition of components, parts, and the driver himself.

Since 06.07.2022, due to Regulation 2019/2144, specific driver assistance systems that also monitor the condition of the driver are mandatory for all classes of motor vehicles in the EU when they are newly registered. These include a device for installing an alcohol-sensitive immobilizer, a warning system for drowsiness and declining driver attention, and a seat belt warning system (Reg. (EU) 2019/2144, 2019). Accordingly, it should be possible to retrofit an immobilizer to new vehicles that prevent people from driving with an excessively high alcohol level. The drowsiness detection system records and analyzes the driver's steering behavior and recognizes changes that can result from microsleep. If he threatens to fall asleep, he is warned and advised to take a break. The seat belt system detects if a person in the passenger compartment is not wearing a seat belt and draws attention to this utilizing a warning sound.

To ensure the roadworthiness of the car, a variety of components are monitored by sensors. This starts with essential functions such as the fuel tank level or, in the case of an electric vehicle, the battery status. Furthermore, the engine temperature, malfunctions, and defects in important system components such as the light, the battery, and the brake are monitored and communicated to the driver by error messages.

The tires bear the car's weight, which is why high longitudinal and lateral forces act on them while driving (Rajamani, 2006). They form the only connection to the road and significantly influence vehicle behavior and safety. In Germany, between 2018 and 2021, a share of 27.9 percent of accidents resulting in personal injury could be attributed to technical defects in the tire (Statistisches Bundesamt, 2022). Due to the UN/ECE 64 vehicle regulation of the EU, it has been mandatory for all passenger vehicles to be equipped with tire pressure monitoring systems since November 2014, which should warn the driver of changes in tire pressure (Reg. No 64 UN/ECE, 2010). This improves road safety and is also advantageous from an environmental point of view because low tire pressure increases fuel consumption (Szczucka-Lasota, Kamińska, and Krzyżewska, 2019). An innovative CMS has been installed in Audi's luxury vehicles (A6, A7, A8, and Q8) since 2018 that detects whether a wheel is loose. Changes in the wheel speed sensor signal are used to detect a loose wheel. This system is intended to increase road safety further because, in the United Kingdom alone, there are between 3 and 7 fatalities each year in accidents caused by wheel loss (Dodd, 2010).

2.4.2 *Applications in Research*

Before a technical product can be sold and used, it must be verified that it is sufficiently safe. *Functional safety* is the field that deals with the correct and safe functioning of a product. The automotive sector covers this area by the *ISO 26262 standard* (Wilhelm, Ebel, and Weitzel, 2015). It specifies guidelines, development, and control methods for the functional safety of electrical and electronic components, including CMSs. Even for comparatively uncritical functions, low failure rates must be demonstrated during development, which can quickly make development expensive. Brake lights and headlights, whose failure entails low risks, should have a random hardware failure rate of less than $10^{-7}/\text{hour}$ according to the ISO 2626 standard (Das and Taylor, 2016; Xie et al., 2023). However, the high requirements ensure product quality and safety. Due to the high requirements in automotive functional safety, there is a large gap between CM applications operating in vehicles and topics that have yet to be dealt with in scientific publications. However, automotive CM is an active research area

that provides impetus and proofs-of-concept for future applications of CM in production vehicles.

The following presents the current state of research for automotive CM applications based on ML. The papers are grouped according to the components or parts for which the CM is performed. The explanation details the types of failures that are identified and the sensor signals utilized for detection. Most publications mentioned below are discussed in more detail in the review paper by (Theissler et al., 2021). They have been extended in the remainder to reflect the state of research up to 2023.

Damping System Faults: Wang and Yin (2014) and Yin and Huang (2015) proposed the detection of failures in damping systems using accelerometers on the four corners of the vehicle body. They detected spring failures and evaluated the methodology using a simulation model for vehicle damping. Zehelein, Hemmert-Pottmann, and Lienkamp (2020) simulated failures in the damping system. They kept the damper current constant during test drives, which resulted in lower damping forces. Their data source consisted of 18 hours of driving on different road surfaces with an upper-class sedan vehicle, equally distributed between intact and defective dampers. They used the wheel speed sensors, lateral and longitudinal acceleration, and yaw rate as sensor signals. All signals were already present in the vehicle's electronic stability control (ESC) system, so no additional sensor technology was installed. Hu, Luo, and Deng (2021) developed a health monitoring system for estimating the remaining life of automotive suspensions using a long short-term memory (LSTM) network. The system used vibration sensory data obtained from durability tests under various driving cycles as training data. To determine ground truth data for the fatigue state of the components on the test bench, they used special sensors that measure the mechanical stress on the components.

Brake System Faults: Sankavaram et al. (2012) performed failure detection of regenerative braking systems of electric and hybrid vehicles. They used a vehicle power train simulation model with 25 state variables, e.g., wheel speed, wheel torque, and battery temperature. They detected twelve different failure types, including battery temperature, current flow faults, and vehicle speed sensor faults. Jegadeeshwaran and Sugumaran (2015) used accelerometers mounted close to the brake drum to detect failures such as brake oil spills on the disc brake, air in the brake fluid, disc brake pad wear, and drum brake pad wear, among others. The experiments were conducted on a brake test rig with a passenger vehicle. Their approach was based on extracting statistical features from the vibration signal, which they used to train a biological methods-

inspired classifier (Sharma and Sharma, 2011). In another publication (Kumar et al., 2021), the research group improved their results by applying a boosting algorithm that used logistic regression models as weak-learners (Friedman, Hastie, and Tibshirani, 2000).

Engine Faults: Lin (2021) proposed a *support vector machine* (SVM) classifier for detecting motor bearing faults with vibration signals. The method constructed a feature space by extracting statistical parameters of vibration signals and reliably detected bearing ball, inner, and outer ring faults. A publicly available data set for motor bearing faults was used as training data (Smith and Randall, 2015). Jung and Sundström's (2019) research addressed failures related to airflow in a combustion engine. Their study identified failures in the air mass flow sensor and abnormalities in intake manifold pressure, temperature, and intercooler pressure. To detect these failures, their model used sensor signals such as engine speed, pressure at different engine positions, and temperature, among others. Wolf et al. (2018) researched pre-ignition failures in petrol engines. The data were based on more than 1000 signals from Electronic Control Units (ECUs) in the car, which are used to control vehicle functions, such as torque at the gearbox or revolutions per minute. Wong et al. (2016) dealt with the detection of simultaneous failures in engines. The underlying data were signals from a 4-cylinder Honda engine, specifically the engine noise, ignition, and air ratio. Wang et al. (2010) proposed using the engine's vibration data to detect failures at the fuel injection and spark plugs.

State-of-health of the Battery of Electric Vehicles: The state-of-health (SoH) of a battery indicates the level of degradation. It is expressed as a percentage of the battery capacity from the initial state. Pan et al. (2018) determined the SoH using physical indicators extracted from the battery's internal resistance. Yang et al. (2018) focused on the detection of short circuits and used the current flow, voltage, and the battery's temperature as data source. The tests were performed with real batteries under laboratory conditions. You, Park, and Oh (2017) collected the current and voltage signals of battery charging and discharging processes from actual driving profiles. Based on these signals, they developed a data-driven approach to predict SoH.

Tire Faults: Siegel (2018) presented two different approaches to tire monitoring. In the first paper, a 20 percent increase or decrease in tire pressure is detected using the GPS and acceleration signals recorded from a car's smartphone. In the second paper, image recognition is proposed to detect cracks on the surface of tires using photos taken by a smartphone. For this, the photos should be uploaded by the car's owner to a cloud-based diagnostic application that detects

whether the tires are in normal condition (Siegel, Sun, and Sarma, 2018). Vasan et al. (2023) introduced a transfer learning-based CNN approach for tire CM using vibration signals obtained through low-cost acceleration sensors mounted at the rear axle. Using well-established CNN architectures, they classified three different tire pressure states (low, regular, high, and low speeds).

Fuel Cell Faults: Zuo et al. (2021) conducted a more than 1000 hours lasting durability test of a fuel cell on a test bench. They developed an algorithm predicting fuel cell voltage degradation based on the current load. Mohammadi et al. (2015) used a physical simulation model for a fuel cell, which they validated by experimenting with a fuel cell on a test bench. The distribution of currents in the simulated fuel cell was used as data to train an ML algorithm. Using the trained algorithm, they could classify flooding and drying of the fuel cell caused by water management problems.

Faults in Power Steering: Ghimire et al. (2011) introduced a hybrid data-driven and model-based approach to detect power steering failures. For this purpose, they first created a physical model of the power steering system and then used various ML algorithms to classify faulty states. They simulated the failures with different severity. In their work, the authors recognized four different failure types, including a torque sensor malfunction and increased steering wheel friction. In a subsequent publication, they presented an improved approach that also worked robustly on missing data (Ghimire, Zhang, and Pattipati, 2018).

Faults in Electric Motors, Starter-Motors, and Generators: Seera et al. (2014) proposed an ensemble of ML models to detect stator winding faults and eccentricity problems of induction motors. They used the three-phase current signals of the induction motor for CM. Data collection was done on a test rig. The measurements were performed with different motor loads and noise levels. Peters et al. (2020) investigated the detection of failures in vehicle-engine start systems. They also performed experiments on a test rig, detecting two mutually dependent failures. These were battery and start-stop engine failures. They also simulated failures of different intensities here. As features for a multinomial regression model, they used the current, voltage, and motor revolutions per minute. Simsir, Bayir, and Uyaroğlu (2015) introduced a feed-forward *artificial neural network* (ANN) for real-time monitoring of a hub motor. This motor is located in the wheel and is utilized in solar vehicles or electric bicycles due to its compactness. They used seven different main parameters of the motor as sensor signals, which they recorded under laboratory conditions. These were electrical and mechanical

parameters, including the voltage and current of the source, the output torque, and the speed of the motor. Wu and Kuo (2010) utilized a hybrid fuzzy logic and ANN to classify failures of automotive generators. They used the generator's output voltage as a feature for fault detection. Their model detected diode faults, single-phase stator coil faults, and if the voltage regulator was disconnected.

Full vehicle faults: Routray, Rajaguru, and Singh (2010) proposed a method to detect failures independent of a specific component in the car. Their clustering-based approach used information from parameter identifiers (PIDs), of which there are several thousand in modern cars. These PIDs are serial data collected continuously in the ECUs both by sensors in the car and by diagnostic software routines that check the status of subsystems. They tested their method for detecting failures of the heated oxygen sensor, which measures the oxygen content of the car's exhaust stream. Tagawa, Tadokoro, and Yairi (2015) introduced a novel ANN architecture for fault detection and analysis. They utilized 43 different sensor signals, which come from existing sensors in the car and can be read out from the in-vehicle network. With their structured approach, they could identify the true causes of the faults. They evaluated their approach to actual driving data. However, this evaluation is limited because there were no real failures in the trips, so they used hill descents or acceleration and braking maneuvers as faulty data.

In their research, Shafi et al. (2018) addressed the detection of failures in a fleet of vehicles. They collected data from the in-vehicle network and did not use additional sensors. This data is transmitted via Bluetooth to a smartphone, which sends it to a server running the evaluation algorithms. When a failure is detected, the driver is notified via a mobile notification on the smartphone. The vehicle fleet consisted of 70 Toyota Corollas, which collected data from normal conditions and subsystem failures. Their work focused on detecting cooling, exhaust, fuel, and ignition failures.

Theissler (2017) also examined data from the in-vehicle network and trained an ensemble of two ML algorithms to classify known and detect unknown faults. Test drives were performed with a Renault Twingo 1. The eight sensor signals used to train the models included engine load, vehicle speed, and accelerator pedal position. The work focused on detecting intermittent faults, i.e., faults that were present in the sensor signals for only a short period. Permanent failures are usually easier to detect. The injected failures involved actuators, sensors, and the wiring harness. *Actuators* are components that convert an electrical signal from a control unit into mechanical movements.

Faults in autonomous vehicles: Fang et al. (2020) developed a method for detecting and localizing failures in a sensor cluster in an autonomous vehicle. Their multi-stage method allowed the detection of known and unknown failures, up to isolating the failure and stopping the vehicle. The sensor cluster consisted of a GPS module, gyroscope, accelerometer, LiDar, and camera data, among others. Test drives were performed with an autonomous car on a test track for evaluation. Fault conditions were simulated by adding fault patterns to the data, such as a constant offset or the failure of a sensor.

Jeong et al. (2018) proposed a system for self-diagnosing autonomous vehicles. They introduced a new communication network for this purpose. Data from the sensors in the car were analyzed and evaluated using edge computing. As a result, the results were sent to the cloud, informing other nearby vehicles to avoid accidents. Optimizing the message protocol in the car increased the message transmission speed by 15.25%. The system was implemented in a computer-generated environment.

Wyk et al. (2020) formed an ensemble of ANNs and classical ML algorithms to detect anomalies in the sensor data of an autonomous or connected vehicle. They evaluated their model on the *Safety Pilot Model Deployment* data set (Bezzina and Sayer, 2014). In their study, they used vehicle speed, vehicle acceleration, and GPS data as sensor signals. They generated the anomalies artificially by manipulating the sensor data. Their anomaly types consisted of bias, gradual drift, temporarily constant value, sharp change, and missing data.

2.5 CONDITION MONITORING IN OTHER INDUSTRIES

Wind Power: The importance of wind power for the energy transition in Germany is enormous since the share of wind power in the German electricity mix was about a quarter in 2022, accounting for slightly more than half of the total electricity generated by renewables (Statistisches Bundesamt, 2023). For off-shore plants, operations and maintenance (O&M) costs contribute up to 30% of the price of a kilowatt-hour (Bussel and Schöntag, 1997). According to Carroll et al. (2017), lost revenue due to downtime and transportation costs for maintenance each account for about 45% of O&M costs. Staff and repair costs each account for approximately 5%. Therefore, there are great efforts in the industry to reduce downtimes by optimizing maintenance strategies (Bangalore and Patriksson, 2018). McMillan and Ault (2007) investigated the economic advantage of CMSs. Their study showed that CM is particularly worthwhile for off-shore plants with higher maintenance costs if the detection of failures works with high accuracy.

Aerospace: An aircraft is subjected to extreme dynamic loads in its operational environment, so regular maintenance must be performed to guarantee safety and reliability (Ahmed and Nandi, 2020). CM is also used in improving the mission readiness of military aircraft, as there is a trend towards flight-critical electronic systems that need to be monitored (Keller et al., 2006). In modern aircraft, automated flight control systems are used to ensure maximum handling qualities and safe operation. Advanced systems integrate load reduction functions and a flight protection area to prevent critical loads on components due to extreme flight maneuvers. CM helps to analyze whether the respective condition of the aircraft allows certain flight maneuvers (Voskuijl, van Tooren, and Walker, 2015).

Railway: The development of the rail network and rail transport is a crucial transformative factor in a country's economic and social development. Reliable and functioning rail transport is the essential prerequisite for this. When components of trains fail unexpectedly, delays in deliveries may occur (Ahmed and Nandi, 2020). CM helps monitor the rail network and critical components of trains. The industry focuses on optimal rail renewal and maintenance planning that minimizes long-term costs and failure probabilities. Using the combination of CM and *reinforcement learning* (Sutton and Barto, 1998), for example, an optimal strategy was found, simultaneously reducing rail renewal expenses and increasing network reliability and safety (Mohammadi and He, 2022).

Manufacturing: All manufactured goods face international competition in a globalized world. Depending on social developments, customers' preferences for quality, safety, and environmental performance are changing in these markets. Hence, the demands on machinery and production processes are also changing. Companies are developing new maintenance strategies in highly competitive markets to achieve maximum operational efficiency and remain competitive.

Higher plant availability and reliability should be achieved with the most cost-effective means. These requirements have led to the growth of maintenance 'on condition', minimizing unplanned downtime in production processes (Shrieve and Hill, 1998).

The most popular sensors for rotating components such as bearings or gearboxes are *accelerometers* (see Subsection 3.3), which pick up the component's vibrations. In addition, microphones are also applied in industrial CMSs for acoustic monitoring. Oil analysis and lubricant monitoring are used as indicators to detect wear of oil-wetted components. Electrical parameters such as voltage, current, and resistance are collected and analyzed for CM of electronic components in

production processes (Ahmed and Nandi, 2020). CM in manufacturing is part of *Industry 4.0* (Czichos, 2019), which refers to integrating digitalization into production processes using elements of *artificial intelligence* (Fetzer, 1990). Industry 4.0 covers the entire life cycle of a product, i.e., development and production, use, maintenance, and recycling. CM, as part of Industry 4.0, thus contributes to increased efficiency and productivity (Mockenhaupt, 2021).

2.6 OUTLOOK

CM is an essential component of modern technical systems, providing more safety and improving maintenance measures' planning. The provided application areas are only a selection of important areas for CMS and can be extended to almost every industrial sector using complex technical systems. A frequently criticized limitation, especially in the automotive field, is the lack of public data sets. This prevents the comparability of CMS, as no benchmark can be made between a novel approach and the state-of-the-art. Quantitative comparability using performance metrics is also impossible due to the different problem settings, sensors, sensor placements, and data sets (Arena et al., 2022). Automobile companies consider data sets highly confidential and do not share them publicly (Theissler et al., 2021).

Academia research has limited access to actual vehicle data, so either collaboration is made with industry partners, simulation data is generated, or data is collected on test benches. The question remains about how well these simulations and data from test benches can be compared to driving behavior in real road traffic. An ongoing initiative at the EU level, which obliges large corporations to publish data sets and thus gives universities and start-ups access to them, can accelerate research in the field of CM (EU Vehicle Data Initiative, 2022).

A further challenge of CMS development is the *system and component level gap*. Complex systems such as vehicles, ships, or trains consist of numerous subsystems and components. CMSs are usually developed at the lowest level, the component level. For the user of a technical system, however, the main interest is to optimize maintenance at the highest system level since the overall system's functionality should be ensured. Ideally, the condition of all components and subsystems would have to be monitored, but this is not feasible in practice. The *critical-part selection* is an auxiliary tool for determining critical components, which are decisive for the failure behavior of a technical system. Another challenge is the interpretation of the monitored data. Nowadays, in modern machines, all systems are interconnected, sensors occur in a variety, and storage capacity is no longer a problem. Thus, a large amount of data is recorded, expecting such a technical system can also be monitored condition-based. However, translating the raw sensor data into maintenance actions

is often challenging, and experts with a good understanding of the system in normal and fault conditions are needed (Tinga and Loendersloot, 2019).

When developing a CMS, initially, the difficult decision of which physical quantities to monitor, which model type to use, where to place the sensor, and which sensor type is most suitable must be made. Mouatamir (2018) introduced a framework to find systemically answers to these questions. However, in the end, a company always faces the question: Do the economic benefits of the investment in the CMS outweigh the costs? A methodology to estimate these costs and benefits is introduced by Tinga (2013).

3

VEHICLE VIBRATIONS AND ACCELEROMETERS

In simple terms, a vibration is "the motion of a machine, or machine part, back and forth from its position of rest" (Gardiner, 1998, p. 269). Four physical quantities determine the behavior of a vibration: the initiating force, the mass, the stiffness, and the damping characteristics of the vibrating system. The initiating force is the source of the vibration. The mass, stiffness, and damping forces act in opposition. They thereby control and minimize the system's vibration (Gardiner, 1998). In summary, CM of vibration signals aims to analyze the relation between the input signal (initiating force) and the output response (vibration) over time and detect the dynamic changes in the system behavior with increasing wear (Jauregui Correa and Lozano Guzman, 2020b). This chapter introduces the fundamentals of vibration monitoring and mechanical vibration. These are considered in the context of vehicles. Furthermore, sensor technology used to measure vibrations is discussed.

3.1 FUNDAMENTALS OF MECHANICAL VIBRATIONS

In order to be able to describe mechanical vibrations, some basic terms of mechanics are defined below.

3.1.1 *Basic Terms of Mechanics*

Mechanics, as a branch of physics, deals with the motion of bodies and the laws that apply to them. There are three fundamental quantities to which all relevant quantities in mechanics can be traced back (Binnewies et al., 2016). These quantities are: The *mass* m in kilograms (kg), the *distance* s in meters (m) and the *time* t in seconds (s). A body's *velocity* results from the derivative of the distance s with respect to the time t. In a vectorized form, this is:

$$\vec{v} = \frac{\partial \vec{s}}{\partial t}, \tag{1}$$

measured in $m \cdot s^{-1}$. The change in velocity of a body is called *acceleration* and results from the second derivative:

$$\vec{a} = \frac{\partial^2 \vec{s}}{\partial^2 t}, \tag{2}$$

measured in $m \cdot s^{-2}$. A body that moves has a *momentum* $\vec{p}$, which depends on its mass and velocity.

$$\vec{p} = m \cdot \vec{v}. \tag{3}$$

The momentum can be imagined as a measure of the difficulty of bringing a moving body to rest. The unit is $kg \cdot \frac{m}{s}$. For the movement in one dimension, the vector notation simplifies to $p = m \cdot v$.

Isaac Newton established classical mechanics in his main work entitled *Philosophiae Naturalis Principia Mathematica*, published in 1687.

Theorem 1 (Newton's fist law) *A body remains in a state of rest or a constant motion in a straight line unless a force acts on it.*

According to Newton's first law, a body is inert, and a force is the cause of a body's change in motion. Newton's second law, also called the *fundamental equation of mechanics*, formulates the relationship between force and acceleration:

Theorem 2 (Newton's second law)

$$\vec{F} = m \cdot \vec{a}.$$

The force $\vec{F}$ that gives acceleration $\vec{a}$ to a body of mass m is the product of m and a. To honor Newton's merits, the unit for force is named after him, where $1\ N = 1\ \frac{kg \cdot m}{s^2}$. A force from body A on body B is accompanied by an equal but opposite force from body B on body A, which is stated in Newton's third law:

Theorem 3 (Newton's third law)

$$\vec{F}_{A \to B} = -\vec{F}_{B \to A}.$$

In physics, springs are often used as examples to illustrate the behavior of elastic bodies. For a spring in a vertical position, from which a mass m is hanging, the mass at rest is located in the *static equilibrium position*. The static equilibrium position is where the opposing forces of the spring (upward, negative sign) and those of the mass's gravitational force (downward, positive sign) are equal in magnitude. The equality of these two forces occurs here because of Newton's third law. If a spring is to be deflected by a distance x from its static equilibrium position, then a force F_x must be applied, which is proportional to the deflection Δx. The relationship between spring force and deflection is specified by *Hooke's law*:

Theorem 4 (Hooke's law)

$$F_x = -k \cdot \Delta x.$$

The spring constant k has the unit $N \cdot m^{-1}$.

Oscillation is a movement about an equilibrium point that repeats after a time interval. When a body oscillates, it is called *vibration* (Rao, 2018). Let x be the displacement of an oscillation. If there is a constant time interval T after the motion repeats, the motion is called *periodic*, i.e.,

$$x(t + T) = x(t). \tag{4}$$

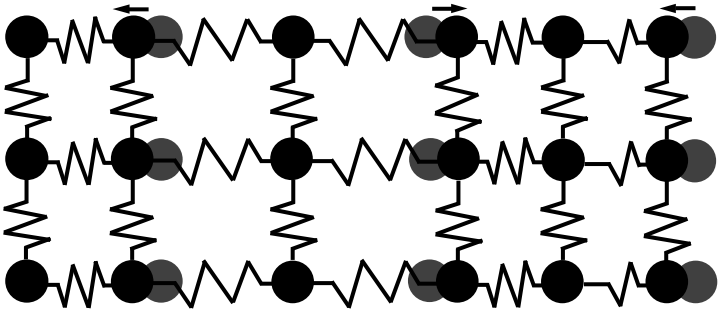

Figure 5: Model for the vibration of an elastic medium (Obst, Hardt, and Fuhrmann, 2018).

T is referred to as the *period of oscillation*. The reciprocal $F = \frac{1}{T}$ is called *frequency* and is given in the unit Hertz (Hz), where $1\ \text{Hz} = \frac{1}{\text{s}}$. A special case of a periodic oscillation is a *harmonic oscillation*. If it is harmonic, it can be represented in the following functional form:

$$x(t) = A\cos(2\pi Ft + \theta), \tag{5}$$

where A is the *Amplitude*, i.e., the largest displacement, and θ is the *phase angle* (Balke, 2020). The angular frequency Ω measured in *radians per seconds* (rad/s) is derived from F and corresponds to $\Omega = 2\pi F$.

Sound waves are vibrations that propagate in a medium. The most common one is *airborne sound*, which can be perceived through the human ear. This thesis focuses on *structure-borne sound*, i.e., the sound propagating in a solid body, such as a mechanical component in a car. Figure 5 showcases the illustration of density fluctuations that are both local and temporal in an elastic medium. The binding forces of the particles ensure that they are at a constant distance from their neighbors in the neutral position. The density of the particles is then uniformly distributed in the medium.

3.1.2 *Vibration Systems*

The following section is based on excerpts from Sections 2.4 and 3.3 of the detailed introduction to mechanical vibration by Rao (2018).

3.1.2.1 *Free Vibration*

The simplest mechanical vibration to describe is the free vibration of an undamped single-degree-of-freedom (SDOF) spring-mass system. Figure 6 shows the schematic structure of such a system. In this simplified representation, the mass as a single point represents the machine. In a real machine, the mass is distributed, but a single-point mass can be assumed for approximation. Single-degree-of-freedom systems can be used as idealized representations for various mechanical and structural systems. The *degree of freedom* indicates how many

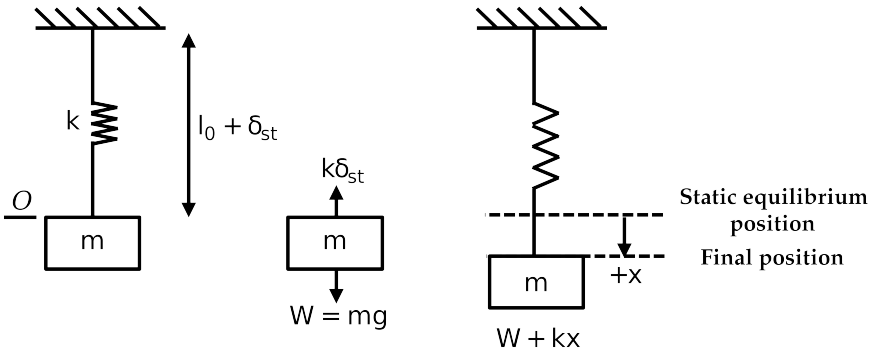

Figure 6: SDOF spring-mass system (Rao, 2018).

coordinates are needed to determine the position of the mass. *Free vibration* means the mass has been set in motion by an initial force, but no external forces are acting on it. An example of free vibration is the vertical oscillation experienced by a cyclist riding over a bump in the road.

The equation of motion of a free vibration of an undamped SDOF spring-mass system is derived as follows. It will be demonstrated that harmonic oscillations occur naturally there. When the mass m is in static equilibrium, the gravitational force W pulling it downward with $W = mg$, is balanced by the upward spring force $-k\delta_{st}$, i.e.,

$$0 = -k\delta_{st} + W \tag{6}$$

with g as acceleration due to gravity, k as spring constant, and δ_{st} as static deflection. If the mass is deflected by $+x$, the spring force equals $-k(x + \delta_{st})$. In addition, the force W acts in the opposite direction. In total, this results in

$$F_m = -k(x + \delta_{st}) + W, \tag{7}$$

as a force F_m on the mass m. After applying Newton's second law, this is equal to

$$m\ddot{x} = -k(x + \delta_{st}) + W. \tag{8}$$

The common physical dot notation is used here for derivatives. Due to the equilibrium of forces $W = k\delta_{st}$, the following differential equation is obtained

$$m\ddot{x} + kx = 0. \tag{9}$$

A solution is given by the exponential function

$$x(t) = Ce^{st} \tag{10}$$

with $C \neq 0 \in \mathbb{R}$ and $s \in \mathbb{C}$. Inserting in eq. 9 results in $s = \pm i\Omega_n$, where $\Omega_n = \sqrt{\frac{k}{m}}$. The quantity Ω_n is called *natural frequency*. The

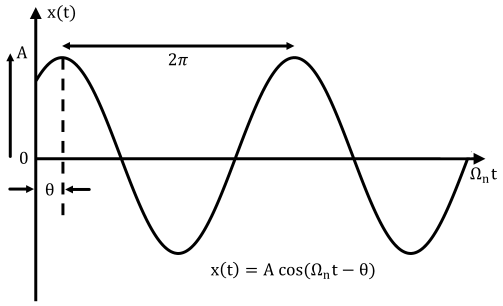

Figure 7: Graphical visualization of the equation of motion of a harmonic oscillator (Rao, 2018).

general solution of eq. 9 for $x(t)$ is obtained by substituting the two solutions for s into eq. 10 and adding these exponential functions, i.e.,

$$x(t) = C_1 e^{i\Omega_n t} + C_2 e^{-i\Omega_n t}. \tag{11}$$

Applying Euler's formula $e^{izt} = \cos(zt) + i\sin(zt)$ with $z \in \mathbb{R}$ leads

$$x(t) = (C_1 + C_2)\cos(\Omega_n t) + (C_1 - C_2)i\sin(\Omega_n t). \tag{12}$$

Let $x(0) = x_0$ and $\dot{x}(0) = \dot{x}_0$ be the initial conditions of $x(t)$ and $\dot{x}(t)$. Inserting and transforming the equations of $x(t)$ and $\dot{x}(t)$ yields $C_1 + C_2 = x_0$ and $C_1 - C_2 = \frac{\dot{x}_0}{i\Omega_n}$. Hence,

$$x(t) = x_0 \cos(\Omega_n t) + \frac{\dot{x}_0}{\Omega_n}\sin(\Omega_n t). \tag{13}$$

By transformations of eq. 13, it can be shown that the equation of motion corresponds to a harmonic oscillator (see Figure 7). For this, let $x_0 = A\cos(\theta)$ and $\frac{\dot{x}_0}{\Omega_n} = A\sin(\theta)$. Recalculation yields for the amplitude $A = \sqrt{x_0 + \left(\frac{\dot{x}_0}{\Omega_n}\right)}$ and phase angle $\theta = \tan^{-1}\left(\frac{\dot{x}_0}{x_0\Omega_n}\right)$. Overall,

$$x(t) = A\cos(\Omega_n t - \theta), \tag{14}$$

which is indeed a harmonic oscillator.

3.1.2.2 *Forced Vibration*

Having analyzed how a system oscillates after a single excitation, the case of a harmonic excitation is now considered in more detail. In the vehicle, harmonic excitations occur, for example, due to imbalances on the tire, which are transmitted to the body, or on the combustion engine's crankshaft, which converts the forces generated by combustion into rotary motion (Mitschke and Wallentowitz, 2014a). Let an undamped SDOF spring-mass system (see Figure 6) be given again but with additional acting harmonic force $F_H(t) = F_0\cos(\Omega t)$ on the

mass m. Here, Ω is the angular frequency. This changes the equation of motion eq. 9 to

$$m\ddot{x} + kx = F_H(t). \tag{15}$$

According to eq. 12 the homogeneous solution $x_h(t)$ has the form

$$x_h(t) = W_1 \cos(\Omega_n t) + W_2 \sin(\Omega_n t). \tag{16}$$

Recalculation shows that

$$x_p(t) = A \cos(\Omega t) \tag{17}$$

is a particular solution, where

$$A = \frac{F_H}{k - m\Omega^2} = \frac{\delta_{st}}{1 - \left(\frac{\Omega}{\Omega_n}\right)^2}. \tag{18}$$

The general solution of the linear inhomogeneous second order differential eq. 15 is $x_h + x_p$. Overall, this results in

$$\begin{aligned} x(t) = &\left(x_0 - \frac{\delta_{st}}{1 - \left(\frac{\Omega}{\Omega_n}\right)^2} \right) \cos(\Omega_n t) + \frac{\dot{x}_0}{\Omega_n} \sin(\Omega_n t) \\ &+ \frac{\delta_{st}}{1 - \left(\frac{\Omega}{\Omega_n}\right)^2} \cos(\Omega t), \end{aligned} \tag{19}$$

where W_1 and W_2 were determined by substituting the initial conditions x_0 and $\dot{x}_0$.

Case 1: $0 < \frac{\Omega}{\Omega_n} < 1$
In this case, a positive prefactor is obtained, and the harmonic system response x_p has the same phase as the external excitation.

Case 2: $\frac{\Omega}{\Omega_n} > 1$
In this case, a negative prefactor A is obtained, and the harmonic system response x_p is out of phase by π compared to the external excitation. Moreover, $\frac{\Omega}{\Omega_n} \to \infty$ leads to $A \to 0$, i.e., the system hardly responds to high-frequency external excitations.

Case 3: $\frac{\Omega}{\Omega_n} = 1$
This case is also called *resonance*. Transformations and application of L'Hospital rule, yield for $x(t)$ then

$$x(t) = x_0 \cos(\Omega_n t) + \frac{\dot{x}_0}{\Omega_n} \sin(\Omega_n t) + \frac{\delta_{st} \Omega_n t}{2} \sin(\Omega_n t). \tag{20}$$

Here, the amplitude increases linearly over time.

A parameter not considered further for free vibration and harmonically excited vibration due to the focus of the thesis is *damping*. It

causes the amplitudes of the oscillating system in the case of free oscillation to go towards zero with time if no further energy is supplied to the system. In the case of the excited harmonic oscillation, the damping leads to the system's vibration being dominated by x_p and the x_h term going towards zero (Mitschke and Wallentowitz, 2014a).

3.2 VEHICLE VIBRATIONS

Vehicle vibration is an everyday problem affecting drivers and passengers. Although often considered a mere inconvenience, vehicle vibration can have several negative effects, both on the occupants and the vehicle itself. Determining vehicle vibrations is crucial to increasing driver and passenger safety and improving ride comfort. In addition, knowledge gained in this area can also be used to increase vehicle life by reducing components' wear and tear.

This section first presents the causes and effects of vehicle vibrations. Then, various strategies for reducing and eliminating vehicle vibrations are explained. In the previous section, simple mechanical vibrations and their equation of motions were described. In contrast, a vehicle is a highly complex vibration system whose equations of motion and behavior can be determined analytically or by numerical simulation. This is beyond the scope of this thesis. Detailed mathematical and physical discussions of models for describing vehicles as a vibration system can be found in (Zeller, 2012b).

3.2.1 *Causes*

According to Newton's first law, a body remains in a state of rest unless an external force acts on it. For a vehicle that vibrates, knowledge of *excitations* that cause vibrations is therefore of interest. These can be divided into the categories of *internal* and *external excitations*. The most crucial external excitation influencing the vibration comfort in the vehicle is due to the road unevenness (Küçükay, 2022). Vertical motions up to 30 Hz in the vehicle are excited by them. Since the road surface is generally not uniform, the roadway excitations are also referred to as *stochastic excitation*, i.e., the roadway unevenness occurs with different amplitude and wavelength at irregular intervals (Sauer, Kramer, and Ersoy, 2017). Another external excitation is the wind acting on the vehicle. The driver, who influences the driving behavior by utilizing the steering wheel, accelerator, brake, and clutch pedals, is also an external excitation source (Küçükay, 2022).

The powertrain is one of the two primary sources of internal excitation. These include the periodic mass and gas forces in internal combustion engines and the friction and contact processes in the transmission, roller bearings, and clutches. In an internal combustion engine, forces and torques are induced by the movements of the pistons and

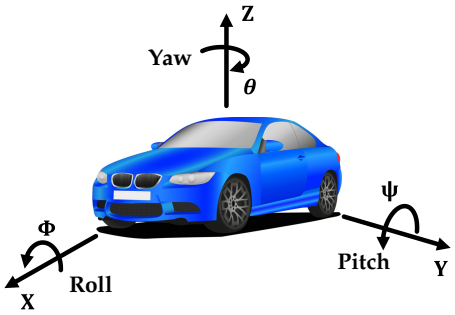

Figure 8: The vehicle coordinate system.

the combustion processes. Via the engine suspension, which connects the engine to the vehicle body, the vehicle body vibrates, which can cause disturbing noises for the driver (Mitschke and Wallentowitz, 2014b).

The second primary source is the internal excitation of chassis components. These include imbalances on wheels, tires, or brakes. Under load, these imbalances lead to fluctuations in the radial force when the wheel rolls. The radial force is the force acting in the running direction of the wheel. At higher speeds, this causes the vehicle to vibrate disruptively (Zeller, 2012b).

In addition to how excitation is induced, it is also possible to distinguish in which direction vibration phenomena occur in the vehicle. Vibrations in the direction of the three translational degrees of freedom of the longitudinal, lateral, and vertical dynamics (x, y, and z direction) specified in the standardized vehicle coordinate system can arise. Likewise, they can occur in the direction of the rotational directions of motion ψ, ϕ, θ, referred to as *pitch*, *roll*, and *yaw*. Figure 8 shows the vehicle coordinate system. Vertical dynamic vibrations occur due to uneven road surfaces or imbalance and out-of-roundness of the wheels.

One goal in vehicle development is to avoid unpleasant pitching movements. When driving over an uneven surface, the vehicle body should ideally have a parallel movement in the z-direction. This is achieved by tuning the front and rear axles, which reduces pitching movements. The powertrain dynamics mainly cause longitudinal vibrations. Rolling motions are, for instance, the source of either the driver's steering movements or different excitations of the road acting on the left and right sides of the vehicle (Zeller, 2012b).

3.2.2 *Effects*

The transmission of excitations within a vehicle is a complex process that involves various components. These excitations originate from the engine and the wheel. They are transmitted to the bodywork, allowing the passenger to perceive them through the seat, the floor,

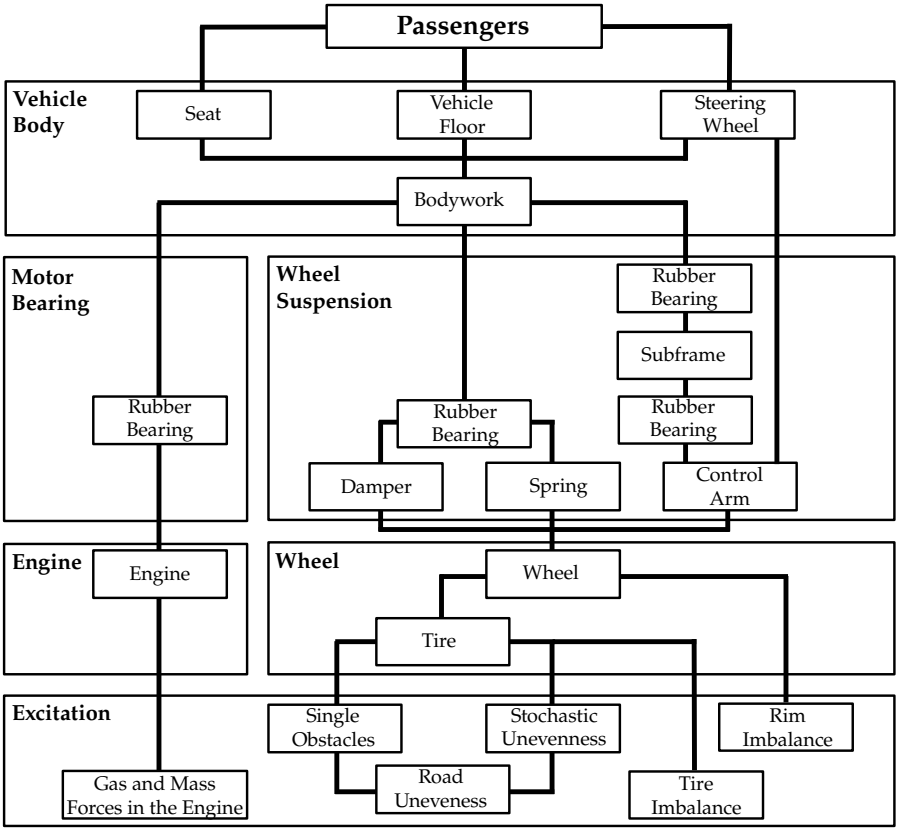

Figure 9: Transmission paths within the vehicle from the excitation to the passenger (Wallentowitz, 2005).

and the steering wheel. Figure 9 outlines the primary paths through which a single excitation travels to the passenger, who can perceive it both tactically and acoustically. These excitations give rise to a range of vibration phenomena summarized in Table 1. The table provides information on the frequency ranges associated with each vibration phenomenon and identifies the corresponding excitation responsible for it (Wallentowitz, 2005).

Vibrations tangible to humans are typically limited to frequencies up to 30 Hz. Nevertheless, it should be noted that this particular threshold is highly dependent on the individual. The human auditory range encompasses frequencies between 15 Hz to approximately 20 kHz. The emergence of noise arises from a vibrating object causing the surrounding air molecules to vibrate and can be perceived by the human ear. As people age, their ability to hear higher-frequency sounds decreases. An 80-year-old person normally cannot hear frequencies above roughly 5 kHz. The transition range between tangible and audible vibrations, referred to as *roughness*, is from 20 to 100 Hz (Küçükay, 2022). Due to the occurrence of primarily frequency-mixed signals in vehicles, oscillations can be simultaneously perceptible to touch and hearing. The overall mechanical and acoustic vibrations experienced by passengers are what constitute *driving comfort*. In the

field of vehicle-specific vibration technology, this is commonly referred to as *NVH*, which stands for *Noise, Vibration, and Harshness* (Pletschen, 2010).

The level of driving comfort experienced by a driver depends on several factors that can be considered in vehicle development. These include driving characteristics (smooth or sporty), suspension tuning (soft or hard), and the presence of features that make driving easier (e.g., driver assistance systems or power steering. Interior noise also contributes to driving comfort, with customers of higher-end vehicles expecting lower noise levels. Driving comfort is relevant not only when the vehicle is moving but also when the vehicle is stationary with the engine idling. Proper tuning of spring stiffness and damper constants can greatly enhance driving comfort. Active suspension systems, which allow the spring and damper parameters to be adapted to different vehicle maneuvers, can also significantly improve driving comfort (Sauer, Kramer, and Ersoy, 2017).

In addition to passengers and their driving comfort, vibrations also affect the components in the vehicle. This impact can result in component failures, material fatigue, loosening of components, and increased friction between elements. Components can only function for a shorter period when exposed to strong vibrations, i.e., the wear reserve decreases more quickly. Therefore, there is a positive correlation between the vibration amplitude and stress levels. The loosening of components in the vehicle can be caused by incorrect assembly. Over time, loosening problems can increase, leading to misalignment or imbalance and ultimately causing mechanical systems to fail. Additionally, vibrations can increase friction between individual vehicle components, leading to wear and tear. In the worst-case scenario, this can result in catastrophic failures as the vibrations cause components to collide, resulting in damage or even destruction. Such collisions can occur between rotating components and their housings, causing damage to both (Jauregui Correa and Lozano Guzman, 2020a).

3.2.3 *Mitigations*

The extent to which vibrations are permitted depends on the market positioning of a vehicle. Consumers are more likely to expect and accept these in a sporty, agile vehicle than in a comfort-oriented SUV (Sauer, Kramer, and Ersoy, 2017). However, if vibrations exceed an acceptable level, countermeasures must be taken in vehicle development. They can be divided into passive, semi-active, and active measures based on energy consumption.

Passive measures aim to influence the transmission behavior of vibrations on the transfer paths (see Figure 9) by adjusting component parameters. They do not require any additional energy. *Semi-active measures* also influence the transmission behavior of vibrations

Vibration Phenomenon			Excitation		
	f(Hz) from – to		Road	Imbalance	Powertrain
Vehicle Body Vibration	0.5	5	++		
Riding, Freeway Hop	2	5	++		
Longitudinal Jerking	4	10			++
Jerking, Shaking	7	15	++	+	
Bouncing	7	25	++		
Backlash	8	20			++
Axle Vibration	10	15	++	+	
Steering Unsteadiness	10	20		+	
Brake Rubbing	15	25		+	
Engine Trembling, Shaking	15	40			++
Idling Shaking	20	30			++
Exhaust System	20	1000			++
Roar	30	70	++	+	++
Axle Harshness	30	80	++		
Rolling	30	300	++		
Engine Noise	200	5000			++
Gearbox Noise	400	500			++

Table 1: Vibration phenomena in the vehicle (Wallentowitz, 2005).

on individual transfer paths, but individual adjustments are made depending on the driving condition. Therefore, actively controllable or adjustable vehicle components are installed that can change their physical properties. They require an additional energy supply for operation. In contrast to the first two measures, *active measures* do not influence transfer paths but use auxiliary systems to generate compensation forces to counteract vibrations. However, the systems required for this need a considerable energy supply, as they are typically in continuous operation.

Passive measures in the field of vibration reduction involve altering the resonant frequencies of components. This is achieved through modifications to stiffnesses or masses that impact the resonant frequency. *Elastic mounting* is the most common passive measure and can be accomplished by either decoupling the excitation source from the environment or isolating the excited component from the excitation. For example, the engine mount connects the engine to the body. It isolates the component bodywork from the excitation source by reducing vibrations to the bodywork through the elastic isolating element. The bearing element is designed to transmit the excitation frequency's amplitude only at a weakened level. Elastomers such as rubber have good damping properties and are also used for bearing elements. Damping reduces kinetic energy from the vibrating system and converts it into thermal energy, thus reducing the amplitude of the vibration. Innovations in the field of engine mounts enable semi-

active measures, making it switchable depending on the operating condition (Zeller, 2012b).

In the chassis, semi-active dampers are used to adapt damping to different axle loads, driving conditions, and routes. Fully active damping systems are currently not installed in road vehicles due to their high energy consumption and price (Sauer, Kramer, and Ersoy, 2017). However, active measures are already being utilized in some cases in vehicle interiors to reduce noise. The *Active noise cancellation* (ANC) technology, often integrated into modern headphones, can also counteract the wind and rolling noises in the vehicle interior. The basis of this technique lies in the principle of sound *superposition*, wherein the interference of sound waves can result in their mutual cancellation. First, ANC uses a microphone to detect a noise field. Then a sound compensation field is generated via a loudspeaker so that the interference source is superimposed and the sound pressure for the occupant is minimized. The success of this methodology depends heavily on the accuracy of the sound compensation field (Zeller, 2012b).

3.3 ACCELEROMETERS

To observe and analyze the vibrations of components in a vehicle, corresponding sensor technology is necessary. For this purpose, acceleration sensors are employed, commonly referred to as *accelerometers*. These sensors generate a signal proportional to the acceleration experienced by the sensor in the direction of measurement. The acceleration experienced is related to the equation of motion of the vibration as the second derivative.

Accelerometers are versatile because they detect a wide range of frequencies, particularly very high frequencies in the kilohertz range (Ahmed and Nandi, 2020). They are also lightweight, usually weighing only a few grams. In vehicles, they are used in the control system for triggering airbags and seat belt pre-tensioners, in the *anti-lock braking system* (ABS), or in the chassis control system for detecting vehicle body acceleration. The acceleration is usually specified using the acceleration due to gravity, where 1 g is approximately $9.81 \frac{m}{s^2}$. The measurement range of accelerometers can be several hundred g. The measuring principle for accelerometers is based on determining the inertial force acting on a small part called the *proof mass* located in the sensor. The second Newton's law ($F = ma$) can be employed to infer the acceleration (Reif, 2012). The proof mass is fixed in the sensor via an elastically deformable mount, such as a *leaf spring*. The deflection of the proof mass is then used to derive acceleration given linear spring forces.

The most prominent sensor variants generate a change in resistance, capacitance, or electrical charge via the deflections of the mass.

They are *electrical transducers*, i.e., they transfer the physical quantity of the acceleration into an electrical signal. The acceleration signal can then be inferred from the value of the electrical signal, e.g., the current. A distinction is made between *AC* and *DC accelerometers*. The first group can only measure dynamic accelerations, whereas the second can also measure static accelerations, such as the acceleration due to gravity. Capacitive, resistive, and piezoresistive are the most common DC accelerometers. Details on the transduction principles and the operation of the sensor types can be found in (Watzka, Scheler, and Wilhelm, 2012). Piezoelectric accelerometers are the most prevalent AC accelerometers. The *piezoelectric effect* describes the appearance of an electrical charge on a solid body when it is subjected to mechanical stress. The *mechanical stress* τ describes the internal stress on a body when it is subjected to an external load and is expressed in *Pascal* ($1\ \mathrm{Pa} = 1\ \frac{\mathrm{N}}{\mathrm{m}^2}$). Piezoelectric materials are, for instance, quartz crystals, widely used in accelerometers. The deflected proof mass in the accelerometer causes stress in the crystal. The piezoelectric effect produces a charge whose amplitude is measurable.

Transduction Principle	**Measurement Range in *g***	**Frequency Range in *Hz***	**Operating Temperature Range in *°C***
Capactive	-500 – 500	0 – 1.000	-40 - 80
Resistive	-1.000 – 1.000	0 – 5.000	-20 - 71
Piezoresistive	-60.000 – 60.000	0 – 5.000	-20 - 85
Piezoelectric	-120.000 – 120.000	0.2 – 20.000	-54 - 250

Table 2: Measurement and frequency ranges of commercial accelerometers based on the study by (Elies and Ebenhöch, 2015).

A market evaluation of more than 100 commercial acceleration sensors with prices between 1 and 3000 Euro, used in aerospace, automotive, railway, and consumer electronics, was conducted by Elies and Ebenhöch (2015). Table 2 shows the differences between the transduction principles and their measurement and frequency ranges. The capacitive acceleration sensors have the lowest measurement and acceleration range. However, they are also inexpensive to manufacture due to modern semiconductor technology, and they can also measure static accelerations (Weber, 2012). Resistive and piezoresistive were in the middle field in the measurement and frequency range. Nevertheless, they can also detect very low frequencies down to 0 Hz, which is impossible with the piezoelectric ones. These had the highest measurement and frequency range, but they can only measure dynamic accelerations. Furthermore, they have the broadest range of operating temperatures, which allows their use in hot operating locations.

The study showed no significant correlation between the measurement range and energy consumption. The maximum value among all tested sensors was 1 *Watt*. Most of the sensors have a volume of less

than 10 cm^3. Almost all sensors weigh between 0.1 and 100 g. Overall, all sensors require little installation space and are lightweight.

The sensor type selection considerably influences the measurement results, which is why the decision must be made carefully, considering the respective application's financial and technical requirements. Piezoelectric sensors were used for test drives as part of this thesis since dynamic driving-dependent vibrations in the chassis needed to be recorded. Therefore, no DC accelerometer was required, and the piezoelectric sensors with a wide frequency range were the favored type. A guide from TE Connectivity (2017), a leading sensor technology manufacturer, provides use case dependent detailed instruction for selecting the optimal accelerometer type.

3.4 VIBRATION-BASED MONITORING

Vibrations frequently occur in technical systems, originating from various internal sources such as motors and turbines or external sources such as weather conditions like rain and wind. The key is that the structure is set in motion. The CM technique, also known as *vibration* or *vibration-based monitoring*, is utilized to analyze these signals (Tinga and Loendersloot, 2019). These techniques are well-suited for mechanical components in machinery and operating equipment, making them an integral part of a CM program in the industrial environment (Mobley, 1998).

Feature extraction is a crucial aspect of vibration monitoring to identify system response characteristics, allowing for inferring the structure's state. Vibration monitoring often focuses on the measured vibration and statistical parameters, such as vibration level, kurtosis, or skewness. Conversely, vibration-based monitoring employs advanced signal processing methods to identify specific failure causes. Raw vibration signals are no longer considered, and instead, signals based on them, like derivatives or Fourier transforms, are analyzed (Tinga and Loendersloot, 2019). Refer to Chapter 4 for more information on these transformations and feature extractions of vibration signals.

The advantages of vibration-based monitoring include the following (Ahmed and Nandi, 2020):

(i) Accelerometers enable a non-intrusive form of diagnostics. No component of a machine needs to be destroyed for this purpose.

(ii) Vibration analysis is effective because nearly 80% of all rotating machinery problems are due to imbalance or misalignment.

(iii) Accelerometers are easily accessible and affordable. They can even be found in smartphones.

(iv) The hardware to convert the analog signals into digital ones and store them is affordable due to technological progress.

(v) They can be evaluated directly at the machine but also online.

(vi) The techniques for diagnosing failures of rotating components have been well-established and have been proven for decades. Furthermore, the failures are explainable on a physical level. These include the detection of bearing failures (Dyer and Stewart, 1978), cracks (Mayes and Davies, 1984), and shaft imbalance (Bishop and Parkinson, 1965).

3.5 OUTLOOK

The current chapter has introduced the fundamental aspects of mechanical vibrations, outlining vibrations that occur in vehicles, their underlying causes, and some methods for their prevention. Additionally, the use of acceleration sensors as a measurement technology for recording vibrations and vibration-based monitoring was examined.

In the discussion of mechanical basics, it was determined that the free vibration of an SDOF system results in a harmonic vibration. However, in the case of vehicles, vibrations involve multiple degrees of freedom, are damped, and are influenced by various excitation sources. The next chapter will demonstrate that even such complex vibrations are composed of harmonic oscillations and can be decomposed into them via mathematical transformations.

It is now apparent that a vehicle is a complex vibration system with various influencing factors and transmission paths. Therefore, optimizing acoustic behavior based on customer needs is essential when developing and integrating new vehicle components. The *V-model*, which is widely used in the automotive industry for the development process, assumes that every requirement for functions that can be broken down into a system and component level is also matched by a test and verification. This ensures that acoustic requirements are also met in the production vehicle. Further details of the V-model can be found in (Gonter et al., 2021). While computer simulations of acoustic vehicle properties were not discussed in this chapter, it is worth noting that such simulations can be carried out using *finite element methods* (FEM) (Jung and Langer, 2001). Modern FEM models, which include several million elements that describe the powertrain, axles, interior, and body structure, are available today. As a result, the development process is supported by vehicle simulation, which makes predictions about acoustic vehicle behavior (Zeller, 2012a).

The trend toward electric mobility is also significantly impacting vehicle acoustics. Generally, electric cars are quieter than internal combustion vehicles. However, the electric drive and power electronics give rise to new airborne and structure-borne sound sources that

must be considered in the acoustic design of vehicle development (Seeck et al., 2021). For instance, bearings installed to dampen excitations from the powertrain must be designed for other frequency ranges (Pletschen, 2010).

The cause, effect, location, and measurement of vibrations in the vehicle were introduced, laying the groundwork for data acquisition, which is the first step of a vibration-based CMS (see Figure 4). The recorded data is validated in the subsequent data processing step, and features are extracted. Therefore, the next chapter will explore the methodology for analyzing and extracting features from vibration data.

4

VIBRATION SIGNAL ANALYSIS

The analysis of vibration signals is an essential tool for characterizing and diagnosing mechanical systems and structures. This analysis provides insights into mechanical components' behavior, condition, and remaining functionality (Mobley, 1998). This chapter gives a detailed overview of techniques and methods used in the field of vibration analysis. These originated in the engineering subfield of *signal processing* (Palani, 2022b), so a brief introduction to signals and their types is first presented to classify those of accelerometers. After that, properties describing vibration data in the time domain are discussed. This is followed by considering signals in the frequency and time-frequency domains. Finally, graph domain analysis is introduced, representing vibration signals in graph form and enabling analysis techniques of *complex networks* (Strogatz, 2001).

4.1 SIGNALS

According to Scheithauer (1998), we have become an *information society* in which information or messages are generated, sent, received, and traded. Information needs a carrier, and this is called a *signal*. For human speech, this is air pressure, which is changed through the vocal cords, causing sound waves to propagate. For radio and television, the receiver processes electromagnetic waves to decode the message (Scheithauer, 1998). Information is knowledge content, and the representation of this knowledge as a physical quantity is a signal. For example, the body temperature of a human being is a signal that provides information about the state of health (Meyer and Mildenberger, 2002). In the same way, the vibration data in the vehicle considered in this thesis are signals that give information about the wear condition of a component. Oppenheim, Willsky, and Nawab (1996, p. xxvii) define signals as *"functions of one or more independent variable"* containing *"information about the behavior or nature of some phenomenon"*.

In most cases, signals are functions depending on time, but they can also depend on other quantities (Palani, 2022a). For instance, an image can be interpreted as a 2D signal, where the pixel values depend on the position. Due to the focus of this thesis on vibration data, time-dependent signals are classified in more detail below.

4.1.1 *Continuous and Discrete Signals*

Let $x(t)$ be a signal with $x : D_t \to \mathbb{R}, t \mapsto x(t)$. This is called a *continuous-time* or *analog signal* if t is a continuous variable (Hsu, 2011). A variable t is called *continuous* if and only if D_t is uncountable, for example, when $D_t \subset \mathbb{R}$ is an interval of real numbers. On the other hand, a *discrete* variable t takes only finitely many or countably many values, and the respective signal is called *discrete-time* signal (Fahrmeir et al., 2004). If the image of the signal x is continuous, the signal is called *value-continuous* and otherwise *value-discrete* (Scheithauer, 1998). A discrete-time signal $x[n]$, $n \in \mathbb{Z}$, can arise because the signal is inherently discrete like the daily closing price of a stock or because it arises from *sampling* at the points $t_0, \ldots, t_n$ of a continuous-time signal $x(t)$, i.e.,

$$x[n] = x(t_n). \tag{21}$$

For vibration data measured with an accelerometer, the sensor ensures that the sampling is *uniform*, i.e.,

$$x[n] = x(nT), \tag{22}$$

where $T \in \mathbb{R}$ is the *sampling interval* and $F_s = \frac{1}{T}$ the *sampling rate* (samples per second). In other fields, discrete-time signals are often called *time series*. When processing the vibration data, the signal is converted by an analog/digital converter into a digital number, e.g., with 16 or 32 bits. Such a discrete-time and value-discrete signal is called *digital signal*. The representation as a digital number, named *quantization*, has hardly any influence in practice nowadays because of the high number of digits and can often be neglected (Scheithauer, 1998).

4.1.2 *Sinusoids and Complex Exponentials*

The following section is based on the definitions and discussions in (Proakis and Manolakis, 2006).

A continuous-time signal or a discrete-time signal x is called *periodic* if and only if

$$x(t) = x(t + T)\ \forall t \in \mathbb{R} \tag{23}$$

$$x[n] = x[n + N]\ \forall n \in \mathbb{Z}, \tag{24}$$

respectively. Here, $0 < T \in \mathbb{R}$ and $0 < N \in \mathbb{N}$ are the smallest values for which the corresponding equality holds. These values are called *fundamental period* of x. Their reciprocals are called *fundamental frequency*. The condition for the periodicity is similar to the motion equation in Section 3.1 for mechanical vibrations. A *sinusoid*, which also

appears in harmonic oscillations, is a special periodic signal, which for continuous-time signals $x(t)$, $t \in \mathbb{R}$, has the functional form

$$x(t) = A\cos(\Omega t + \theta) \tag{25}$$
$$= A\cos(2\pi F t + \theta), \tag{26}$$

where A is the amplitude, Ω the angular frequency given in *radians per second* (rad/s), and θ as phase in radians. Alternatively, the frequency F in *cycles per second* (Hz) with $\Omega = 2\pi F$ is used to represent x.

Analogously, the discrete-time sinusoidal $x[n]$, $n \in \mathbb{Z}$, is represented as

$$x[n] = A\cos(\omega n + \theta) \tag{27}$$
$$= A\cos(2\pi f n + \theta), \tag{28}$$

where ω is now the angular frequency in *radians per sample*. Alternatively, x can be expressed using the frequency f with unit *cycles per sample* where $\omega = 2\pi f$.

Since this thesis focuses on vibration data as discrete-time signals, two essential differences between discrete-time and continuous-time sinusoids should be pointed out. Discrete-time sinusoids are only periodic if the frequency f is a rational number. Furthermore, all discrete-time sinusoids x_k whose frequencies differ by multiples of 2π are identical, i.e.,

$$x_k[n] = A\cos(\omega_k n + \theta)\ \forall k \in \mathbb{N} \tag{29}$$
$$\omega_k = \omega_0 + 2\pi k,\ -\pi \leqslant \omega_0 \leqslant \pi, \tag{30}$$

which results from the 2π periodicity of cosine. Any 2π interval $\omega_1 \leqslant \omega \leqslant \omega_1 + 2\pi$ thus contains *all* distinct discrete-time sinusoids. Therefore, in the following, the interval for ω is fixed as $-\pi \leqslant \omega \leqslant \pi$ or $0 \leqslant \omega \leqslant 2\pi$, the most common ones in the literature (Proakis and Manolakis, 2006). If the sinusoid has a frequency $|\omega| > \pi$ or $|f| > \frac{1}{2}$, there exists a sinusoid identical to it with $|\omega| < \pi$. Hence, the sinusoid with $|\omega|$ is called *alias*. In contrast, distinct sinusoids occur for continuous-time sinusoids for all Ω, F with $-\infty < \Omega < \infty$ and $-\infty < F < \infty$, respectively. The sinusoids are closely related to complex exponentials $x(t)$ given by

$$x(t) = Ae^{i(\Omega t+\theta)} = A(\cos(\Omega t + \theta) + i\sin(\Omega t + \theta)), \tag{31}$$

where the second equality holds due to *Euler's formula* (Moskowitz, 2002). It is easy to conclude from this that the determined properties of discrete-time and continuous-time sinusoids also apply to discrete-time and continuous-time complex exponentials. A real-valued sinusoid can be represented as a complex exponential by

$$A\cos(\Omega t + \theta) = \frac{A}{2}e^{i(\Omega t+\theta)} + \frac{A}{2}e^{-i(\Omega t+\theta)}, \tag{32}$$

where it consists of two complex exponentials, also called *phasors*, rotating in opposite directions with $\pm\Omega$ radians.

4.1.3 *Further Classes of Signals*

If the course of a signal is known in advance, it is called a *deterministic signal*. If, on the other hand, the course is unknown and random, as is the case with vibration data in a vehicle, then it is a *stochastic signal* (Hsu, 2011). For instance, the road surface is a source of excitation that causes stochastic vibrations in the vehicle (Ersoy et al., 2017).

In addition, signals can also be distinguished by their energy and power. The *energy* $W(t_1, t_2)$ of a continuous-time signal is equal to

$$W(t_1, t_2) = \int_{t_1}^{t_2} |x(t)|^2 \, dt. \tag{33}$$

This definition of energy is proportional to the physical quantity of energy. For example, in a circuit with voltage $v(t)$ and resistor with resistance R, the energy dissipated at the resistor is $\frac{1}{R}\int_{t_1}^{t_2} v^2(t)dt$.

The signal's *total energy* is then

$$W = \int_{-\infty}^{\infty} |x(t)|^2 \, dt. \tag{34}$$

The signal $x(t)$ is called *energy signal* if it has a finite total energy. For discrete-time signals the total energy is given by the sum

$$W = \sum_{k=-\infty}^{\infty} |x[k]|^2 \, T. \tag{35}$$

According to the physical definition of power, the *average power* of $x(t)$ for the continuous and discrete case is as follows

$$P = \lim_{L\to\infty} \frac{1}{L} \int_{-\frac{L}{2}}^{\frac{L}{2}} |x(t)|^2 \, dt, \tag{36}$$

$$P = \lim_{N\to\infty} \frac{1}{2N+1} \sum_{k=-N}^{N} |x(kT)|^2 . \tag{37}$$

If the average power is finite, the signal $x(t)$ is a *power signal*. The definition of an energy signal indicates that its average power is 0. Hence, energy signals are always power signals. (Scheithauer, 1998). Energy and power signals play an essential role in the context of the *Fourier transform* (Oppenheim, Willsky, and Nawab, 1996). Since the vibration signals recorded in the vehicle are simultaneously limited in time and amplitude, they are energy signals.

4.2 TIME DOMAIN ANALYSIS

The vibration data recorded by the accelerometer are available in their raw form as discrete-time signals, respectively, time series. As discussed in Chapter 3, in complex vibration systems such as a vehicle,

several excitation sources are often responsible for the vibrations of a component. This makes it difficult to directly infer the state of a component from the raw signal. The standard approach is to extract features from the raw signal that summarize the characteristics of the signal and can be used as indicators for the CMS (Ahmed and Nandi, 2020).

4.2.1 *Statistical Features*

Statistical features do not necessitate significant computing resources and are, as a result, relatively simple to integrate into a CMS. These features can be evaluated against predefined thresholds to classify the condition of a machine (Sánchez et al., 2018). Additionally, the statistical features can be employed to train ML models that can predict the state of a machine. The statistical features discussed here are the most commonly utilized ones for condition monitoring of machines, according to a comprehensive review of the field by (Ahmed and Nandi, 2020). The features are presented only for discrete-time signals x with

$$x : \{0, \dots, N-1\} \to \mathbb{R}, n \mapsto x[n], \tag{38}$$

since negative indices are irrelevant for measured vibration signals. For the continuous-time case, versions exist where integrals are used instead of sums.

(i) The *mean amplitude* is defined as

$$\bar{x} = \frac{1}{N} \sum_{n=0}^{N-1} x[n].$$

(ii) The *variance* σ_x^2 is given as

$$\sigma_x^2 = \frac{1}{N-1} \sum_{n=0}^{N-1} (x[n] - \bar{x})^2,$$

and the *standard deviation* is equal to σ_x.

(iii) The *root mean square* value x_{RMS} is expressed as

$$x_{RMS} = \sqrt{\frac{1}{N} \sum_{n=0}^{N-1} |x[n]|^2}.$$

(iv) Let x_{max} be the maximum and x_{min} be the minimum value of $x[n]$ for $0 \leqslant i \leqslant N-1$. The *peak-to-peak amplitude* is then the difference between the maximum and minimum amplitude, i.e., $x_{PTP} = x_{max} - x_{min}$.

(v) The *crest factor* x_{CF} measures the ratio of the peak values in the signal to a type of average signal value. It is calculated as

$$x_{CF} = \frac{1}{2}\frac{x_{PTP}}{x_{RMS}}.$$

(vi) The *shape factor* x_{SF} is the ratio of the root mean square value to the average absolute value of the signal, i.e.,

$$x_{SF} = \frac{x_{RMS}}{\frac{1}{N}\sum_{n=0}^{N-1}|x[n]|}.$$

(vii) The *clearance factor* x_{CLF} is a well-established statistical parameter for detecting damage to bearings based on vibration signals (Shrivastava and Wadhwani, 2013). Inner and outer race faults of bearings, for example, show lower clearance factors than bearings in normal conditions. It is defined as

$$x_{CLF} = \frac{x_{max}}{\frac{1}{N}\left(\sum_{n=0}^{N-1}\sqrt{|x[n]|}\right)^2}.$$

(viii) The third normalized central moment is called *skewness*. It is a measure of the asymmetry of the *probability density function* $p(x)$ of the vibration signal. If the vibration data is considered as a random variable, $\int_a^b p(x)dx$ gives the probability that the amplitude lies between a and b (Tappe, 2013). The skewness is expressed as

$$x_{SK} = \frac{\sum_{n=0}^{N-1}(x[n]-\bar{x})^3}{N\sigma_x^3}.$$

(ix) The *kurtosis* is the fourth centralized moment. It is a shape parameter that measures the peakedness of a probability density function.

$$x_{KU} = \frac{\sum_{n=0}^{N-1}(x[n]-\bar{x})^4}{N\sigma_x^4}.$$

4.2.2 *Correlations*

In addition to statistical features extracted from a single signal, the measurement of the similarity between multiple signals is of interest. One similarity measure is the *(unbiased) cross-correlation*. This computes the similarity of two signals with different time lags. It is used to determine whether one signal is a time-shifted version of the other or to identify similar patterns in two signals (Tranquillo, 2014). For discrete-time signals x and y, the unbiased cross-correlation is defined as

$$C_{xy}(k) = \frac{1}{N-L}\sum_{n=0}^{N-L-1} x[n]y[n+k],\ 1 \leqslant k \leqslant L, \tag{39}$$

where $L << N$, so there is a sufficient number of summands. The cross-correlation is called *unbiased* because it is divided by $N - L$ instead of N. What is calculated here is actually the "sample cross-correlation," an estimator for the cross-correlation corresponding to the expected value $\mathbb{E}[x[n]y[n+k]]$ under the assumption that x and y are realizations of *ergodic stochastic processes* (Smith, 2007). For more details on stochastic processes and their role in signal processing, refer to (Park, 2018). By the maximum determination of C_{xy}, it can be recognized with which delay k of the signals to each other the largest correlation can be reached. The case $x[n] = y[n]$ in eq. 39 is called *auto-correlation*. The cross-correlation value depends on the signals' amplitude. By using the *covariance*,

$$CV_{xy} = \frac{1}{N} \sum_{n=0}^{N-1} (x[n] - \bar{x})(y[n] - \bar{y}) \tag{40}$$

the *correlation coefficient* can be defined. The correlation coefficient is equal to

$$\rho_{xy} = \frac{CV_{xy}}{\sigma_x \sigma_y}, \tag{41}$$

which lies between -1 and 1 and measures the (linear) correlation between the signals x and y on a uniform scale (Meyer and Mildenberger, 2002).

4.3 FREQUENCY DOMAIN ANALYSIS

As derived in Section 3.1.2, harmonic oscillations occur naturally in free, damped, and forced vibrations of mechanical components. However, the numerous excitation sources and transmission paths in the vehicle (see Section 3.2.1 and 3.2.2) lead to the superposition of different vibrations so that an accelerometer mounted on a component in the vehicle generally measures a complex vibration signal where the harmonic components are no longer immediately recognizable. The following introduces methods from frequency analysis to decompose a signal into its harmonic components

This section relates, for the most part, to the discussion in (Oppenheim, Willsky, and Nawab, 1996), which gives a detailed introduction to signal processing. If not stated otherwise, the information is taken from there, especially Sections 3.6, 4.1, 5.1, and 7.1.

4.3.1 *Fourier Series*

First, let $x[n]$ be a discrete-time periodic signal, i.e.,

$$x[n] = x[n+N], \ \forall n \in \mathbb{Z} \tag{42}$$

with fundamental period N and fundamental frequency $\omega_0 = \frac{2\pi}{N}$. This type of signal is generated, for example, by vibrations of rotating machines at a constant speed (Randall, 2021). The goal is to represent the signal $x[n]$ as a sum of harmonically related complex exponentials $\Phi_k[n]$ expressed compactly as

$$x[n] = \sum_k a_k \Phi_k[n], \tag{43}$$

where the parameters $a_k \in \mathbb{C}$ are called *spectral coefficients* and $\Phi_k[n]$ is the k^{th} *harmonic* (Palani, 2022b) equal

$$\Phi_k[n] = e^{ik\omega_0 n} = \cos(k\omega_0 n) + i\sin(k\omega_0 n),\ k \in \mathbb{N}. \tag{44}$$

Notice that all Φ_k have multiples of $\frac{2\pi}{N}$ as the fundamental frequency and that

$$\Phi_k[n] = \Phi_{k+rN}[n] \text{ for } r \in \mathbb{N}. \tag{45}$$

Hence, there are only N many different complex exponentials of the type given in eq 44. Due to this linear dependency, it is sufficient to sum only over $0, \dots, N-1$ to represent $x[n]$, i.e.,

$$x[n] = \sum_{k=0}^{N-1} a_k \Phi_k[n]. \tag{46}$$

This results in a system of N equations with N unknowns a_k since the equality must hold for $n = 0, \dots, N-1$. For the proof of the linear independence of the set of these equations, refer to the literature. It follows that there exists a unique solution. This solution is given by the *discrete-time Fourier series* (DTFS), which is defined below.

Definition 5 *The discrete-time Fourier series (DTFS),* a_k, $0 \leqslant k \leqslant N-1$, *of a periodic discrete-time signal* x *with fundamental period* N *is*

$$a_k = \frac{1}{N} \sum_{n=0}^{N-1} x[n] e^{-ik\omega_0 n} \textit{ (analysis equation)},$$

where

$$x[n] = \sum_{k=0}^{N-1} a_k e^{ik\omega_0 n} \textit{ (synthesis equation)}.$$

From eq. 45 it can be concluded that $a_k = a_{k+N}$, i.e., the spectral coefficients repeat after N successive values. This periodicity is the reason why it is sufficient in the definition to consider only the a_k of $k = 0, \dots, N-1$. However, any successive sequence of length N can be used as values for k.

For the complex conjugate signal $x^*[n]$ the relation $x^*[n] \overset{\text{DTFS}}{\longleftrightarrow} a^*_{-k}$ holds. It follows that for real-valued signals $a_k = a^*_{-k}$. The spectral

coefficients decompose $x[n]$ into complex exponentials. However, for real-valued signals like vibration signals, by exploiting the symmetry properties, it can be shown that the synthesis equation can also be represented through sinusoids. The imaginary parts of the complex exponentials are canceled out, resulting in

$$x[n] = a_0 + 2\sum_{k=1}^{L} |a_k| \cos\left(\frac{2\pi}{N} kn + \theta_k\right), \tag{47}$$

where $L = \frac{N}{2}$ for the case if N is even and $\frac{N-1}{2}$ if it is odd (Proakis and Manolakis, 2006). The DTFS is a linear operation. By applying the synthesis equation, the *frequency-domain* representation of x is obtained, and by applying the analysis equation, the signal is converted back to the *time domain*. It is important to note that the representation of a periodic discrete-time signal using discrete-time Fourier series is a finite sequence, unlike continuous-time signals, which are represented by an infinite sequence.

4.3.2 *Discrete-Time Fourier Transform*

The next goal is decomposing an aperiodic discrete-time signal $x[n]$ into complex exponentials. The idea is to construct a periodic discrete-time signal $\tilde{x}$ that matches x over one period and then let the length of that period approach infinity so that both signals match for any finite value. First, let $x[n]$, $n \in \mathbb{Z}$, have a finite length with

$$x[n] = 0 \text{ for } n \notin \{0, \dots, N_1 - 1\},\ N_1 \in \mathbb{N}. \tag{48}$$

A periodic discrete-time signal $\tilde{x}$ with

$$\tilde{x}[n] = x[n] \text{ for } n \in \{0, \dots, N_1 - 1\} \tag{49}$$

can be constructed from $x[n]$ by choosing a fundamental period N with $N > N_1$ where

$$\tilde{x}[n] = x[n \bmod N] \text{ for } n \in \mathbb{Z}. \tag{50}$$

If $N \to \infty$, then $\tilde{x}$ coincides with x for any finite value n. Now consider the spectral coefficients a_k of $\tilde{x}$ equal

$$a_k = \frac{1}{N}\sum_{n=0}^{N-1} \tilde{x}[n] e^{-ik\frac{2\pi}{N}n} = \frac{1}{N}\sum_{n=0}^{N_1-1} x[n] e^{-ik\frac{2\pi}{N}n} \tag{51}$$

$$= \frac{1}{N}\sum_{n=-\infty}^{\infty} x[n] e^{-ik\frac{2\pi}{N}n}, \tag{52}$$

exploiting the fact that x outside $0, \dots, N_1 - 1$ is equal to 0. The function $X_{DTFT}(\omega)$, also called the *spectrum* of x, is defined as

$$X_{DTFT}(\omega) = \sum_{n=-\infty}^{\infty} x[n] e^{-i\omega n}. \tag{53}$$

The convergence is not a problem here, since x has only a finite length. It is noticeable that the a_k of $\tilde{x}$ are only scaled samples of this function, i.e.,

$$a_k = \frac{1}{N} X_{DTFT}(k\omega_0), \tag{54}$$

with $\omega_0 = \frac{2\pi}{N}$. Rewritten, $\tilde{x}$ is then

$$\tilde{x}[n] = \sum_{k=0}^{N-1} \frac{1}{N} X_{DTFT}(k\omega_0) e^{ik\omega_0 n} \tag{55}$$

$$= \frac{1}{2\pi} \sum_{k=0}^{N-1} X_{DTFT}(k\omega_0) e^{ik\omega_0 n} \omega_0 \tag{56}$$

Eq. 56 converges for $N \to \infty$ to an integral with a width of 2π. Since $\tilde{x}[n] = x[n]$ for $n \to \infty$, $x[n]$ is equal to

$$x[n] = \frac{1}{2\pi} \int_0^{2\pi} X_{DTFT}(\omega) e^{i\omega n} d\omega. \tag{57}$$

Because $X_{DTFT}(\omega)e^{i\omega n}$ is 2π periodic, an arbitrary interval of length 2π can be chosen for calculating the integral.

Definition 6 *The discrete-time Fourier transform (DTFT) of a finite aperiodic discrete-time signal x is*

$$X_{DTFT}(\omega) = \sum_{n=-\infty}^{\infty} x[n] e^{-i\omega n}, \text{ (analysis equation)},$$

where

$$x[n] = \frac{1}{2\pi} \int_{2\pi} X_{DTFT}(\omega) e^{i\omega n} d\omega. \text{ (synthesis equation)}.$$

The DTFT can also be defined for a broader class of signals with infinite lengths. If x is absolutely summable, i.e., $\sum_{n=-\infty}^{\infty} |x[n]| < \infty$, then the analysis equation converges uniformly (this implies pointwise) to a continuous function $X_{DTFT}(\omega)$. Suppose x has finite energy but is not absolutely summable. Then the analysis equation converges in mean squared error, i.e., in $L^2[-\pi, \pi]$ but not pointwise (Haykin and Veen, 1998). Alt (2012) provides an introduction to the theory of the function space L^2 and more generally *Lebesgue spaces*. The synthesis equation, on the other hand, has no convergence issues because the integral is calculated over a finite interval.

Since $X_{DTFT}(\omega)$ is generally complex-valued, it can also be represented in polar coordinate form as $X_{DTFT}(w) = |X_{DTFT}(w)|e^{i\phi(w)}$ (Palani, 2022b). For real-valued signals $x[n]$, $|X_{DTFT}(w)|$ is an even function and is called *magnitude spectrum* and $\phi(w)$ is an odd function and is called *phase spectrum*. For general signals the relation $x^*[n] \overset{DTFT}{\longleftrightarrow} X^*_{DTFT}(-\Omega)$ holds and therefore for real-valued signals like the vibration signals $X_{DTFT}(\Omega) = X^*_{DTFT}(-\Omega)$ (Proakis and Manolakis, 2006).

4.3.3 *Fourier Transform*

Since accelerometers measure the continuous physical quantity of acceleration that is only converted into a discrete-time signal by the sensor and its sampling, the relationship between the spectrum of the continuous-time signal given as the *Fourier Transform* (FT) and the DTFT is of interest. In the application case of this thesis, the aim is to assign the discrete frequencies ω unambiguously to continuous frequencies Ω that can be observed on a vehicle's component and which may change over its lifetime. Under which conditions this is possible is clarified in the following.

Definition 7 *The Fourier transform (FT) of a continuous-time signal* x *is*

$$X_{FT}(\Omega) = \int_{-\infty}^{\infty} x(t) e^{-i\Omega t} dt, \text{ (analysis equation)},$$

and the inverse Fourier transform (IFT) is

$$\hat{x}(t) = \frac{1}{2\pi} \int_{-\infty}^{\infty} X_{FT}(\Omega) e^{i\Omega t} d\Omega. \text{ (synthesis equation)}. \tag{58}$$

Let $\hat{x}_m = \frac{1}{2\pi} \int_{-m}^{m} X_{FT}(\Omega) e^{i\omega t} d\Omega$, and x be an energy signal. Then, for $m \to \infty$, $\hat{x}_m$ converges to x in L^2. However, this does not guarantee pointwise convergence. If x satisfies the so-called *Dirichlet conditions* (Singh et al., 2022), then $\hat{x}(t) = x(t)$ except for the t for which $x(t)$ is not continuous. The conditions are that $x(t)$ is absolutely integrable and has a finite number of minima, maxima, and discontinuities for each finite interval. In addition, the discontinuities must have a finite value.

The DTFT of a discrete-time signal $x[n] = x(nT)$ sampled with $F_s = \frac{1}{T}$ can be expressed through the FT of the continuous-time signal $x(t)$ as follows

$$X_{DTFT}(\omega) = \frac{1}{T} \sum_{n=-\infty}^{\infty} X_{FT}\left(\Omega - n\Omega_s\right), \tag{59}$$

where $\Omega = \frac{w}{T}$ and $\Omega_s = \frac{2\pi}{T}$. From eq. 59, it can also be derived that X_{DTFT} is periodic with period 2π. The DTFT of $x[n]$ is the superposition of shifted and scaled by $\frac{1}{T}$ versions of the FT of $x(t)$. However, under what conditions do these versions of the FT not overlap? Let $x(t)$ be *band-limited*, i.e., $X(\Omega) = 0$ for $|\Omega| > \Omega_B$. They do not overlap if

$$\Omega_B < \Omega_s - \Omega_B \iff \Omega_B < \frac{1}{2}\Omega_s \iff F_B < \frac{1}{2}F_s. \tag{60}$$

Figure 10 shows the influence of Ω_s on the DTFT. The results are summarized in the *Nquist-Shannon sampling theorem*.

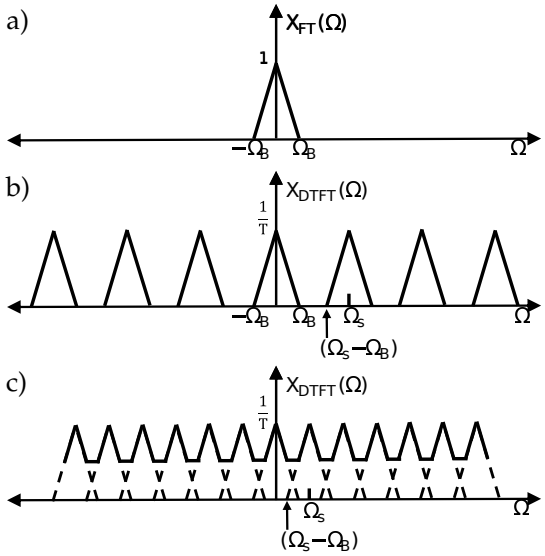

Figure 10: Influence of sampling on the frequency domain: In (a), the FT of the original signal is presented, where (b) and (c) show the continued DTFT for the cases $\Omega_s > 2\Omega_B$ and $\Omega_s < 2\Omega_B$ (Oppenheim, Willsky, and Nawab, 1996).

Theorem 8 (Nquist-Shannon sampling theorem) *For a continuous-time band-limited signal* $x(t)$, $t \in \mathbb{R}$, *with* $X(\Omega) = 0$ *for* $\Omega > \Omega_B$, x *is uniquely determined by the sampled signal* $x[n] = x(nT)$, $n \in \mathbb{Z}$ *and* $\frac{1}{T} = F_s$, *if*

$$\Omega_B < \frac{1}{2}\Omega_s \iff F_B < \frac{1}{2}F_s. \tag{61}$$

This is a remarkable result because some information is lost through sampling. It reveals that the accelerometer in the vehicle, even if it only measures a sampled version of the vibration signal, encodes the complete information about the vibration in the sampled signal (apart from the quantization error) if the vibrations are band-limited, and the sample rate is chosen sufficiently. It also shows that selecting a sensor with a sufficiently high sample rate is crucial for further analysis.

4.3.4 *Discrete Fourier Transform*

The DTFT $X_{DTFT}(\omega)$ is a continuous function depending on the frequency ω. Frequency analysis is usually performed on digital signal processors, which can only process and store a finite number of values. Accordingly, the DTFT is not a computationally favorable representation for frequency analysis (Proakis and Manolakis, 2006). Instead, the *discrete Fourier Transform* (DFT) is computed in real applications, approximating the DTFT. It corresponds to the sampling of the DTFT in the frequency domain. For this, the discrete-time signal

$x[n]$ is considered only for a finite number of N samples. This section is called a *window* and corresponds to a period of NT seconds (Meyer and Mildenberger, 2002). If this window is considered as a finite-duration signal, i.e., assuming $x[n] = 0$ for $n < 0$ and $n > N-1$, then the DTFT of $x[n]$ is

$$X_{DTFT}(\omega) = \sum_{n=0}^{N-1} x[n]e^{-i\omega n},\ 0 \leqslant \omega \leqslant 2\pi. \tag{62}$$

The DFT is obtained when this function is evaluated at the frequencies $\omega = \frac{2\pi k}{N}$, $0 \leqslant k \leqslant N-1$, which are equally spaced.

Definition 9 *The N-point discrete Fourier transform (DFT) of a discrete-time signal $x[n]$ is defined as*

$$X_{DFT}[k] = \sum_{n=0}^{N-1} x[n]e^{-i2\pi k\frac{n}{N}},\ k = 0, \ldots, N-1$$

and the inverse discrete Fourier Transform (IDFT) as

$$x[n] = \frac{1}{N}\sum_{k=0}^{N-1} X_{DFT}(k)e^{i2\pi k\frac{n}{N}},\ n = 0, \ldots, N-1.$$

Recall that the relation $\Omega = \frac{\omega}{T}$ holds between the discrete-time frequency ω and the continuous-time frequency Ω. For the k^{th} entry of the DFT, this gives the corresponding frequency $\frac{k}{NT}$ Hz, i.e., a *frequency resolution* of $\frac{1}{NT}$ Hz. This assumes that the conditions of the sampling theorem are met. Since $X_{DFT}[k] = X^*_{DFT}[N-k]$ for real-valued x, it suffices to consider only the $X[k]$ from $k = 0, \ldots, \lfloor\frac{N}{2}\rfloor$ (Müller, 2015). The $X[k]$ are called *frequency bins*.

There is a close connection between the DFT and DTFS. If the DFT's window is continued periodically, then for this periodic signal, it holds that $X_{DFT} = Na_k$ (Proakis and Manolakis, 2006). From this, it can be seen that the DFT implies a periodic signal or a periodic continuation. However, suppose the signal from which the window was formed is not periodic or an unsuitable window length was chosen. In that case, the continuation will produce discontinuities that do not exist in the original signal. The effect on the DFT is called *leakage effect* because the spectrum is smeared. This effect is prevented using window functions, which act like weighting functions. The signal's considered window is multiplied before applying the DFT with the window function, which lets the values disappear at the edges (Meyer and Mildenberger, 2002). The most commonly used window function is the *Hanning window* (Lyon, 2009) given by

$$hann[n] = \frac{1}{2}\left(1 - \cos\left(\frac{2\pi n}{N-1}\right)\right),\ 0 \leqslant n \leqslant N-1. \tag{63}$$

If x and X_{DFT} are written in vector notation, it is easy to express the DFT as a matrix $W \in \mathbb{C}^{N \times N}$ that maps x to X_{DFT}, i.e., the DFT is a linear transformation and the time complexity of the computation is $O(n^2)$ (Proakis and Manolakis, 2006). By exploiting symmetries in the matrix, the runtime can be reduced to $O(N \log(N))$. These optimized algorithms are called *fast Fourier transforms* (FFTs). For a window length of $N = 4096$, there is already a factor of 341.3 between the computing times of the DFT and the FFT (Scheithauer, 1998). The most common FFT algorithm is the *Cooley-Turkey algorithm*, which recursively divides the DFT of length $N = N_1 \cdot N_2$ into smaller DFTs of length N_1, N_2 (Cooley and Tukey, 1965). Since there is limited computational capacity on a microcontroller for executing a CMS, efficient feature extraction algorithms are critical to successfully applying a CMS in practice.

4.4 TIME-FREQUENCY DOMAIN ANALYSIS

It was pointed out in the last section that the DFT implicitly assumes that the signal is periodic. In this case, the frequency components do not change over time. However, it is known from subsection 3.2.1 that in the vehicle, for example, stochastic excitations are generated by the road surface, which produces a signal with a non-constant spectrum (Ersoy et al., 2017). Similarly, the vibration signal of rotating machines that increase their number of revolutions per minute, like during a speed-up, generates a spectrum that changes over time (Ahmed and Nandi, 2020). This also occurs during acceleration in the vehicle's gas engines and piston movements. The signal is transferred into the *time-frequency* domain for analyzing such time-varying vibrations. The adapted version of the FT is called *short-time Fourier transform* (STFT), and it was first introduced by Gabor (1946). For the discrete case, the STFT describes the computation of successive N-point DFTs, where the windows of the DFTs are $x[nH]$ to $x[nH + N - 1]$, respectively (Garrido, 2016). The variable $H \in \mathbb{N}$, $H \leqslant N$, is called *hop size*, and with its choice, the percentage overlap $\frac{N-H}{N}$ of the DFT windows can be specified.

Definition 10 *Let x be a discrete-time signal. The short-time Fourier transform is given by*

$$X_{STFT}[n, k] = \sum_{m=nH}^{nH+N-1} x[m]h[n-m]e^{-i2\pi k \frac{m}{N}},$$

where h is a N-point window function and $H \in \mathbb{N}$ is the hop size.

The *(power) spectrogram* results from the STFT through

$$Spec[n, k] = \left|STFT[n, k]^2\right|, \tag{64}$$

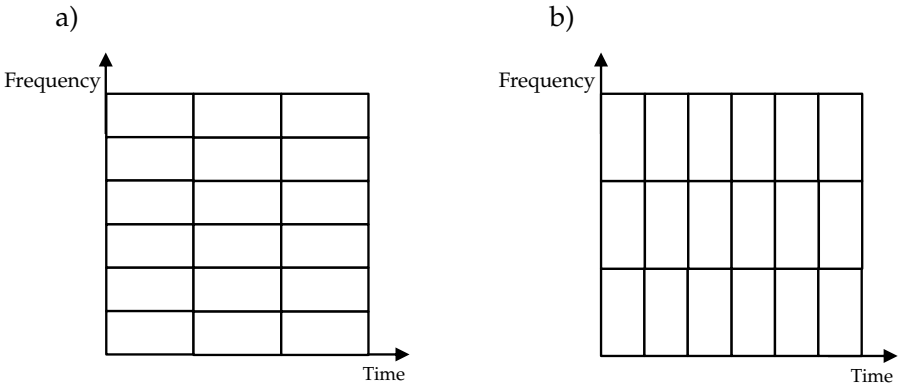

Figure 11: Spectrogram a) has a high frequency resolution, whereas b) has a high time resolution.

i.e., it specifies how the energy of a signal is distributed in the time-frequency domain (Kehtarnavaz and Kim, 2005). For the *magnitude* spectrogram, the squaring of the STFT value is omitted. Let $n_{wind} \in \mathbb{N}$ be the number of windows used for calculating the STFT of a real-valued signal x, then is $Spec \in \mathbb{R}^{n_{wind} \times \lfloor \frac{N}{2} \rfloor + 1}$. When calculating a spectrogram, a trade-off exists between the time and frequency resolution (see Figure 11). If a small window length N is chosen for the DFT, corresponding to a short period NT, i.e., a high time resolution, it leads to a low frequency resolution $\frac{1}{NT}$. Alternatively, the frequency resolution can be high due to a large N, but then the time resolution is low. High values for both simultaneously is impossible due to *Heisenberg's uncertainty principle* (Krishnan, 2021). The spectrogram is a well-established feature for monitoring the condition of machines or machine parts (Léonard, 2007; Manhertz and Bereczky, 2021; Wodecki et al., 2019).

Recently, as a feature for audio classification of (structure-born) sound data, a modified version of the spectrogram has been particularly successful. In a subtask for machine condition monitoring of the *DCASE Challenge 2022* (Dohi et al., 2022), the most famous competition for ML with sound data, *Mel-spectrograms* have been the favored and most applied feature. The unit *Mel* is based on the pitch perceived by humans. The Mel scale is a linearized scale of the human auditory system, i.e., a value twice as high on the Mel scale also sounds twice as high to the human ear. According to O'Shaughnessy (2000), the conversion formula for the frequency f_{Hz} to f_{Mel} is given by

$$f_{Mel} = 2595 \log_{10}\left(1 + \frac{f_{Hz}}{700}\right). \tag{65}$$

The transformation of a spectrogram into a Mel-spectrogram with $n_{mels} \in \mathbb{N}$ number of Mels, is done using a triangular filter bank matrix $B \in \mathbb{R}^{\left(\lfloor \frac{N}{2} \rfloor + 1\right) \times n_{mels}}$ (see Figure 12), where $MelSpec = Spec \cdot B \in \mathbb{R}^{n_{wind} \times n_{mels}}$ (Kopparapu and Laxminarayana, 2010). Dörfler, Bam-

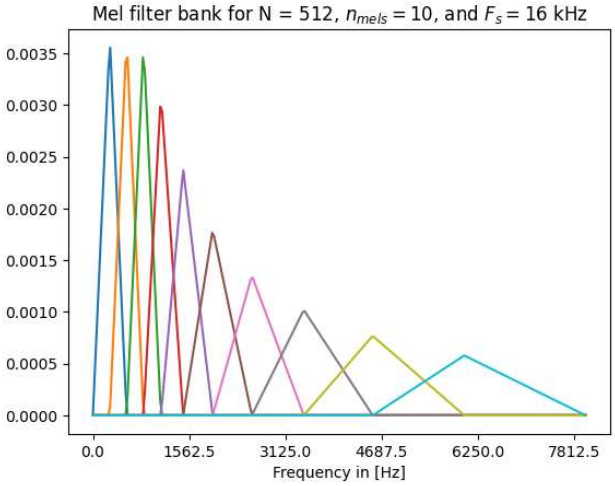

Figure 12: Illustration of a Mel filter bank. As the frequency increases, more frequency bins are utilized to calculate the corresponding Mel bin.

mer, and Grill (2017) argue that the reason for the success of Mel-spectrograms in ML tasks is the property that at typical window lengths of DFTs such as 1024, 2048, or 4096, the frequency dimension is oversampled, and the Mel-spectrogram itself acts like a feature extractor, reducing the dimension in the frequency domain and summarizing higher frequencies, which usually contain little information.

4.5 GRAPH DOMAIN ANALYSIS

Graph-based approaches are another method for analyzing vibration signals. They are a newer form of vibration analysis and were first proposed by Ou and Yu (2016) for the fault diagnosis of roller bearings. They have emerged due to the rise of the field of *complex networks* (Strogatz, 2001). The initial step is to convert the vibration signals into a graph and then extract features from these graphs that can be utilized for CM. The following describes different graphs that can be created from vibration data and are well-established in analyzing vibration signals. Furthermore, the most significant properties of these graphs extracted for CM are introduced.

For a graph G, let V be the set of *vertices* and E be the set of *edges* of G. In shorthand notation, uv is written for an edge $e = \{u, v\} \in E$.

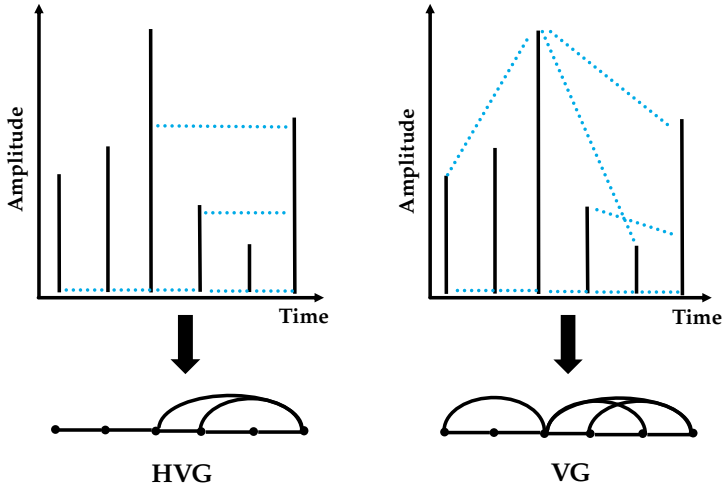

Figure 13: Transformation of a time series into its HVG and VG, respectively.

4.5.1 *Visibility Graphs*

Given the discrete-time signal (time series) $D = ((t_1, d_1), \ldots, (t_N, d_N))$, the *horizontal visibility graph* (HVG) of D is the graph $HVG(D) = (\{1, \ldots, N\}, E)$, where

$$E = \{ij \ : \ d_i > d_k < d_j \text{ for all } 1 \leqslant i < k < j \leqslant N\}. \tag{66}$$

In other words, an edge exists between two vertices in a HVG if and only if the data points can *see* each other, i.e., all data points between these two lie below the horizontal line connecting them (Luque et al., 2009).

A closely related graph is the *visibility graph* (VG) (Lacasa et al., 2008). Its edge set is given by

$$E = \{ij \ : \ d_k < d_i + (d_j - d_i)\frac{t_j - t_k}{t_j - t_i} \text{ for all } 1 \leqslant i < k < j \leqslant N\}, \tag{67}$$

i.e., they can see each other if they can be connected by a straight line without intersecting an intermediate data height. Figure 13 illustrates a HVG and VG generated from the same time series.

Weighted variants of HVGs and VGs can also be defined, where for each edge $e_{ij} \in E$, a weight w_{ij} indicates the strength of the relationship between the vertices i and j. Various recommendations exist in the literature for the weight w_{ij}. For instance, Zhu et al. (2014) propose

$$w_{ij} = \begin{cases} \left|(d_j - d_i)(j - i)\right| + 1, & ij \in E \\ 0, & \text{otherwise.} \end{cases} \tag{68}$$

Supriya et al. (2016) introduce a geometric variant that chooses as weight the angle of the slope line of two data points

$$w_{ij} = \begin{cases} \arctan\left(\frac{d_j - d_i}{j - i}\right), & ij \in E, \\ 0, & \text{otherwise.} \end{cases} \tag{69}$$

The HVG is a subgraph of the VG, and it is, therefore, faster to calculate. The fastest algorithms calculate a HVG in $O(n)$ (Schmidt and Köhne, 2023), whereas the fastest algorithms for the VG are only in $O(n \log n)$ (Fano Yela et al., 2020). The transformation of a time series D into a HVG or VG is invariant under (strictly positive) scaling and arbitrary translations of D (Lacasa et al., 2008). Yela, Stowell, and

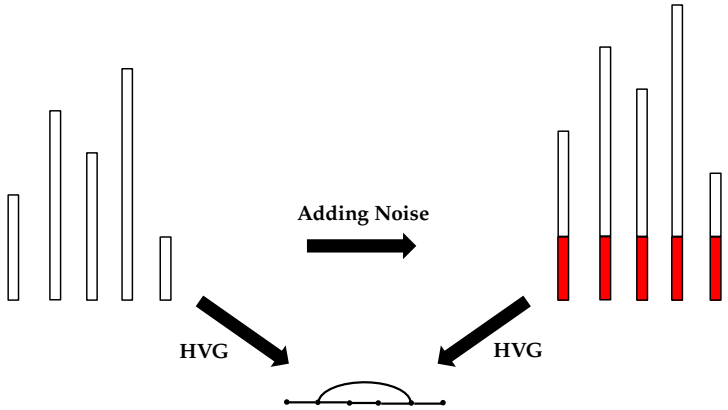

Figure 14: Invariance of HVG under additive noise.

Sandler (2019) used VGs as a similarity measure for analyzing audio signals with harmonic content. Because of their invariances to translations (see Figure 14), superior results could be obtained even for noisy audio data compared to frequency-based methods. The application areas of VGs and HVGs for analyzing and classifying discrete-time signals are very diverse. They range from plasma physics (Acosta-Tripailao, Pastén, and Moya, 2021), fluid dynamics (Manshour, Tabar, and Peinke, 2015), neuroscience (Zhu et al., 2014), and finance (Rong and Shang, 2018; Yang et al., 2009) to chemistry (Kartha et al., 2022). In particular, HVGs and VGs were applied to vibration data for failure detection of roller bearings (Gao et al., 2021; Roy et al., 2022; Zhang et al., 2018).

4.5.2 *Graph Features*

Graph properties provide insight into the structure of a graph. They can refer to individual vertices in the graph but can also provide information about its global structure.

Let $G = (V, E)$ be a graph with $|V| = N$. The vertex v is *incident* with the edge e if $v \in e$, i.e, v is one of the two vertices that e connects. The

degree $\deg(v)$ of a vertex $v \in V$ is the number of edges it is incident to. A *path* P_m in G is a set of vertices $\{v_1, \dots, v_{m+1}\} \subseteq V$ and edges $\{v_1v_2, v_2v_3, \dots, v_mv_{m+1}\} \subseteq E$, where $v_i \neq v_j$ for all $1 \leqslant i < j \leqslant m+1 \leqslant N$. The *length* of the path P_m is equal to m.

The properties presented in the following have been used in the literature to analyze EEG or vibration data (Gao et al., 2021; Zhang et al., 2018; Zhu, Li, and Wen, 2012; Zhu, Li, and Wen, 2014). Here, they are defined only for unweighted graphs, but there are also adapted forms for weighted graphs.

(i) The *degree distribution* $DD \in \mathbb{N}^n$ gives information about how likely it is that vertices have a certain number of edges. The k^{th} entry is obtained by counting the number of vertices with degree k divided by the number of vertices n.

(ii) The *graph entropy* that is derived from the degree distribution with Shannon's entropy formula

$$H = -\sum_{k=0}^{N-1} DD(k) \log(DD(k)).$$

(iii) The *mean vertex degree*

$$\mu(G) = \frac{1}{N} \sum_{v \in V} \deg(v).$$

(iv) The *standard deviation* of the vertex degree

$$\sigma(G) = \sqrt{\frac{1}{N} \sum_{v \in V} (\deg(v) - \mu(G))^2}.$$

(v) The *clustering coefficient* C defined as

$$C = \frac{1}{N} \sum_{v \in V} \frac{\lambda_G(v)}{\frac{1}{2}\deg(v)(\deg(v)-1)},$$

with $\lambda_G(v)$ as the number of triangles on v, i.e., the number of subgraphs of G with 3 edges and 3 vertices of which v is one. The denominator is the maximum number of possible triangles, in this case $\binom{\deg(v)}{2} = \frac{1}{2}\deg(v)(\deg(v)-1)$.

(vi) The *average path length*

$$P = \frac{1}{N(N-1)} \sum_{i \neq j} \text{dist}(i,j),$$

where $\text{dist}(i,j)$ is the length of the shortest path between $i, j \in V$. If no path exists from i to j, then $\text{dist}(i,j)$ is equal to 0.

4.6 OUTLOOK

The analysis methods for vibration signals presented here form the basis for the feature extraction, which is the central part of the data processing step of a CMS in a vehicle with acceleration sensors. Of course, the features are only a careful selection since vibration and audio signals are an active field of research with several emerging approaches. For instance, in deep-learning-based audio classification algorithms, Wang et al. (2017) proposed replacing spectrograms or Mel-spectrograms with trainable layers. In this way, a time-frequency representation is learned in parallel during training. Lostanlen et al. (2019) demonstrate that they can achieve more robustness against noise in environmental sound classification tasks with these learned features. One approach not discussed for the time-frequency analysis is using *wavelets*, which, in contrast to STFTs, do not have an equally-spaced frequency and time resolution. Stéphane (2009) gives an excellent introduction to the theory of wavelets in his book *A Wavelet Tour of Signal Processing*. They achieve a high frequency resolution for lower frequencies and a high time resolution for higher frequencies (Kehtarnavaz and Kim, 2005). However, the frequency-based analysis combined with background knowledge of vehicle vibration phenomena can help improve the explainability of algorithms, as they can be related to concrete physical processes. Therefore, the focus was in this thesis limited to Fourier analysis. *Feature selection* was not directly discussed in this chapter. It was limited to selecting the signal's representation appropriately depending on the properties of the signal. Nevertheless, which feature is ultimately selected for a CMS in the vehicle for a specific use case should be decided based on data by evaluating the performance of the CMS with the respective feature and the algorithms used. Other requirements, such as computational complexity, may influence the selection of the feature. This is particularly relevant for applications that run on edge devices and not in the cloud, i.e., the CMS is computed directly on a microcontroller in the vehicle. The entire CMS, therefore, has only limited computing capacity available, which is why fast feature extraction methods are crucial to ensure the real-time capability of a CMS.

5 TIME SERIES ANOMALY DETECTION

According to Hawkins (1980, p.1) an *anomaly* or also referred to as *outlier* is *"an observation which deviates so much from the other observations as to arouse suspicions that it was generated by a different mechanism"*. Aggarwal (2017) states that in data-generating applications, anomalies occur when the observed system behaves unusually. Detecting anomalies, therefore, provides valuable insights into the system's condition. Applied to the case of this thesis, this means that anomalies may arise when the vehicle is in a faulty operating state, for example, because a component has failed due to wear. Anomaly detection (AD), compared to classification, allows the recognition of deviations from the expected behavior without relying on predefined classes. This flexibility enables a more versatile and adaptive approach to identifying unusual and unknown events in the data, accommodating dynamic operating conditions and emerging fault patterns.

This chapter introduces algorithms used to detect anomalies in time series, including vibration signals, as a special type of time series. The chapter begins by covering the fundamentals of AD and then delves into various algorithms from the fields of statistics, machine learning, and deep learning.

5.1 BASICS OF TIME SERIES ANOMALY DETECTION

The following provides definitions of basic terms in AD, introduces various approaches for detecting anomalies, and presents metrics for evaluating the algorithms.

5.1.1 *Terminology*

An ordered sequence of data points $Y = (y_1, \ldots, y_m)$ with $y_i \in \mathbb{R}^n$ is called a *time series*, i.e., it corresponds to a discrete-time signal. The time series is referred to as *univariate*, if $n = 1$, and for $n > 1$ *multivariate*. For example, when using *tri-axial* accelerometers in the vehicle, the vibrations are recorded in all three dimensions of the vehicle coordinate system, resulting in a multivariate time series. *Subsequences*, denoted as $Y_{i,j} = \{y_i, \ldots, y_j\}$, $1 \leqslant i, j \leqslant m$, of a time series Y correspond to windows of a signal. They are often considered to divide the time series into smaller parts for further analysis. A *equidistant* time series is a time series where the time interval between two successive data points is a fixed constant. The installed accelerometer with uniform sampling guarantees this in case of vehicle vibrations.

The literature has no consistent definition of a time series *anomaly*. Three types are generally distinguished: If individual points are considered anomalous, these are called *point anomalies* or sometimes also *outliers*. A *collective anomaly* describes a subsequence whose single data points are not considered anomalous, but form an anomalous characteristic due to their common occurrence. However, it can also appear that a subsequence itself is not anomalous, but in the respective context, it becomes anomalous. For instance, suppose temperatures above 30 degrees Celsius were measured in a German summer. In that context, this is not anomalous, whereas such a temperature measurement in a German winter is a *contextual anomaly* (Socoró, Alías, and Alsina-Pagès, 2017). Schmidl, Wenig, and Papenbrock (2022) propose the following general definition for a time series anomaly applicable to vibration data:

Definition 11 *A time series anomaly is a sequence of data points* $Y_{i,j}$, $i, j \in \mathbb{N}$, *of length* $j - i + 1 \geqslant 1$ *that deviates w. r. t. some characteristic embedding, model, and/or similarity measure from frequent patterns in the time series* Y.

In the case of vibrations in the vehicle, this is based on the assumption that the vibrations change when the technical condition of the vehicle changes, such as when a wheel becomes loose or the tire pressure drops. *Time series classification*, where the goal is to assign an entire time series to a class correctly, is closely related to time series AD. This is usually done after an anomaly has been detected, and the anomalous parts of the time series are further analyzed to identify, for example, the failed component or function. In the field of CM, this is also called *fault diagnosis* (Galar and Kumar, 2017).

The AD algorithm's input can be a single data point, a subsequence, or features extracted from them. In order to be able to compare different AD algorithms with each other, a uniform output format is required. This is called *anomaly scoring* and assigns a value to each data point of the time series, rating their degree of anomaly. The following definition for an anomaly scoring is based on the one from Schmidl, Wenig, and Papenbrock (2022).

Definition 12 *An anomaly scoring* $S = \{s_1, \ldots, s_m\}$ *with* $s_i \in \mathbb{R}$ *assigns each data point* $y_i \in Y$ *an anomaly score* $s_i \in S$. *For any two scores* s_i *and* s_j, *it must be true that if* $s_i > s_j$, *then* y_i *is more anomalous than* y_j *(in their respective contexts).*

Suppose an AD algorithm receives a subsequence $Y_{i,j}$ or a feature like a Mel-spectrogram extracted from $Y_{i,j}$ as input. If its output is a single anomaly score s, then an anomaly scoring can be generated by setting $s_k = s$ for $i \leqslant k \leqslant j$. In the case of overlapping subsequences, this results in multiple anomaly scores for one data point since it is contained in multiple subsequences. Then, an aggregation function such as mean, median, or maximum determines the final anomaly score.

5.1.2 *Anomaly Detection Approaches*

To abstract from the use case of time series, in the following, the data elements to be analyzed are called *samples*. For times series, the samples are individual data points, subsequences, or features extracted from them. In other contexts, they could also be, for instance, images, text, or rows of tabular data. According to Hodge and Austin (2004), AD distinguishes between three different fundamental learning approaches, described as *Type 1*, *Type 2*, and *Type 3*:

(i) Type 1 algorithms are also called *unsupervised* algorithms in the ML context where there is no explicit training step to learn what is normal or anomalous by an optimization procedure, i.e., anomalies of an unlabeled data set are determined based on the inherent characteristics of the data set itself. In this approach, the data is considered as a static distribution, assuming that samples that are anomalies can be separated from the others because they differ significantly from the majority of the samples, with the method of measuring this depending on the individual algorithm. The approach is initially retrospective, meaning all data must be available before processing. However, predictions can also be made for new samples by comparing them to the existing data. Type 1 is most commonly used in real-world scenarios because it does not require labeled data, which is often unavailable (Barbariol et al., 2022).

(ii) Type 2 algorithms use labeled data to detect anomalies, i.e., this case is equivalent to *supervised classification* problems with the classes 'normal' and 'anomalous' (Kotsiantis, 2007). First, they use a training step to learn the assignment to the classes depending on an algorithm-specific training process. After that, they can make predictions for new unknown samples. However, in real-world applications, it is often very time-consuming or even impossible to generate data of the anomaly class without huge economic losses, e.g., when monitoring the state of an industrial plant and anomalies lead to a stop of production. Therefore this type is used seldom.

(iii) Type 3 is also called *semi-supervised*, where the algorithm is trained only on data of the normal class and consequently learns only this distribution. This approach is appropriate when collecting a large amount of normal class data is more effortless. New samples are then compared to what extent they resemble this normal behavior to determine their anomaly score.

Since it is usually much easier to record data of the normal condition in the context of vibration data in the vehicle, this thesis focuses on

algorithms of Type 3, which can be trained semi-supervised. Besides the learning approach, the AD algorithms differ in their methodology for calculating an anomaly score.

Distance-based methods calculate distances between samples based on metrics. It is assumed that anomalous samples have a larger distance from other samples than normal samples. Depending on the algorithm, the distances are mostly calculated to the nearest neighbors or precomputed cluster centers (Mehrotra, Mohan, and Huang, 2017).

Distribution-based methods assume that the normal data is generated through a *stochastic model*. The assumption is that anomalies correspond to highly improbable values according to this model. Statistical tests can then be used to decide, for example, whether a sample is anomalous or not. If assumptions about the distribution are made, one speaks of a *parametric model*, estimated based on the normal data. If no assumptions are made, it is called a *nonparametric model* (Chandola, Banerjee, and Kumar, 2009).

Forecasting-based methods are an AD approach that is specifically designed for time series data because of their sequential order. The idea is to learn from past data points to predict the following or further data points in the time series. The anomaly score is then determined from the error of the prediction. This methodology assumes that the forecasting error for normal data will be less than for anomalies since these were not present in the training data set, and the anomalies show unknown patterns that are harder to predict (Filonov, Lavrentyev, and Vorontsov, 2016).

Reconstruction-based methods learn the behavior of the normal data by mapping a sample first into a lower dimensional latent vector space and then reconstructing from this latent vector the original sample again. The anomaly score is calculated from the deviation between the reconstruction and the original sample (Pang et al., 2021).

5.1.3 *Evaluation Metrics*

Consider the anomaly class as the positive class and the normal class as the negative class. Predictions are classified as true positives (TPs), false positives (FPs), true negatives (TNs), and false negatives (FNs). The *Area under the Curve* (AUC) metrics, AUC-PR and AUC-ROC, are the most common threshold-independent metrics for AD algorithms (Davis and Goadrich, 2006). Their minimum value is 0, and their maximum is 1. They take the maximum value when an AD algorithm generates a scoring so that the anomaly class can be clearly separated from the normal class. This means that there exists a *threshold* $G \in \mathbb{R}$ such that all scoring values of data points belonging to the anomaly class are greater than G and those of the normal class are all less than or equal to G. AUC-PR represents the area under

the *precision-recall curve*, which describes the *precision* $\left(\frac{TP}{TP+FP}\right)$ as a function of the *recall* $\left(\frac{TP}{TP+FN}\right)$. On the other hand, AUC-ROC represents the area under the curve expressing recall as a function of the *false positive rate* $\left(\frac{FP}{FP+TN}\right)$. Based on the definitions of the two

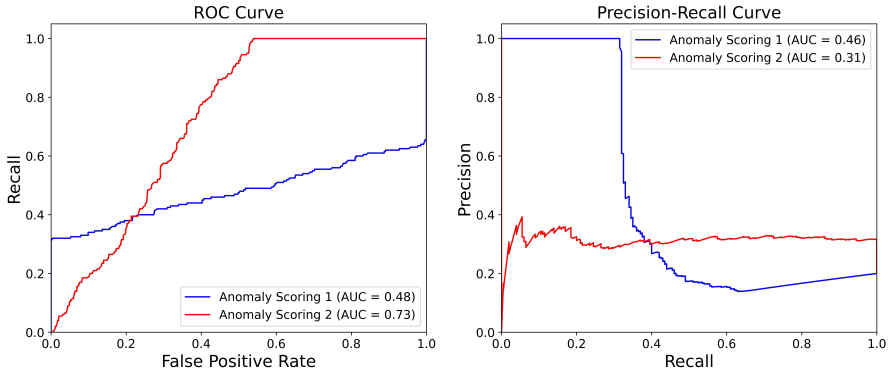

Figure 15: Illustration of a ROC curve and precision-recall curve. The anomaly scoring 1 was generated by an algorithm with high precision and low sensitivity, and the anomaly scoring 2 by an algorithm with low precision and high sensitivity.

metrics, it can be concluded that AUC-PR assigns higher ratings to precise algorithms while AUC-ROC rates sensitive algorithms higher (see Figure 15). AUC-ROC, unlike AUC-PR, is affected by class imbalances. In AD tasks, class imbalances often occur, so paying attention to the proportion of anomalies in the test data is essential because this will affect AUC-ROC. When collecting data through test drives in the case of vehicle condition monitoring, in general, there is much more data from the normal class available since it is more expensive, time-consuming, or even dangerous to collect data from the anomaly class.

AUC-PR or AUC-ROC may be preferred depending on the application and the importance of precision or sensitivity. If, by predicting an anomaly, a CMS triggers a message that is communicated to the driver that, for example, a component is worn and needs to be replaced, then this prediction must be correct with a very high probability. Otherwise, the driver would visit a car repair shop for nothing, which would lead to dissatisfaction with the CMS. So here, high precision would be crucial. Assume that the AD algorithm predicts the condition of the component every second. If it were not so sensitive, this would mean that it would detect the wear of the component slightly later because it would first make a certain number of FNs. The customer will probably rather accept this behavior from the CMS except in very safety-critical use cases.

The binary assignment of the anomaly scores into the normal and anomaly classes using a threshold leads to a trade-off between precision and recall. For example, a customer's request to the AD algorithm may demand a certain level of precision. Then,

the PR curve generated for calculating the AUC-PR can be used to determine which threshold is necessary to reach the required precision and which value the recall in that case takes. However, the higher the precision requirements and, thus, the threshold, the lower the corresponding recall value tends to be.

5.2 STATISTICAL MODELS

The *statistical models* correspond to the distribution-based approach for AD. The underlying stochastic model for the normal data and its distribution is inherently not apparent. However, the idea is to apply statistical methods to estimate the properties of this model based on normal data, which are considered as realizations of the stochastic model.

5.2.1 *Parametric Models*

In the case of the *parametric models*, let the parameters of the stochastic model be denoted by Θ and let $f(x, \Theta)$ be the probability density function. These are going to be estimated from the normal data. For a test sample x, the anomaly score is calculated from the inverse of $f(x, \Theta)$.

Furthermore, it is also possible to determine an anomaly score using a statistical test. The null hypothesis H_0 is that the test sample x was generated by the model with the assumed distribution. The sample is classified as an anomaly if the null hypothesis is rejected. Alternatively, the test statistic can be used to calculate a probabilistic anomaly score from it (Chandola, Banerjee, and Kumar, 2009).

In the simplest case, it is considered that the data were generated from a univariate normal distribution $\mathcal{N}(\mu, \sigma)$, where in practice, these parameters are estimated using the arithmetic mean $\bar{x}$ and empirical standard deviation σ_x. A straightforward technique from the control of industrial manufacturing processes, dating back to Shewhart (1931), classifies all values that fall outside the range $\bar{x} \pm 3\sigma_x$ as an anomaly. An alternative criterion from Chauvenet (1863) which takes into account the number M of samples, determines for a sample x_p that is potentially anomalous first the Z-value $z = \frac{|x_p - \bar{x}|}{\sigma_x}$ and the probability $p_{out} = 1 - \mathbb{P}(-z \leqslant \frac{X - \bar{x}}{\sigma_x} \leqslant z)$, where $\frac{X - \bar{x}}{\sigma_x} \sim \mathcal{N}(0, 1)$. Afterward, the value $p_{out}M$ is calculated corresponding to the expected number of samples that deviate from $\bar{x}$ at least as much as x_p. If $p_{out}M < 0.5$, it is proposed to classify x_p as an anomaly (Mehrotra, Mohan, and Huang, 2017). The *Grubb's test* follows a similar approach

to detect anomalies in univariate data whose distribution is approximately normal (Grubbs, 1950). First, the test statistic

$$G = \frac{\max_{i=1,\dots,M} |x_i - \bar{x}|}{\sigma_x} \tag{70}$$

is determined. The null hypothesis states that the data has no anomaly. Under the null hypothesis, G follows a *t-distribution*. The null hypothesis is rejected at the α significance level, typically 0.05 or 0.01, if

$$z_a > \frac{M-1}{\sqrt{M}} \sqrt{\frac{t^2_{\frac{\alpha}{2M},M-2}}{M-2+t^2_{\frac{\alpha}{2M},M-2}}}, \tag{71}$$

where $t_{\beta,n}$ corresponds to the β-quantile of a t-distribution with n degrees of freedom. This procedure is performed iteratively, i.e., when an anomaly is found, the sample is removed from the data set, M is decreased by one, and the test is repeated until no more anomalies are found in the data set. Laurikkala, Juhola, and Kentala (2000) proposes an adapted version of the test for multivariate data. In the practical application of parametric models, checking the distribution assumptions in advance is crucial. This field of statistical research, also known as *outlier detection*, has a long history with multiple tests that impose different requirements on data distribution and varying degrees of restrictiveness against anomalies (Dixon, 1953; Rosner, 1983). Hawkins (1980) provides a detailed overview of this field in his study.

Unlike the parametric models, the nonparametric models do not assume a distribution for the underlying stochastic model. They are flexible due to the smaller number of assumptions and can also represent very complex distributions (Chandola, Banerjee, and Kumar, 2009). Because of this flexibility, special attention must be taken to prevent overfitting.

5.2.2 *Nonparametric Models*

The simplest nonparametric method is to use histograms to detect anomalies. These estimate the probability density function and can approximate an arbitrary distribution. First, the histograms are created using the training data. For the evaluation of unknown samples, it is checked if this sample falls into one of the existing bins. It is classified as anomalous if it does not fall into existing ones. If it falls into an existing bin, the height corresponding to the frequency of the samples in the bin can also be used to indicate the anomaly score, in which case bins with low height lead to high anomaly scores (Chandola, Banerjee, and Kumar, 2009). One difficulty with histograms is choosing the proper width of bins. If they are too narrow, normal data will be classified as anomalous because they fall into low-frequency

bins, and if they are too wide, anomalous samples may fall into high-frequency bins.

For the case of multivariate data, the histograms can be determined for each dimension individually, and an aggregate function can be used to calculate the final anomaly score. Similarly, it is possible to construct a grid structure where each axis corresponds to a dimension of the multivariate data. The cells of these grids then correspond to the higher-dimensional version of the bins. A problem arises with high-dimensional data, e.g., if a d-dimensional space is divided into grid cells, at least 2^d grid cells are created, i.e., the number grows exponentially. Thus, the expected number of samples in a cell also decreases exponentially (Aggarwal, 2017). This problem can be solved using dimensionality reduction techniques that map the data into a lower dimensional space, such as *PCA* (Ringnér, 2008) or *t-SNE* (Maaten and Hinton, 2008).

With *kernel density estimation*, the probability density function can also be estimated as with histograms, but with smoother functions instead of step functions generated through the binning in histograms (Aggarwal, 2017). The estimated density function $\hat{f}(x)$ is obtained as the sum of the kernel functions K_h centered around each sample in the data set

$$\hat{f}(x) = \sum_{i=1}^{M} K_h(x - x_i), \tag{72}$$

where $h \in \mathbb{R}$ is called the *smoothing parameter* that sets the width of the kernel and the degree of smoothing. An example kernel function is the *Gaussian kernel* (Weglarczyk, Stanislaw, 2018), which in the case of d-dimensional data is defined as

$$K_h(x - x_i) = \left(\frac{1}{h\sqrt{2\pi}}\right)^d e^{-\frac{\|x-x_i\|^2}{2h^2}}. \tag{73}$$

5.3 CLASSICAL MACHINE LEARNING MODELS

The following introduces well-established ML algorithms for AD, each showing a different approach for solving this task.

5.3.1 *Neighbor-based Models*

The neighbor-based models use the distance approach to calculate an anomaly score. The simplest neighbor-based model is formed using the *k-nearest neighbor* (KNN) algorithm, which determines for a sample x its k-nearest neighbors, where the distance is computed using a metric, for example, the *Euclidean* or *Manhattan* metric (Suwanda, Syahputra, and Zamzami, 2020). A sample's set of k-nearest neighbors is called a KNN set in the following. In Ramaswamy, Rastogi,

and Shim's (2000) original version, only the distance to the k^{th} nearest neighbor is used as the anomaly score for a sample x. *KNN-weight* introduced by Angiulli and Pizzuti (2002), proposes to use the sum of the distances between x and all samples from the KNN set to reduce the variance. Alternatively, other aggregation functions, such as the median or mean, can be applied.

If the data set consists of M samples of dimension d, a naive approach to find the KNN set for a single sample lies in the time complexity class $O(k \cdot M \cdot d)$. However, this can be reduced to $O(k \cdot \log(M))$ with optimized data structures like the *k-d tree* (Bentley, 1975). The idea of this data structure is to divide the data space into smaller regions and create a hierarchical structure that allows finding nearest neighbors with fewer operations. The creation of the k-d tree itself is in the time complexity class $O(d \cdot M \cdot \log(M))$, which is why the approach is advantageous, especially if many searches are performed for anomaly score calculation based on the same data set and one benefits from the faster runtime each time.

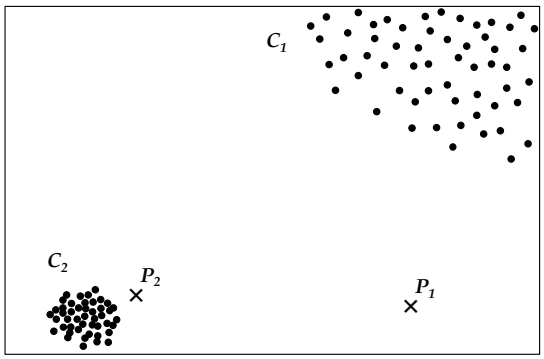

Figure 16: Data set with two clusters and varying local densities (Chandola, Banerjee, and Kumar, 2009).

A problem with distance-based approaches such as KNN is when the data is divided into areas with varying densities. This is illustrated in Figure 16, where two clusters with different densities are shown, but they belong to one data set. If, based on distances in C_1, a threshold is set, from which distance to the KNN set a sample is classified as an anomaly, then this threshold is so large that a sample like p_2 is no longer recognized as an anomaly (Chandola, Banerjee, and Kumar, 2009).

The idea of the *local outlier factor* (LOF) is to take into account the local neighborhood of a sample and its density in the anomaly calculation to overcome this issue (Breunig et al., 2000). In order to be able to describe the LOF, some definitions are first introduced in the following. Let $D_k(x)$ be the distance from x to its k^{th} nearest neighbor with respect to the metric $dist(x, y)$. Furthermore, let the k-neighborhood $L_k(x)$ be the set of all samples with maximum distance $D_k(x)$. Typically, $L_k(x)$ contains k many samples unless multiple samples have

equal distances. The *reachability distance* between sample x and y is defined as

$$R_k(x, y) = \max\{dist(x, y), D_k(x)\}. \tag{74}$$

The *average reachability distance* $AR_k(x)$ is then given as

$$AR_k(x) = \frac{1}{|L_k(x)|} \sum_{y \in L_k(x)} R_k(x, y). \tag{75}$$

The LOF is defined as the average of the ratios of $AR_k(x)$ and all average reachabilities in its k neighborhood, i.e.,

$$LOF_k(x) = \frac{1}{|L_k(x)|} \sum_{y \in L_k(x)} \frac{AR_k(x)}{AR_k(y)}. \tag{76}$$

If the density in individual cluster regions is homogenous, the LOF of samples of any of these clusters will be close to 1, although the density differs between clusters (Aggarwal, 2017). In order to handle cases where the data is not spherically distributed, alternative versions such as *connectivity-based outlier factor* (COF) have been developed, where the k-neighborhood is determined via a *shortest-path* approach (Tang et al., 2002).

5.3.2 *Autoregressive Models*

Autoregressive models (AR) are an essential methodology from the field of *econometrics* for modeling time series that describe, for example, trends and relationships in economies and financial markets (Hayashi, 2000). Autoregressive models assume that the current values of a time series depend on past values of the time series, with values in the near past having more influence than older past values (Mehrotra, Mohan, and Huang, 2017). They, therefore, attempt to model the time series as a function of its past values. Let $Y = (y_1, \ldots, y_M)$ be a univariate time series. The simplest autoregressive model is the $AR(p)$ model

$$y_t = \sum_{i=1}^{p} = a_i y_{t-i} + \mu + \epsilon_t, \tag{77}$$

where the parameter $p \in \mathbb{N}$ indicates how many historical values are included, a_i is the i^{th} *regression coefficients*, $\mu \in \mathbb{R}$ is the *mean term*, and ϵ_t is the *error term*. The ϵ_t are assumed to be uncorrelated, have expected value 0, and constant variance σ^2 (Aggarwal, 2017). The error terms can be used to generate anomaly scores because they represent unpredicted behavior. Eq. 77 gives $M - p$ linear equations for a time series of length M. Normally, $M \gg p$, so it results in an overdetermined system of equations. Therefore, the parameters are estimated by the *least-squares method* (Björck, 1996). The $AR(p)$ model can be

combined with a *moving average* (MA) model. The $MA(q)$ model is defined as

$$y_t = \sum_{i=1}^{q} b_i \epsilon_{t-i} + \mu + \epsilon_t. \tag{78}$$

where the regression parameters b_i must also be learned using the training data. This is more complex than in the case of the $AR(p)$ model since the errors can only be determined once the b_i are known. Therefore, they are determined sequentially using an iterative non-linear procedure (Braei and Wagner, 2020).

The combination of $AR(p)$ and $MA(q)$ model is called *autoregressive moving average* (ARMA) model given by

$$y_t = \sum_{i=1}^{p} a_i y_{t-i} + \sum_{i=1}^{q} b_i \epsilon_{t-i} + \mu + \epsilon_t, \tag{79}$$

The coefficients are typically determined using a *maximum likelihood method* (Neusser, 2009). This method assumes a joint probability distribution for $y_1, \ldots, y_M$ and calculates the coefficients that maximize the probability that the given time series is observed. However, p and q must first be chosen to estimate the coefficients. For this purpose, the *Box-Jenkins method* is applied where the *autocorrelation function* and *partial autocorrelation function* are examined (Box and Jenkins, 1970). All models presented so far assume that the time series is *stationary*, i.e., its distribution y_t does not depend on t. However, some time series contain a trend and thus do not fulfill the stationarity assumption. For instance, this can be observed in global temperatures rising due to climate change. For this case, the *autoregressive integrated moving average* (ARIMA) model was developed as a generalization of the ARMA model, where $y_t^* = y_t - y_{t-1}$ is fitted instead of y_t, called the *first-order difference*. If this new time series is non-stationary, the process is iteratively repeated with y_t^* (Neusser, 2009).

5.3.3 *One-class Support Vector Machine*

Support vector machines (SVMs) proposed by Cortes and Vapnik (1995) are one of the most famous supervised machine learning algorithms for classification. In a modified form, they can also be applied for AD. Schölkopf et al. (1999) introduced a one-class SVM algorithm where only the data of the normal class are used as training data. The goal is to learn a discriminative boundary around the normal samples with a maximum margin classifier so that all samples outside are classified as anomalies (Chandola, Banerjee, and Kumar, 2009).

Let $X = \{x_1, \ldots, x_M\}$ be the set of all training data and $\Phi : X \to F$ be a feature map that maps the training data into a inner product space F, where the inner product is denoted as $\langle \cdot \rangle$. Usually, Φ maps into a

high-dimensional space to better separate the data that may not be linearly separable in the sample space. The inner product between $\Phi(x)$ and $\Phi(y)$ is calculated using a simple *kernel function*, i.e.,

$$K(x, y) = \langle \Phi(x), \Phi(y) \rangle. \tag{80}$$

A simple kernel function is advantageous from a computational perspective since it expects the lower-dimensional samples as input but computes the inner product in the higher-dimensional feature space without explicitly evaluating Φ. This procedure is called *kernel trick*. If a map Φ and inner product space F are chosen, it is not straightforward to find the kernel function. Therefore, in practice, the approach is the other way around. First, a simple symmetric and positive semidefinite function is chosen as the kernel. Then *Mercers theorem* is applied (Lampert et al., 2009), which states that for any symmetric and positive semidefinite function $K(x, y)$, there exists a mapping Φ into an inner product space F such that $K(x, y) = \langle \Phi(x), \Phi(y) \rangle$ as required in eq. 80. The map Φ does not have to be constructed explicitly. The existence is sufficient since it is not evaluated due to the kernel trick.

In the following, an algorithm is defined to generate a function f that assigns the value 1 to a small area containing the majority of the samples and -1 to the rest. The decision function f is based on a hyperplane whose value depends on which side of the hyperplane the sample is located

$$f(x) = \operatorname{sgn}(\langle x, \Phi(x) \rangle - \rho), \tag{81}$$

where sgn is the *sign function* and ρ the *bias term*. Schölkopf et al.'s (1999) idea is to separate the samples in the feature space from the origin using a maximum margin. They propose to solve the convex quadratic programming problem

$$\min_{w \in F, \epsilon \in \mathbb{R}^M, \rho \in \mathbb{R}} \frac{1}{2}\|w\|^2 + \frac{1}{\nu M} \sum_{i=1}^{M} \xi_i - \rho \tag{82}$$

$$\text{subject to} \quad \begin{cases} \langle w, \Phi(x_i) \rangle & \geqslant \rho - \xi_i, \\ \xi_i & \geqslant 0 \ \forall i = 1, \dots M. \end{cases}$$

Here, ξ_i denotes the *slack variables*, and $\nu \in (0, 1)$ is the *regularization parameter*. The smaller ν is chosen, the more the optimization problem becomes that of the *hard margin* SVM algorithm (Lampert et al., 2009), allowing less misclassification in the training data set. However, this

bears the risk of building an overfitted model. By considering the dual problem

$$\min_{\alpha} \frac{1}{2} \sum_{j=1}^{M} \sum_{i=1}^{M} \alpha_i \alpha_j K(x_i, x_j) \tag{83}$$

$$\text{subject to} \quad \begin{cases} 0 \leqslant \alpha_i \leqslant \frac{1}{\nu M}, \\ \sum_{i=1}^{M} \alpha_i = 1. \end{cases}$$

and determining the coefficients α_i, it can be shown that for f holds

$$f(x) = \operatorname{sgn}\left(\sum_{i=1}^{M} \alpha_i K(x_i, x) - \rho \right). \tag{84}$$

All x_i for which $\alpha_i \neq 0$ are called *support vectors*. The authors suggest the *gaussian kernel* $K(x, y) = e^{-\frac{\|x-y\|}{2\sigma^2}^2}$ as the kernel function. Other popular kernels are, for example the *polynomial kernel* or the *sigmoid kernel* (Bounsiar and Madden, 2014).

5.4 DEEP LEARNING MODELS

Applying *deep learning* models has significantly improved detecting anomalies in real-world time series compared to classical ML algorithms (Pang et al., 2021). The following presents the most widely used ANN architectures for AD in time series.

5.4.1 *Autoencoders*

An *Autoencoder* (AE) is a special ANN architecture consisting of an *encoder* and a *decoder*, which are executed one after the other. The encoder maps a sample x into a low-dimensional latent space, and the decoder maps the latent vector back into the original data space (Braei and Wagner, 2020). In the case of AD, the AE is trained exclusively on the normal class data to learn to recover approximately x. The anomaly score results from the error that occurs during the recovery of the sample using the AE.

Let $X \subset D$ be the training data set and D the data space. In the case of vibration data, a sample $x \in X$ could be, for example, a subsequence or a magnitude spectrum. In this case, D would then correspond to $\mathbb{R}^{n \times m}$ with $n, m \in \mathbb{N}$. Let the encoder be E_Φ with learnable weights Φ, mapping the sample $x \in X$ to the latent vector $z = E_\Phi(x) \in Z$. The decoder D_Θ with learnable weights Θ then maps z back to the original data space. The AE network $A_{\Phi,\Theta}$ is therefore the composition of both functions

$$A_{\Phi,\Theta}(x) = D_\Theta(E_\Phi(x)). \tag{85}$$

The encoder and decoder are arbitrary ANNs whose exact architecture depends on the application (Lempitsky, 2019). In the simplest case, they are *multi-layer perceptrons* (Rosenblatt et al., 1962). For image-like inputs such as spectrograms, *convolutional architectures* are also commonly used (Khan et al., 2021). During the training, the goal is to minimize the *loss function* L

$$L(\Phi, \Theta) = \frac{1}{|X|} \sum_{x \in X} \Delta(x, A_{\Phi,\Theta}) \tag{86}$$

where Δ is a function that describes the dissimilarity between the sample and its reconstruction by the AE. A common choice is the Euclidean distance (Lempitsky, 2019). The loss function is minimized during training with *stochastic gradient descent* (Ketkar, 2017).

One challenge with AEs is that when the latent space has a large dimension, they tend to learn the identity mapping since it minimizes the loss function. However, the AE should learn a compact and simpler representation of the data in the latent space. By applying regularization techniques, a large norm of latent vectors or weights Φ and Θ can be penalized during training to learn a sparse representation in the latent space (Ng, 2011; Rifai et al., 2011). Another possibility is to add noise to the samples during training so that the AE performs denoising and reconstruction simultaneously, which prevents it from learning the identity mapping (Vincent et al., 2008).

5.4.2 *Recurrent Neural Networks*

Classical *feed-forward* ANNs have the disadvantage that they cannot incorporate the dependencies in sequential inputs like time series since they have no memory and implicitly assume the samples are independent. *Recurrent neural networks* (RNNs) offer a solution to this, as they have *hidden states* and cycles, which allow them to take into account information that has already been processed and include them in the current prediction (Zollanvari, 2023). Due to these advantageous properties, they are widely used for modeling sequential data and also for detecting anomalies in time series (Su et al., 2019).

Let $(x_1, \ldots, x_M)$ be the input sequence of training samples and $(y_1, \ldots, y_M)$ be the target sequence, where $x_i \in \mathbb{R}^n$ and $y_i \in \mathbb{R}^q$. In the following, the architecture of a *vanilla* RNN is explained, which aims to learn to predict the samples of the target sequence based on the input sequence. For this, let $(\hat{y}_1, \ldots, \hat{y}_M)$ be the *output sequence*, $\hat{y}_i \in \mathbb{R}^q$, and $(h_1, \ldots, h_M)$, $h_i \in \mathbb{R}^l$, be the hidden states. The forward pass of a vanilla RNN is given by the recursive equation

$$h_t = a(W_{xh} x_t + W_{hh} h_{t-1} + b_h), \tag{87}$$

$$\hat{y}_t = W_{hy} h_t + b_y, \tag{88}$$

where $W_{xh} \in \mathbb{R}^{l \times n}$ is the input-to-hidden weight matrix, $W_{hh} \in \mathbb{R}^{l \times l}$ is the hidden-to-hidden weight matrix, $W_{hy} \in \mathbb{R}^{q \times l}$ is the hidden-to-output weight matrix, $b_h \in \mathbb{R}^l$ and $b_y \in \mathbb{R}^q$ are bias terms, and a is a non-linear element-wise activation function (Goodfellow, Bengio, and Courville, 2016). Deeper RNNs can be created by stacking $s \in \mathbb{N}$ hidden state layers, i.e., the hidden states h_t from eq. 87 are used as input for the next hidden state layer, and only after the s^{th} hidden state layer $\hat{y}_t$ is calculated as in eq. 88 (Zollanvari, 2023).

The weights of the RNN are adjusted during training to minimize a loss function that calculates the deviation between the predicted sequence and the target sequence. Stochastic gradient descent is used to accomplish this task. However, the classical *backpropagation algorithm* cannot be applied to determine the gradients (Rojas, 1996). Instead, an adapted version called *backpropagation through time* is used, where the RNN is unrolled to essentially become a feed-forward network again (Werbos, 1990).

It is difficult for the vanilla RNNs to learn relationships that extend over long intervals in sequences since *vanishing gradients* occur during training, so earlier time points only have a diminishing effect on later ones, and no long-term dependencies can be learned (Bengio, Simard, and Frasconi, 1994). Advanced RNNs, such as *long short-term memory* (LSTM) networks, have been developed to overcome this weakness. These contain gating mechanisms so the network can better learn which information to retain and which to forget, with improving capability for learning long-term dependencies (Hochreiter and Schmidhuber, 1997).

Often, RNNs are trained in AD tasks with the objective to predict future samples based on a sequence of historical samples, i.e., they try to perform forecasting, and the anomaly score results from the error between forecast and ground truth (Nguyen et al., 2021). Another variant is integrating them as part of the encoder and decoder of an AE and using a reconstruction error to determine the anomaly score (Homayouni et al., 2020). In both cases, the RNN is trained only on sequences of normal samples. It is assumed that a sequence of anomalous samples has unknown patterns, making it harder for the RNN to predict them accurately and leading to more significant errors.

5.4.3 *Convolutional Neural Networks*

Convolutional neural networks (CNNs) are a class of neural networks proposed by LeCun (1989) that operate on grid-like structures. Therefore, they are widely used for image data applications (2D grid), such as image recognition and segmentation (Goodfellow, Bengio, and Courville, 2016). However, their scope is not limited to machine vision applications. They can also effectively detect

anomalies in time series interpreted as 1D grid structures. A CNN is an ANN that contains at least one *convolutional layer*. In this layer, a operation called *convolution* is executed on the grid-structured data. For the 1D discrete-time signals x and k, the *discrete convolution* of x and k is defined as

$$y[m] = (x * k)[m] = \sum_{i=-\infty}^{\infty} x[i]k[m-i], \forall m, \tag{89}$$

where x is the *input signal*, y the *feature map*, and k the *kernel* . The values of the kernel are parameters that are adjusted during training. In the 1D case, the size of the kernel is called *width*, which corresponds to the length of the discrete-time signal, whereas in the 2D case, it has the form $width \times height$. In practice, the summations in eq. 89 are finite because the signals are of finite length, with the kernel typically being much smaller. The convolution operation can be imagined as sliding a flipped version of the kernel over the input signal x and computing the sum of the element-wise products of both signals for the overlapping region. This operation can also be defined on higher dimensions using multidimensional arrays as input and kernel. In order to be able to learn also non-linear relations, a non-linear activation function a is applied after the convolution in the CNN layer, as well as adding a *bias* term $b \in \mathbb{R}$, i.e., the final output becomes $a(y[m] + b)$. After the convolutional layer, a *pooling layer* is usually added in a CNN, where neighboring inputs are combined into one by an aggregation function like the maximum. This reduces dimensionality and makes the network invariant to small input translations (Zollanvari, 2023).

CNNs have *sparse connectivity*. For instance, given a kernel with $width = 5$, $u[m]$ is affected only by five inputs, whereas in MLPs, all inputs are used due to the weight matrix. This makes CNNs computationally very efficient. Since a single kernel has only a few parameters but slides over the entire signal or image, CNNs are also highly efficient from a memory perspective. This property is called *parameter sharing*. It has the additional advantage that the CNN layer becomes *equivariant* to translations (Goodfellow, Bengio, and Courville, 2016). This is precious for tasks like time series analysis, where translations mean shifts in time. CNNs leverage temporal equivariance to efficiently detect patterns (e.g., trends, periodicities, or anomalies) at different time positions in a time series without the need for separate learning for each position.

For AD in vibration data, CNNs can be used as encoders and decoders in AEs. Here, they are trained semi-supervised to reconstruct the time domain signal (1D) or a time-frequency representation (2D) like a spectrogram (Khan et al., 2021).

5.4.4 *Graph Neural Networks*

Graph neural networks (GNNs) are a special class of ANNs that operate on graph-structured data. A graph $G = (V, E)$ is a set of vertices V and edges E, where an edge $uv \in E$ connects the vertices u and v. Images with their 2D grid structure, as well as univariate time series as 1D grids, can be viewed as special cases of graphs that have only a certain subset of edges (Bronstein et al., 2021). Vertices are often considered as objects or entities and edges describe relations between them.

Many modern technical systems have an increasing number of interconnected sensors that measure time series. Graphs as a data structure provide a way to model the relationships between these sensors, which are viewed as vertices. GNNs can learn the complex relationships and interdependencies between different sensors and detect deviations caused by anomalous events (Deng and Hooi, 2021).

Let $N(u)$ be the *neighborhood* of a vertex $u \in V$, i.e., the set of all vertices $v \in V$ with $uv \in E$. The basic GNN consists of a set of vertex features $X \in \mathbb{R}^{d \times |V|}$ in addition to the input graph G. Since the vertices correspond to objects, the vertex features provide additional information about them in vectorial form. The goal during the training of the GNN is to learn embeddings for the vertices so that the information about the local neighborhood of the vertices is preserved in the low-dimensional embedding space $E \subset \mathbb{R}^d$. These embeddings can then be used in downstream tasks, for example, to classify vertices, to predict edges, or to assign an entire graph to a class (Hamilton, 2020).

At the beginning, the *hidden embedding* h_u^0 of a vertex u corresponds to the vertex feature. The essential operation of the GNN *neural message passing* is iteratively applied during training, which can be considered a generalization of the convolution operation on graphs. Similar to a kernel aggregating information of the surrounding pixels in a CNN for 2D images, a GNN aggregates information from a vertex neighborhood at each message-passing and then updates the hidden embedding of the vertex:

$$h_u^{k+1} = \text{UPDATE}^k\left(h_u^k, \text{AGGREGATE}^k(\{h_v^k, \forall v \in N(u)\})\right) \tag{90}$$

$$= \text{UPDATE}^k\left(h_u^k, m_{N(u)}^k\right) \tag{91}$$

The AGGREGATE function takes as input the hidden embeddings of the neighboring vertices and forms from them a message $m_{N(u))}^k$, which is then combined by the UPDATE function with the previous hidden embedding h_u^k to generate the new hidden embedding h_u^{k+1} of the vertex u. The AGGREGATE and UPDATE functions are arbitrary, differentiable functions like neural networks. The message-passings performed are also sometimes called the *layers* of the GNN. If stopped after K iterations, the K^{th} hidden embedding can be taken

as the final embedding for each vertex. The vertex embeddings can also be combined into one embedding for the whole graph through further aggregation functions (Hamilton, 2020).

5.5 OUTLOOK

The introduced algorithms for AD represent the step of data interpretation in the context of CMSs for vibration signals in vehicles. Due to the focus of the thesis, the algorithms presented were limited to those that process only vibration data as a single data source. However, advanced ANN architectures can also process multi-modal inputs. Since an increasing number of sensors are installed in modern vehicles, there is more application potential for this in the future. For example, Bogatinovski and Nedelkoski (2021) propose a novel forecasting-based LSTM architecture for AD in multi-modal data sources. An advantage of such approaches is that they can learn correlations between signals from different modalities. A multi-modal trained AD algorithm can leverage the strengths of different data sources and use them together to give a more accurate view of a technical system's condition.

The chapter did not address properties like algorithm *explainability*. For this topic, refer to the work of Atakishiyev et al. (2023), who present the current state of research in explainable ML algorithms in automotive and propose an end-to-end framework for developing explainable algorithms for autonomous vehicles. Explainable algorithms are advantageous for the application in the automotive sector since high standards exist on the reliability and accuracy of the algorithms during the development towards series production. They provide transparency in decision-making, enabling engineers, regulators, and users to understand why a specific outcome or prediction was generated. This transparency builds trust and confidence in the system's behavior, ensuring that safety-critical components and functions are robustly designed and verified. Furthermore, explainable algorithms can provide the necessary documentation and justification for regulatory compliance. They help demonstrate that the CMS operates as intended and meets the required safety and reliability standards.

Part II

RESEARCH

6

COUNTING HORIZONTAL VISIBILITY GRAPHS

Juhnke-Kubitzke, Martina, Daniel Köhne, and Jonas Schmidt (2021). *Counting Horizontal Visibility Graphs*. DOI: https://doi.org/10.48550/arXiv.2111.02723.

ABSTRACT

Horizontal visibility graphs (HVGs, for short) are a common tool used in the analysis and classification of time series with applications in many scientific fields. In this article, extending previous work by Luque and Lacasa (2017a), we prove that HVGs associated to data sequences without equal entries are completely determined by their ordered degree sequence. Moreover, we show that HVGs for data sequences without and with equal entries are counted by the Catalan numbers and the large Schröder numbers, respectively.

7

DENSITY BASED ANOMALY DETECTION FOR WIND TURBINE CONDITION MONITORING

Bernhard, Johannes, Jonas Schmidt, and Mark Schutera (2022). "Density based Anomaly Detection for Wind Turbine Condition Monitoring." In: *Proceedings of the 1st International Joint Conference on Energy and Environmental Engineering - CoEEE,* INSTICC. SciTePress, pp. 87–93. ISBN: 978-989-758-599-9. DOI: https://doi.org/10.5220/0011358600003355.

ABSTRACT

Unsupervised and explainable approaches are critical in anomaly detection for mechanical systems. This work proposes a density-based k-nearest neighbor method to combine an unsupervised learning setup with the added value of explainability. The algorithm is applied to detect anomalies in vibration data from acceleration sensors or microphones. In a training phase, we transform healthy vibration data into Mel-spectrograms and extract feature patches representing healthy turbines' vibration energy distribution. We determine anomaly scores by calculating a k-nearest neighbor similarity between operational feature patches and healthy feature patches. Hence, we use basic statistical methods with interpretable results, which contrasts with deep learning techniques. The evaluation paradigm is data from damaged and healthy wind turbines and a secondary machine audio data set. This work introduces and explores a novel sensor-level anomaly score. The model identified all damaged sequences as anomalies on the wind turbine sequences. Furthermore, the method achieved competitive results on the more complex DCASE sound anomaly data set (Koizumi et al., 2020). Concluding, our anomaly score lays the foundations for an interpretable condition monitoring system

8

TIRE PRESSURE MONITORING USING WEIGHTED HORIZONTAL VISIBILITY GRAPHS

Schmidt, Jonas (2022). "Tire Pressure Monitoring using Weighted Horizontal Visibility Graphs." In: *2022 International Conference on Control, Automation and Diagnosis (ICCAD)*, pp. 1–6. DOI: https://doi.org/10.1109/ICCAD55197.2022.9853892.

ABSTRACT

Tire pressure monitoring systems have been proven to reduce fuel consumption and increase driver safety. Today, direct measuring systems are installed in the car, which measure the tire pressure with sensors inside the tire, or indirect systems, which detect a drop in tire pressure through the relative change in the wheel speed. This work proposes a novel way of detecting tire pressure conditions by transforming the vibration data of chassis components into a weighted horizontal visibility graph. Graph features are extracted from this representation to serve as input to an XGBoost classifier. Drives on a test track with tri-axial accelerometers on the upper control arm with low and normal tire pressure are performed to evaluate the method. The results indicate that the proposed method classifies the reduced tire pressure with high precision while also allowing changes in tire pressure to be detected quickly.

9

DETECTING LOOSE WHEEL BOLTS OF A VEHICLE USING ACCELEROMETERS IN THE CHASSIS

Schmidt, Jonas, Kai-Uwe Kühnberger, Dennis Pape, and Tobias Pobandt (2023). "Detecting Loose Wheel Bolts of a Vehicle Using Accelerometers in the Chassis." In: *Pattern Recognition and Image Analysis*. Cham: Springer Nature Switzerland, pp. 665–679. ISBN: 978-3-031-36616-1. DOI: https://doi.org/10.1007/978-3-031-36616-1_53.

ABSTRACT

Increasing road safety has been a society's goal since the automobile's invention. One safety aspect that has not been the focus of research so far is that of a loose wheel. Potential accidents could be prevented with the help of early detection of loose wheel bolts. This work investigates how acceleration sensors in the chassis can be used to detect loose wheel bolts. Test drives with tightened and loosened wheel bolts were carried out. Several state-of-the-art semi-supervised anomalous sound detection algorithms are trained on the test drive data. Evaluation and optimization of anomalous sound detection algorithms shows that loose wheel bolts can be reliably detected when at least three out of five wheel bolts are loose. Our study indicates that acoustic preprocessing and careful selection of acoustic features is crucial for performance and more important than the choice of a special algorithm for detecting loose wheel bolts.

10

A SIMPLE SCALABLE LINEAR TIME ALGORITHM FOR HORIZONTAL VISIBILITY GRAPHS

Schmidt, Jonas and Daniel Köhne (2023). "A simple scalable linear time algorithm for horizontal visibility graphs." In: *Physica A: Statistical Mechanics and its Applications* 616, p. 128601. ISSN: 0378-4371. DOI: https://doi.org/10.1016/j.physa.2023.128601.

ABSTRACT

Horizontal Visibility Graphs establish a connection between time series and complex networks. As a feature, they have shown strong results in time series classification. For real-world applications, algorithms for computing HVGs are necessary that work efficiently on streamed data, that can be parallelized, and whose runtime is independent of the type of time series. Our proposed algorithm extends the fast horizontal visibility algorithm of Zhu, Li, and Wen (2012). satisfying all these desirable properties. The extended version stays worst-case in O(n), works additionally efficiently on streamed data, and becomes parallelizable. Contrary to recent publications, it does not require a complex data structure. This approach enables the computation of HVGs with millions of vertices in a short period, opening up new application areas of HVGs for time series generated batch-wise or resulting from measurements with a high sampling rate.

11

PATENT: COMPUTER-IMPLEMENTED METHOD FOR THE CALCULATION OF CONVOLUTIONAL NETWORKS

Schmidt, Jonas, Michael Hertkorn, and Martin Damian Trochowski (2021). "Computer-implemented method for the calculation of convolutional networks." Pat. DE 10 2020 202 871 A1.

ABSTRACT

The present invention enables faster inference of convolutional neural networks (CNNs) for overlapping input data. The patent claim applies to using CNNs on microcontrollers for detecting siren signals with microphones mounted on the outside of the vehicle. However, the methodology can also be transferred to vibration data. The approach works as follows: A stream of audio input data is converted into a feature representation $x_1 \in \mathbb{R}^2$ that serves as the CNN's input. Suppose the subsequent input x_2 overlaps with x_1. By caching the CNN's intermediate layers output of the input x_1 for the related parts that overlap, the output of x_2 can be computed with fewer computational operations by reusing the cached outputs of the hidden layers and calculating all intermediate outputs only for the non-overlapping parts of x_2 and x_1.

12 DISCUSSION

With the proposed simple and scalable algorithm for faster computation of HVGs for streamed data, such as vibration signals, feature extraction as part of the data processing of a CMS is implemented more efficiently (Schmidt and Köhne, 2023). For in-vehicle applications where the condition monitored by the CMS must be communicated with high frequency to other vehicle systems, efficient data processing and feature extraction is crucial. In this case, edge computing is often the only viable option since transferring the data to be processed to the cloud creates additional latencies. Due to their limited computing power, edge computing systems rely heavily on efficient data processing and benefit particularly from optimized feature extraction methods.

The transformation of vibration signals in HVGs, which were then analyzed in the graph domain, has proven effective for detecting low tire pressure using acceleration sensors mounted on the upper control arm (Schmidt, 2022). Here, we also used graph features related to the degree sequence. These features, such as graph entropy, were very informative for classifying time series with HVGs also in other studies (Luque and Lacasa, 2017b). We provided a reason for this observation with the proof that if the HVG originated from a data sequence containing no equal entries, it is completely determined by its (ordered) degree sequence, i.e., all its information is encoded in it (Juhnke-Kubitzke, Köhne, and Schmidt, 2021). This was previously known only for a special case when the first and last values of the data sequence of the HVG are the two largest (Luque and Lacasa, 2017b). However, there is still the restriction that no equal entries may occur in the data sequence. Imagine a data sequence consisting of 1024 entries that originates from a vibration signal. The quantization for this sequence is done using 32-bit floating point numbers. In that case, one can easily calculate (assuming an uniform distribution and independence) that the probability for equal entries is only about 0.01%. This gives a heuristic explanation of why, in practice, the case of equal entries with sufficient quantization has little relevance.

For tire pressure recognition, sensors that measure the pressure in each tire directly or indirect systems that detect a pressure drop using differences in the wheel speed signal are typically used. The presented work has shown that a distinction between 1.0 bar (low) and 2.3 bar (normal) is also feasible with an acceleration sensor. This gives the option of either dispensing with direct measurement of the pressure in the tire and saving costs for these sensors or, alternatively,

using the information from the acceleration sensors to be still able to make statements about the tire pressure if other sensors fail. Together with semi-supervised AD algorithms, accelerometers mounted on the upper control arm have also proven their value in detecting loose wheel bolts (Schmidt et al., 2023). Here, we reliably detected these as an anomaly if at least three of the five wheel bolts were loose.

One physical explanation for this result is that when a third wheel bolt is loosened, an additional degree of freedom always occurs so the wheel can move around this axis, i.e., it can wobble more. Considering the five wheel bolts on one wheel of our BMW series 5 test vehicle, their arrangement forms a regular pentagon. Any selection of three tight wheel bolts spans a plane, but when a further one is loosened, the two remaining ones form a straight line so that the wheel can wobble slightly about the axis perpendicular to it. The AD algorithm will likely detect these additional vibrations as anomalies.

The window length, hop size, and the selection of acoustic features had a decisive influence on the AD performance, which underlined the importance of optimizing the acoustic hyperparameters and applying domain knowledge. We also tested a MobileNetV2, a CNN architecture designed to work particularly well on mobile devices, for loose wheel bolt detection (Sandler et al., 2018). This used overlapping Mel-spectrograms for the final determination of the anomaly score. A future implementation on an in-vehicle microcontroller would benefit from our patent's approach to optimize the inference of CNNs with overlapping inputs, in which intermediate layers outputs are cached to reuse these outputs and save computational operations on future inputs (Schmidt, Hertkorn, and Trochowski, 2021).

For the low tire pressure and loose wheel bolts experiments, the test drives were carried out with a BMW 5 series (model F10), and the trained ML algorithms are, therefore, only applicable to this vehicle model. The transmission paths of vibrations and the installed components vary depending on the chassis concepts of different models. As a result, the vibrations measured by accelerometers also differ. Therefore, we assume that such an ML-based CMS has to be adapted for different vehicle models.

The factors influencing vibration data in the chassis are various. These include road conditions, weather conditions, load, and driving behavior. For the test drives with the loosened wheel bolts, for example, vibration data could only be recorded for a very limited speed range of up to 30 km/h and on an even road surface. However, for the further development of such CMSs for series production, they must function reliably for any road surfaces and speeds. Adjusting the semi-supervised AD algorithms is necessary to detect loose wheel bolts in more natural driving environments.

From the perspective of an ML-based CMS, there are several options to deal with these issues in the future. The first and most obvi-

ous option is to record additional test drives and increase the training data set, so the model can learn to determine the condition even from this new vibration data distribution. However, it must be weighed for the particular use case to what extent the costs incurred by additional test drives are proportional to the added value for the model's performance. The challenge is the exponential growth of the parameter combination, which can thus become very large even with a small number of influencing factors.

A second option, and the approach we suggest to investigate further, is to focus more on feature extraction of the vibration data and incorporate domain knowledge into developing the AD algorithms. Suppose the vibration signal is transferred from the time domain to the frequency domain. In that case, we propose to study in future work to what extent specific frequency ranges are affected by individual influencing factors such as braking, accelerating, or vehicle load. For road excitation, for example, it is known from the literature that it only causes vibrations up to 30 Hz (Ersoy et al., 2017). If this frequency range is excluded from the AD algorithm by using high-pass filters, it can be prevented that a surface such as an icy road, which was not part of the training data, is falsely detected as an anomaly. A CMS that works more robustly can be developed with close collaboration between machine learning developers and engineers with expertise in the chassis field, who are familiar with the factors influencing the vibrations at the respective sensor position.

Another aspect that has yet to be addressed due to the lack of data in the current work is the differences between components of the same type that result from tolerances in manufacturing processes. For this, it needs to be investigated for the respective application and the component to be monitored how strongly these tolerances affect the observed vibrations in the vehicle. Alternatively, the algorithm used for the CM can be trained on data from a fleet of vehicles so that a generalization effect is achieved regarding component tolerances.

The explainability of the decisions is beneficial for the acceptance and validation of a CMS in an industrial application. For this purpose, we proposed a method based on a density-based KNN algorithm for detecting anomalies in wind turbine vibration signals (Bernhard, Schmidt, and Schutera, 2022). In contrast to deep-learning approaches, the anomaly values can be more easily traced to specific frequency ranges. By carefully selecting hyperparameters, the algorithm beat the deep-learning-based baseline model on a more complex audio AD data set. A KNN algorithm using Mel-spectrograms as acoustic features for loose wheel bolt detection also performed remarkably well. Although the best results were obtained with deep-learning-based AD algorithms, the differences were mainly in detecting only one or two loosened wheel bolts as anomalies. At the same time, the ANN architectures tested were intentionally kept small or

optimized for edge computing, such as MobileNetV2, to guarantee in-vehicle executability. Overall, we concluded that very deep complex neural network architectures are not necessarily required for AD in vehicle vibration data.

As ZF Friedrichshafen AG is an automotive supplier, my research has mainly focused on a single component or function, giving me a limited view of the vehicle's overall condition. In contrast, the car manufacturer that installs a CMS in their vehicle has complete access to all information, data, and sensors. There is great potential to further improve CMSs by using additional sensors that allow conclusions to be drawn about the condition of the component or function. By combining information from multiple sensors and systems, *sensor fusion* enables a more comprehensive view of the vehicle's condition (Muldoon, Kowalczyk, and Shen, 2002). This becomes particularly relevant when different driving functions become more interconnected and interdependent. However, car manufacturers often deny access to the entire sensor information collected in their vehicle fleet. This information deficit, which affects not only suppliers but even more so research institutions, universities, and start-ups, is an inhibitor of innovation. As mentioned in the section on CMSs in automotive applications, there is a lack of large public data sets with internal vehicle data. One reason for the rapid progress in image recognition is that large labeled public data sets such as *ImageNet* have been published (Deng et al., 2009). Similar spurts of innovation are imaginable for vehicle CMSs if more researchers had access to these data and could test new approaches on them so that the results would also be comparable.

The EU initiative *"Access to vehicle data, functions and resources"*, intended to define conditions for using and accessing in-vehicle generated data, gives rise to hope (EU Vehicle Data Initiative, 2022). An innovation- and competition-friendly framework should be developed to allow start-ups to enter the market with their digital services. Allowing everyone to test their own approaches, ideas, and models is the quickest and fairest way to achieve ZF Friedrichshafen AG's vision of zero accidents. May the best model win!

13

CONCLUSION

This dissertation aimed to develop computational efficient and advanced methods for anomaly detection in vibration-based CMSs, focusing on automotive applications. The research demonstrated that accelerometers can be combined with AD algorithms to reliably detect damage to gearboxes, low tire pressure, and loose wheel bolts as anomalies. In addition, methods were developed to accelerate feature extraction from vibration signals and inference of CNNs on edge devices.

The groundwork has been set for future vehicles to analyze and monitor more of their internal parts, components, and functions besides recognizing their external environment. Integrating such novel CMSs into autonomous vehicles will improve road safety and increase human acceptance and trust in this technology. The automotive industry's transformation trend toward zero-emission and autonomous vehicles is a major challenge. The success and acceptance depend not only on faultless vehicle control on the road but also on safety-supporting systems such as CMSs.

However, the investment in its success is worth it. Ultimately, we are expected to live in a society with less traffic congestion, cleaner air, and more green spaces instead of parking areas. For passengers, there will be increased safety on the road, more comfort and relaxation during the ride instead of stress, and better accessibility of mobility for people who cannot drive due to age or disabilities. Overall, it is a more efficient and beneficial form of transportation for people as individuals, society as a whole, and our global environment.

Part III

APPENDIX

A

RUNTIME DATA OF HORIZONTAL VISIBILITY ALGORITHMS FOR SYNTHETIC AND EMPIRICAL TIME SERIES

Schmidt, Jonas (2022). *Runtime Data of Horizontal Visibility Algorithms for synthetic and empirical Time Series*. Version V2. DOI: https://doi.org/10.26249/FK2/MXFPLV.

DESCRIPTION

This repository contains the computed runtimes of state-of-the-art horizontal visibility algorithms for synthetic and empirical time series. The provided Python code was used to compute the runtime data and includes implementations of various horizontal visibility algorithms. The main contribution is a newly developed algorithm that extends the fast weighted horizontal visibility algorithm of Zhu, Li, and Wen (2012). The proposed algorithm works efficiently on streamed data, is multi-processing capable, and has linear runtime in the worst case.

BIBLIOGRAPHY

Acosta-Tripailao, Belén, Denisse Pastén, and Pablo S. Moya (2021). "Applying the Horizontal Visibility Graph Method to Study Irreversibility of Electromagnetic Turbulence in Non-Thermal Plasmas." In: *Entropy* 23.4. ISSN: 1099-4300. DOI: https://doi.org/10.3390/e23040470.

Aggarwal, Charu C. (2017). "Proximity-Based Outlier Detection." In: *Outlier Analysis*. Cham: Springer International Publishing, pp. 111–147. ISBN: 978-3-319-47578-3. DOI: https://doi.org/10.1007/978-3-319-47578-3_4.

Ahmed, Hosameldin and Asoke K Nandi (2020). *Condition monitoring with vibration signals: Compressive sampling and learning algorithms for rotating machines*. John Wiley & Sons. ISBN: 978-1-119-54462-3. DOI: https://doi.org/10.1002/9781119544678.

Alt, Hans Wilhelm (2012). "Funktionenräume." In: *Lineare Funktionalanalysis: Eine anwendungsorientierte Einführung*. Berlin, Heidelberg: Springer Berlin Heidelberg, pp. 39–98. DOI: https://doi.org/10.1007/978-3-642-22261-0_3.

Anderson, James M., Nidhi Kalra, Karlyn D. Stanley, Paul Sorensen, Constantine Samaras, and Tobi A. Oluwatola (2016). *Autonomous Vehicle Technology: A Guide for Policymakers*. Santa Monica, CA: RAND Corporation. DOI: https://doi.org/10.7249/RR443-2.

Anderson, Ronald T (1976). *Reliability design handbook*. Tech. rep.

Angiulli, Fabrizio and Clara Pizzuti (2002). "Fast Outlier Detection in High Dimensional Spaces." In: *Principles of Data Mining and Knowledge Discovery*. Ed. by Tapio Elomaa, Heikki Mannila, and Hannu Toivonen. Berlin, Heidelberg: Springer Berlin Heidelberg, pp. 15–27. ISBN: 978-3-540-45681-0. DOI: https://doi.org/10.1007/3-540-45681-3_2.

Arena, Fabio, Mario Collotta, Liliana Luca, Marianna Ruggieri, and Francesco Gaetano Termine (2022). "Predictive Maintenance in the Automotive Sector: A Literature Review." In: *Mathematical and Computational Applications* 27.1. ISSN: 2297-8747. DOI: https://doi.org/10.3390/mca27010002.

Atakishiyev, Shahin, Mohammad Salameh, Hengshuai Yao, and Randy Goebel (2023). *Explainable Artificial Intelligence for Autonomous Driving: A Comprehensive Overview and Field Guide for Future Research Directions*. DOI: https://doi.org/10.48550/arXiv.2112.11561. arXiv: 2112.11561.

BMWK (2022a). *Automobilindustrie*. URL: https://www.bmwk.de/Redaktion/DE/Textsammlungen/Branchenfokus/Industrie/

branchenfokus - automobilindustrie . html (visited on 06/03/2023).

BMWK (2022b). *FAQ Liste Umweltbonus*. URL: https://www.bmwk.de/Redaktion/DE/Downloads/F/faq-liste-umweltbonus.pdf?__blob=publicationFile&v=1 (visited on 06/04/2023).

Balke, Herbert (2020). "Schwingungen von Systemen mit dem Freiheitsgrad 1." In: *Einführung in die Technische Mechanik: Kinetik*. Berlin, Heidelberg: Springer Berlin Heidelberg, pp. 105–123. ISBN: 978-3-662-59096-6. DOI: https://doi.org/10.1007/978-3-662-59096-6_4.

Bangalore, P. and M. Patriksson (2018). "Analysis of SCADA data for early fault detection, with application to the maintenance management of wind turbines." In: *Renewable Energy* 115, pp. 521–532. ISSN: 0960-1481. DOI: https://doi.org/10.1016/j.renene.2017.08.073.

Barbariol, Tommaso, Filippo Dalla Chiara, Davide Marcato, and Gian Antonio Susto (2022). "A Review of Tree-Based Approaches for Anomaly Detection." In: *Control Charts and Machine Learning for Anomaly Detection in Manufacturing*. Ed. by Kim Phuc Tran. Cham: Springer International Publishing, pp. 149–185. ISBN: 978-3-030-83819-5. DOI: https://doi.org/10.1007/978-3-030-83819-5_7.

Bengio, Y, P Simard, and P Frasconi (1994). "Learning long-term dependencies with gradient descent is difficult." en. In: *IEEE Trans Neural Netw* 5.2, pp. 157–166.

Bentley, Jon Louis (1975). "Multidimensional Binary Search Trees Used for Associative Searching." In: *Commun. ACM* 18.9, 509–517. ISSN: 0001-0782. DOI: https://doi.org/10.1145/361002.361007.

Bernhard, Johannes, Jonas Schmidt, and Mark Schutera (2022). "Density based Anomaly Detection for Wind Turbine Condition Monitoring." In: *Proceedings of the 1st International Joint Conference on Energy and Environmental Engineering - CoEEE*, INSTICC. SciTePress, pp. 87–93. ISBN: 978-989-758-599-9. DOI: https://doi.org/10.5220/0011358600003355.

Bertoncello, Michele and Dominik Wee (2015). *Ten ways autonomous driving could redefine the automotive world*. URL: https://www.mckinsey.com/industries/automotive-and-assembly/our-insights/ten-ways-autonomous-driving-could-redefine-the-automotive-world (visited on 07/08/2023).

Bezzina, Debby and James Sayer (2014). "Safety pilot model deployment: Test conductor team report." In: *Report No. DOT HS* 812.171, p. 18.

Binnewies, Michael, Maik Finze, Manfred Jäckel, Peer Schmidt, Helge Willner, Geoff Rayner-Canham, and Geoff Rayner-Canham (2016). "Anhang A: Einige Grundbegriffe der Physik." In: *Allgemeine und Anorganische Chemie*. Berlin, Heidelberg: Springer Berlin Heidel-

berg, pp. 869–889. ISBN: 978-3-662-45067-3. DOI: https://doi.org/10.1007/978-3-662-45067-3_26.

Bishop, Richard Evelyn Donohue and AG Parkinson (1965). "Second order vibration of flexible shafts." In: *Philosophical Transactions of the Royal Society of London. Series A, Mathematical and Physical Sciences* 259.1095, pp. 1–31. DOI: https://doi.org/10.1098/rsta.1965.0052.

Björck, Åke (1996). *Numerical Methods for Least Squares Problems*. Society for Industrial and Applied Mathematics. DOI: https://doi.org/10.1137/1.9781611971484.

Bogatinovski, Jasmin and Sasho Nedelkoski (2021). "Multi-source Anomaly Detection in Distributed IT Systems." In: *Service-Oriented Computing – ICSOC 2020 Workshops*. Cham: Springer International Publishing, pp. 201–213. ISBN: 978-3-030-76352-7. DOI: https://doi.org/10.1007/978-3-030-76352-7_22.

Bounsiar, Abdenour and Michael G. Madden (2014). "One-Class Support Vector Machines Revisited." In: *2014 International Conference on Information Science & Applications (ICISA)*, pp. 1–4. DOI: https://doi.org/10.1109/ICISA.2014.6847442.

Box, G.E.P. and G.M. Jenkins (1970). *Time Series Analysis: Forecasting and Control*. Holden-Day series in time series analysis and digital processing. Holden-Day. ISBN: 9780816210947.

Braei, Mohammad and Sebastian Wagner (2020). *Anomaly Detection in Univariate Time-series: A Survey on the State-of-the-Art*. DOI: https://doi.org/10.48550/arXiv.2004.00433.

Breunig, Markus M., Hans-Peter Kriegel, Raymond T. Ng, and Jörg Sander (2000). "LOF: Identifying Density-Based Local Outliers." In: *SIGMOD Rec.* 29.2, 93–104. ISSN: 0163-5808. DOI: https://doi.org/10.1145/335191.335388.

Bronstein, Michael M., Joan Bruna, Taco Cohen, and Petar Veličković (2021). *Geometric Deep Learning: Grids, Groups, Graphs, Geodesics, and Gauges*. DOI: https://doi.org/10.48550/arXiv.2104.13478. arXiv: 2104.13478 [cs.LG].

Brown, Austin, Jeffrey Gonder, and Brittany Repac (2014). "An Analysis of Possible Energy Impacts of Automated Vehicles." In: *Road Vehicle Automation*. Ed. by Gereon Meyer and Sven Beiker. Cham: Springer International Publishing, pp. 137–153. ISBN: 978-3-319-05990-7. DOI: https://doi.org/10.1007/978-3-319-05990-7_13.

Bussel, Gerhard van and Christian Schöntag (Oct. 1997). "Operation and maintenance aspects of large offshore windfarms." In: *European Wind Energy Conference : Proceedings of the International Conference*. Irish Wind Energy Association, pp. 272–275. URL: https://www.researchgate.net/publication/228742049_Operation_and_Maintenance_Aspects_of_Large_Offshore_Windfarms.

Carroll, James, Alasdair McDonald, Iain Dinwoodie, David McMillan, Matthew Revie, and Iraklis Lazakis (2017). "Availability, opera-

tion and maintenance costs of offshore wind turbines with different drive train configurations." In: *Wind Energy* 20.2, pp. 361–378. DOI: https://doi.org/10.1002/we.2011.

Chandola, Varun, Arindam Banerjee, and Vipin Kumar (2009). "Anomaly Detection: A Survey." In: *ACM Comput. Surv.* 41.3. ISSN: 0360-0300. DOI: https://doi.org/10.1145/1541880.1541882.

Chauvenet, W. (1863). *A Manual of Spherical and Practical Astronomy: Spherical astronomy*. A Manual of Spherical and Practical Astronomy. J. B. Lippincott & Company.

Cooley, James W and John W Tukey (1965). "An algorithm for the machine calculation of complex Fourier series." In: *Mathematics of computation* 19.90, pp. 297–301. DOI: https://doi.org/10.1090/S0025-5718-1965-0178586-1.

Cortes, Corinna and Vladimir Vapnik (1995). "Support-vector networks." In: *Machine Learning* 20.3, pp. 273–297. ISSN: 1573-0565. DOI: https://doi.org/10.1007/BF00994018.

Czichos, Horst (2019). "Industrie 4.0." In: *Mechatronik: Grundlagen und Anwendungen technischer Systeme*. Wiesbaden: Springer Fachmedien Wiesbaden, pp. 345–348. ISBN: 978-3-658-26294-5. DOI: https://doi.org/10.1007/978-3-658-26294-5_17.

Das, Nabarun and William Taylor (May 2016). "Quantified fault tree techniques for calculating hardware fault metrics according to ISO 26262." In: pp. 1–8. DOI: https://doi.org/10.1109/ISPCE.2016.7492848.

Davies, Aled (1998). "Preface." In: *Handbook of Condition Monitoring: Techniques and Methodology*. Springer Dordrecht. ISBN: 978-0-412-61320-3. DOI: https://doi.org/10.1007/978-94-011-4924-2.

Davis, Jesse and Mark Goadrich (2006). "The Relationship between Precision-Recall and ROC Curves." In: *Proceedings of the 23rd International Conference on Machine Learning*. ICML '06. Pittsburgh, Pennsylvania, USA: Association for Computing Machinery, 233–240. ISBN: 1595933832. DOI: https://doi.org/10.1145/1143844.1143874.

Deng, Ailin and Bryan Hooi (2021). "Graph Neural Network-Based Anomaly Detection in Multivariate Time Series." In: *Proceedings of the AAAI Conference on Artificial Intelligence* 35.5, pp. 4027–4035. DOI: https://doi.org/10.1609/aaai.v35i5.16523.

Deng, Jia, Wei Dong, Richard Socher, Li-Jia Li, Kai Li, and Li Fei-Fei (2009). "ImageNet: A large-scale hierarchical image database." In: *2009 IEEE Conference on Computer Vision and Pattern Recognition*, pp. 248–255. DOI: https://doi.org/10.1109/CVPR.2009.5206848.

Deutsches Institut für Normung e. V. (June 2019). *Grundlagen der Instandhaltung*. Norm.

Dixon, W. J. (1953). "Processing Data for Outliers." In: *Biometrics* 9.1, pp. 74–89. ISSN: 0006341X, 15410420. DOI: https://doi.org/10.2307/3001634. (Visited on 07/16/2023).

Dodd, M (2010). *Heavy vehicle wheel detachment and possible solutions - phase 2 - final report*. URL: https://trid.trb.org/view/919611 (visited on 04/12/2022).

Dohi, Kota, Keisuke Imoto, Noboru Harada, Daisuke Niizumi, Yuma Koizumi, Tomoya Nishida, Harsh Purohit, Takashi Endo, Masaaki Yamamoto, and Yohei Kawaguchi (2022). *Description and Discussion on DCASE 2022 Challenge Task 2: Unsupervised Anomalous Sound Detection for Machine Condition Monitoring Applying Domain Generalization Techniques*. DOI: https://doi.org/10.48550/ARXIV.2206.05876.

Dyer, D. and R. M. Stewart (Apr. 1978). "Detection of Rolling Element Bearing Damage by Statistical Vibration Analysis." In: *Journal of Mechanical Design* 100.2, pp. 229–235. ISSN: 0161-8458. DOI: https://doi.org/10.1115/1.3453905.

Dörfler, Monika, Roswitha Bammer, and Thomas Grill (2017). "Inside the spectrogram: Convolutional Neural Networks in audio processing." In: *2017 International Conference on Sampling Theory and Applications (SampTA)*, pp. 152–155. DOI: https://doi.org/10.1109/SAMPTA.2017.8024472.

EEA (2019). *Greenhouse gas emissions from transport in Europe*. URL: https://www.eea.europa.eu/data-and-maps/indicators/transport-emissions-of-greenhouse-gases/transport-emissions-of-greenhouse-gases-12 (visited on 06/04/2023).

Elies, S and S Ebenhöch (2015). "Performance analysis of commercial accelerometers of different technologies." In: *Proceedings of the 6th International Conference on Sensor Device Technologies and Applications*, pp. 54–59.

Ersoy, Metin, Christoph Elbers, Daniel Wegener, Jörn Lützow, Christian Bachmann, and Christian Schimmel (2017). "Fahrdynamik." In: *Fahrwerkhandbuch: Grundlagen – Fahrdynamik – Fahrverhalten– Komponenten – Elektronische Systeme – Fahrerassistenz – Autonomes Fahren– Perspektiven*. Ed. by Metin Ersoy and Stefan Gies. Wiesbaden: Springer Fachmedien Wiesbaden, pp. 51–169. ISBN: 978-3-658-15468-4. DOI: https://doi.org/10.1007/978-3-658-15468-4_2.

Fahrmeir, Ludwig, Rita Künstler, Iris Pigeot, and Gerhard Tutz (2004). "Einführung." In: *Statistik: Der Weg zur Datenanalyse*. Berlin, Heidelberg: Springer Berlin Heidelberg, pp. 1–30. ISBN: 978-3-540-35037-8. DOI: https://doi.org/10.1007/3-540-35037-3_1.

Fang, Yukun, Chaoyi Cheng, Zhen Dong, Haigen Min, and Xiangmo Zhao (2020). "A Fault Diagnosis Framework for Autonomous Vehicles Based on Hybrid Data Analysis Methods Combined with Fuzzy PID Control." In: *2020 3rd International Conference on Un-*

manned Systems (ICUS), pp. 281–286. DOI: https://doi.org/10.1109/ICUS50048.2020.9274856.

Fano Yela, Delia, Florian Thalmann, Vincenzo Nicosia, Dan Stowell, and Mark Sandler (Apr. 2020). "Online visibility graphs: Encoding visibility in a binary search tree." In: *Phys. Rev. Res.* 2 (2), p. 023069. DOI: https://doi.org/10.1103/PhysRevResearch.2.023069.

Fetzer, James H. (1990). "What is Artificial Intelligence?" In: *Artificial Intelligence: Its Scope and Limits*. Dordrecht: Springer Netherlands, pp. 3–27. ISBN: 978-94-009-1900-6. DOI: https://doi.org/10.1007/978-94-009-1900-6_1.

Filonov, Pavel, Andrey Lavrentyev, and Artem Vorontsov (2016). *Multivariate Industrial Time Series with Cyber-Attack Simulation: Fault Detection Using an LSTM-based Predictive Data Model*. DOI: https://doi.org/10.48550/arXiv.1612.06676.

Fredriksson, Gustav, Alexander Roth, Simone Tagliapietra, and Reinhilde Veugelers (2018). "Is the European automotive industry ready for the global electric vehicle revolution?" eng. In: 2018/26. URL: http://hdl.handle.net/10419/208034.

Friedman, Jerome, Trevor Hastie, and Robert Tibshirani (2000). "Additive logistic regression: a statistical view of boosting (With discussion and a rejoinder by the authors)." In: *The Annals of Statistics* 28.2, pp. 337 –407. DOI: https://doi.org/10.1214/aos/1016218223.

Fritz, Alexander (2022). *Die Elektromobilität weltweit auf dem Vormarsch*. URL: https://www.vda.de/de/themen/elektromobilitaet/marktentwicklung-europa-international (visited on 06/03/2023).

Gabor, Dennis (1946). "Theory of communication. Part 1: The analysis of information." In: *Journal of the Institution of Electrical Engineers-part III: radio and communication engineering* 93.26, pp. 429–441.

Galar, Diego and Uday Kumar (2017). "Chapter 5 - Diagnosis." In: *eMaintenance*. Ed. by Diego Galar and Uday Kumar. Academic Press, pp. 235–310. ISBN: 978-0-12-811153-6. DOI: https://doi.org/10.1016/B978-0-12-811153-6.00005-1.

Gao, Yiyuan, Wenliao Du, Xiaoyun Gong, and Dejie Yu (Nov. 2021). "Graph-domain features and their application in rotating machinery fault diagnosis." In: *IOP Conference Series: Materials Science and Engineering* 1207.1, p. 012008. DOI: https://doi.org/10.1088/1757-899X/1207/1/012008.

Gardiner, David W. (1998). "Review of fundamental vibration theory." In: *Handbook of Condition Monitoring: Techniques and Methodology*. Ed. by Aled Davies. Dordrecht: Springer Netherlands, pp. 269–302. ISBN: 978-94-011-4924-2. DOI: https://doi.org/10.1007/978-94-011-4924-2_11.

Garrido, Mario (2016). "The Feedforward Short-Time Fourier Transform." In: *IEEE Transactions on Circuits and Systems II: Express Briefs* 63.9, pp. 868–872. DOI: https://doi.org/10.1109/TCSII.2016.2534838.

Ghimire, Rajeev, Chaitanya Sankavaram, Alireza Ghahari, Krishna Pattipati, Youssef Ghoneim, Mark Howell, and Mutasim Salman (2011). "Integrated model-based and data-driven fault detection and diagnosis approach for an automotive electric power steering system." In: *2011 IEEE AUTOTESTCON*, pp. 70–77. DOI: https://doi.org/10.1109/AUTEST.2011.6058760.

Ghimire, Rajeev, Chao Zhang, and Krishna R. Pattipati (2018). "A Rough Set-Theory-Based Fault-Diagnosis Method for an Electric Power-Steering System." In: *IEEE/ASME Transactions on Mechatronics* 23.5, pp. 2042–2053. DOI: https://doi.org/10.1109/TMECH.2018.2863119.

Gonter, Mark, Peter Knoll, André Leschke, Ulrich Seiffert, and Florian Weinert (2021). "Fahrzeugsicherheit." In: *Vieweg Handbuch Kraftfahrzeugtechnik*. Ed. by Stefan Pischinger and Ulrich Seiffert. Wiesbaden: Springer Fachmedien Wiesbaden, pp. 1073–1160. ISBN: 978-3-658-25557-2. DOI: https://doi.org/10.1007/978-3-658-25557-2_9.

Goodfellow, Ian, Yoshua Bengio, and Aaron Courville (2016). *Deep learning*. MIT press.

Grimmelius, H.T., P.P. Meiler, H.L.M.M. Maas, B. Bonnier, J.S. Grevink, and R.F. van Kuilenburg (1999). "Three state-of-the-art methods for condition monitoring." In: *IEEE Transactions on Industrial Electronics* 46.2, pp. 407–416. DOI: https://doi.org/10.1109/41.753780.

Grubbs, Frank E. (1950). "Sample Criteria for Testing Outlying Observations." In: *The Annals of Mathematical Statistics* 21.1, pp. 27 –58. DOI: https://doi.org/10.1214/aoms/1177729885.

Hameed, Z., S.H. Ahn, and Y.M. Cho (2010). "Practical aspects of a condition monitoring system for a wind turbine with emphasis on its design, system architecture, testing and installation." In: *Renewable Energy* 35.5, pp. 879–894. ISSN: 0960-1481. DOI: https://doi.org/10.1016/j.renene.2009.10.031.

Hamilton, William L (2020). *Graph representation learning*. Morgan & Claypool Publishers.

Hawkins, D. M. (1980). "Introduction." In: *Identification of Outliers*. Dordrecht: Springer Netherlands, pp. 1–12. ISBN: 978-94-015-3994-4. DOI: https://doi.org/10.1007/978-94-015-3994-4_1.

Hayashi, Fumio (2000). *Econometrics*. Princeton Univ. Press. ISBN: 978-0-691-01018-2.

Haykin, Simon S. and Barry Van Veen (1998). *Signals and Systems*. 1st. USA: John Wiley & Sons, Inc. ISBN: 978-0-471-13820-4.

Heinrichs, Dirk (2016). "Autonomous Driving and Urban Land Use." In: *Autonomous Driving: Technical, Legal and Social Aspects*. Ed. by Markus Maurer, J. Christian Gerdes, Barbara Lenz, and Hermann Winner. Berlin, Heidelberg: Springer Berlin Heidelberg, pp. 213–231. ISBN: 978-3-662-48847-8. DOI: https://doi.org/10.1007/978-3-662-48847-8_11.

Hochreiter, Sepp and Jürgen Schmidhuber (1997). "Long Short-Term Memory." In: *Neural Comput.* 9.8, 1735–1780. ISSN: 0899-7667. DOI: https://doi.org/10.1162/neco.1997.9.8.1735.

Hodge, Victoria J. and Jim Austin (2004). "A Survey of Outlier Detection Methodologies." In: *Artificial Intelligence Review* 22.2, pp. 85–126. ISSN: 1573-7462. DOI: https://doi.org/10.1007/s10462-004-4304-y.

Homayouni, Hajar, Sudipto Ghosh, Indrakshi Ray, Shlok Gondalia, Jerry Duggan, and Michael G. Kahn (2020). "An Autocorrelation-based LSTM-Autoencoder for Anomaly Detection on Time-Series Data." In: *2020 IEEE International Conference on Big Data (Big Data)*, pp. 5068–5077. DOI: https://doi.org/10.1109/BigData50022.2020.9378192.

Hsu, Hwei P. (2011). *Signals and systems*. McGraw-Hill New York. ISBN: 978-0-07-163473-1.

Hu, Haoju, Huan Luo, and Xiaoqiang Deng (2021). "Health monitoring of automotive suspensions: a lstm network approach." In: *Shock and Vibration* 2021, pp. 1–11. DOI: https://doi.org/10.1155/2021/6626024.

Jardine, Andrew K.S., Daming Lin, and Dragan Banjevic (2006). "A review on machinery diagnostics and prognostics implementing condition-based maintenance." In: *Mechanical Systems and Signal Processing* 20.7, pp. 1483–1510. ISSN: 0888-3270. DOI: https://doi.org/10.1016/j.ymssp.2005.09.012.

Jauregui Correa, Juan Carlos A. and Alejandro A. Lozano Guzman (2020a). "Chapter Four - Causes and effects of vibration." In: *Mechanical Vibrations and Condition Monitoring*. Ed. by Juan Carlos A. Jauregui Correa and Alejandro A. Lozano Guzman. Academic Press, pp. 75–96. ISBN: 978-0-12-819796-7. DOI: https://doi.org/10.1016/B978-0-12-819796-7.00004-4.

— (2020b). "Chapter One - Fundamentals of mechanical vibrations." In: *Mechanical Vibrations and Condition Monitoring*. Ed. by Juan Carlos A. Jauregui Correa and Alejandro A. Lozano Guzman. Academic Press, pp. 1–26. ISBN: 978-0-12-819796-7. DOI: https://doi.org/10.1016/B978-0-12-819796-7.00001-9.

Jegadeeshwaran, R. and V. Sugumaran (2015). "Brake fault diagnosis using Clonal Selection Classification Algorithm (CSCA) – A statistical learning approach." In: *Engineering Science and Technology, an International Journal* 18.1, pp. 14–23. ISSN: 2215-0986. DOI: https://doi.org/10.1016/j.jestch.2014.08.001.

Jeong, YiNa, SuRak Son, EunHee Jeong, and ByungKwan Lee (2018). "An Integrated Self-Diagnosis System for an Autonomous Vehicle Based on an IoT Gateway and Deep Learning." In: *Applied Sciences* 8.7. ISSN: 2076-3417. DOI: https://doi.org/10.3390/app8071164.

Juhnke-Kubitzke, Martina, Daniel Köhne, and Jonas Schmidt (2021). *Counting Horizontal Visibility Graphs*. DOI: https://doi.org/10.48550/arXiv.2111.02723.

Jung, Daniel and Christofer Sundström (2019). "A Combined Data-Driven and Model-Based Residual Selection Algorithm for Fault Detection and Isolation." In: *IEEE Transactions on Control Systems Technology* 27.2, pp. 616–630. DOI: https://doi.org/10.1109/TCST.2017.2773514.

Jung, Michael and Ulrich Langer (2001). "Grundprinzipien der FEM: Ein 1D-Beispiel." In: *Methode der finiten Elemente für Ingenieure: Eine Einführung in die numerischen Grundlagen und Computersimulation*. Wiesbaden: Vieweg+Teubner Verlag, pp. 62–152. ISBN: 978-3-663-10785-9. DOI: https://doi.org/10.1007/978-3-663-10785-9_3.

Kartha, Moses J., Bilal Ahmad Reshi, Pravin S. Walke, and Davoud Dastan (2022). "Morphological study of thin films: Simulation and experimental insights using horizontal visibility graph." In: *Ceramics International* 48.4, pp. 5066–5074. ISSN: 0272-8842. DOI: https://doi.org/10.1016/j.ceramint.2021.11.044.

Kehtarnavaz, Nasser and Namjin Kim (2005). "Chapter 7 - Frequency Domain Processing." In: *Digital Signal Processing System-Level Design Using LabVIEW*. Ed. by Nasser Kehtarnavaz and Namjin Kim. Burlington: Newnes, pp. 139–145. ISBN: 978-0-7506-7914-5. DOI: https://doi.org/10.1016/B978-075067914-5/50014-3.

Keller, K., K. Swearingen, J. Sheahan, M. Bailey, J. Dunsdon, K.W. Przytula, and B. Jordan (2006). "Aircraft electrical power systems prognostics and health management." In: *2006 IEEE Aerospace Conference*, 12 pp.–. DOI: https://doi.org/10.1109/AERO.2006.1656087.

Kelly, A. (1997). *Maintenance Strategy*. Elsevier Science. ISBN: 978-0-7506-2417-6.

Ketkar, Nikhil (2017). "Stochastic Gradient Descent." In: *Deep Learning with Python: A Hands-on Introduction*. Berkeley, CA: Apress, pp. 113–132. ISBN: 978-1-4842-2766-4. DOI: https://doi.org/10.1007/978-1-4842-2766-4_8.

Khan, Adnan Shahid, Zeeshan Ahmad, Johari Abdullah, and Farhan Ahmad (2021). "A Spectrogram Image-Based Network Anomaly Detection System Using Deep Convolutional Neural Network." In: *IEEE Access* 9, pp. 87079–87093. DOI: https://doi.org/10.1109/ACCESS.2021.3088149.

Kirchberg, Peter, Eberhard Wächtler, D. Goetz, E. Wächtler, I. Winter, and H. Wußing (1981). "Carl Benz." In: *Carl Benz Gottlieb Daimler Wilhelm Maybach*. Ed. by D. Goetz, E. Wächtler, I. Winter, and H. Wußing. Wiesbaden: Vieweg+Teubner Verlag, pp. 18–58. ISBN: 978-3-322-82218-5. DOI: https://doi.org/10.1007/978-3-322-82218-5_2.

Knoll, Peter (2010). "Fahrerassistenzsysteme." In: *Fahrstabilisierungssysteme und Fahrerassistenzsysteme*. Ed. by Konrad Reif. Wiesbaden: Vieweg+Teubner, pp. 104–121. ISBN: 978-3-8348-9717-6. DOI: https://doi.org/10.1007/978-3-8348-9717-6_9.

Koizumi, Yuma et al. (2020). "Description and Discussion on DCASE2020 Challenge Task2: Unsupervised Anomalous Sound Detection for Machine Condition Monitoring." In: *Proceedings of the Detection and Classification of Acoustic Scenes and Events 2020 Workshop (DCASE2020)*, pp. 81–85. URL: http://dcase.community/documents/workshop2020/proceedings/DCASE2020Workshop_Koizumi_3.pdf.

Kopparapu, Sunil Kumar and M Laxminarayana (2010). "Choice of Mel filter bank in computing MFCC of a resampled speech." In: *10th International Conference on Information Science, Signal Processing and their Applications (ISSPA 2010)*, pp. 121–124. DOI: https://doi.org/10.1109/ISSPA.2010.5605491.

Kotsiantis, S. B. (2007). "Supervised Machine Learning: A Review of Classification Techniques." In: *Proceedings of the 2007 Conference on Emerging Artificial Intelligence Applications in Computer Engineering: Real Word AI Systems with Applications in EHealth, HCI, Information Retrieval and Pervasive Technologies*. NLD: IOS Press, 3–24. ISBN: 9781586037802. DOI: https://doi.org/10.5555/1566770.1566773.

Krishnan, Sri (2021). "5 - Advanced analysis of biomedical signals." In: *Biomedical Signal Analysis for Connected Healthcare*. Ed. by Sri Krishnan. Academic Press, pp. 157–222. ISBN: 978-0-12-813086-5. DOI: https://doi.org/10.1016/B978-0-12-813086-5.00003-7.

Küçükay, Ferit (2022). "Einleitung zu Teil IV." In: *Grundlagen der Fahrzeugtechnik: Antriebe, Getriebe, Energieverbrauch, Bremsen, Fahrdynamik, Fahrkomfort*. Wiesbaden: Springer Fachmedien Wiesbaden, pp. 1315–1324. ISBN: 978-3-658-36727-5. DOI: https://doi.org/10.1007/978-3-658-36727-5_30.

Kumar, Harish Senthil, Krishna Anusha Kambhampati, Jegadeeshwaran Rakkiyannan, and Sakthivel Gnanasekaran (2021). "Brake Health Prediction Using LogitBoost Classifier Through Vibration Signals - A Machine Learning Framework." In: *International Journal of Prognostics and Health Management* 12.2. ISSN: 2153-2648. DOI: https://doi.org/10.36001/IJPHM.2021.v12i2.3017.

Lacasa, Lucas, Bartolo Luque, Fernando Ballesteros, Jordi Luque, and Juan Carlos Nuño (2008). "From time series to complex networks:

The visibility graph." In: *Proceedings of the National Academy of Sciences* 105.13, pp. 4972–4975. DOI: https://doi.org/10.1073/pnas.0709247105.

Lampert, Christoph H et al. (2009). "Kernel methods in computer vision." In: *Foundations and Trends® in Computer Graphics and Vision* 4.3, pp. 193–285.

Laurikkala, J., M. Juhola, and E. Kentala (2000). "Informal identification of outliers in medical data." English. In: *Workshop Notes of the 14th European Conference on Artificial Intelligence (ECAI-2000): The Fifth Workshop on Intelligent Data Analysis in Medicine and Pharmacology (IDAMAP-2000)*. Ed. by Nada Lavrac, Silvia Miksch, and Kavsek Branko, pp. 20–24.

LeCun, Yann (1989). "Generalization and network design strategies." English (US). In: *Connectionism in perspective*. Ed. by R. Pfeifer, Z. Schreter, F. Fogelman, and L. Steels. Elsevier.

Leidinger, Bernhard (2014). *Wertorientierte Instandhaltung: Kosten senken, Verfügbarkeit erhalten*. Springer-Verlag. ISBN: 978-3-658-04400-8. DOI: https://doi.org/10.1007/978-3-658-04401-5.

Lempitsky, Victor (2019). "Autoencoder." In: *Computer Vision: A Reference Guide*. Cham: Springer International Publishing, pp. 1–6. ISBN: 978-3-030-03243-2. DOI: https://doi.org/10.1007/978-3-030-03243-2_862-1.

Lin, Shih-Lin (2021). "Application of Machine Learning to a Medium Gaussian Support Vector Machine in the Diagnosis of Motor Bearing Faults." In: *Electronics* 10.18. ISSN: 2079-9292. DOI: https://doi.org/10.3390/electronics10182266.

Lostanlen, Vincent, Justin Salamon, Mark Cartwright, Brian McFee, Andrew Farnsworth, Steve Kelling, and Juan Pablo Bello (2019). "Per-Channel Energy Normalization: Why and How." In: *IEEE Signal Processing Letters* 26.1, pp. 39–43. DOI: https://doi.org//10.1109/LSP.2018.2878620.

Luque, B., L. Lacasa, F. Ballesteros, and J. Luque (Oct. 2009). "Horizontal visibility graphs: Exact results for random time series." In: *Phys. Rev. E* 80 (4), p. 046103. DOI: https://doi.org/10.1103/PhysRevE.80.046103.

Luque, Bartolo and Lucas Lacasa (2017a). "Canonical horizontal visibility graphs are uniquely determined by their degree sequence." In: *The European Physical Journal Special Topics* 226.3, pp. 383–389. ISSN: 1951-6401. DOI: https://doi.org/10.1140/epjst/e2016-60164-1.

— (2017b). "Canonical horizontal visibility graphs are uniquely determined by their degree sequence." In: *The European Physical Journal Special Topics* 226.3, pp. 383–389. ISSN: 1951-6401. DOI: https://doi.org/10.1140/epjst/e2016-60164-1.

Lyon, Douglas A. (Nov. 2009). "The Discrete Fourier Transform, Part 4: Spectral Leakage." In: *Journal of Object Technology*, pp. 23–34. ISSN: 1660-1769. DOI: 10.5381/jot.2009.8.7.c2.

Léonard, François (2007). "Phase spectrogram and frequency spectrogram as new diagnostic tools." In: *Mechanical Systems and Signal Processing* 21.1, pp. 125–137. ISSN: 0888-3270. DOI: https://doi.org/10.1016/j.ymssp.2005.08.011.

Maaten, Laurens van der and Geoffrey Hinton (2008). "Visualizing Data using t-SNE." In: *Journal of Machine Learning Research* 9.86, pp. 2579–2605. URL: http://jmlr.org/papers/v9/vandermaaten08a.html.

Maisonnier, David (2018). "RAMI: The main challenge of fusion nuclear technologies." In: *Fusion Engineering and Design* 136, pp. 1202–1208. DOI: https://doi.org/10.1016/j.fusengdes.2018.04.102.

Manhertz, Gabor and Akos Bereczky (2021). "STFT spectrogram based hybrid evaluation method for rotating machine transient vibration analysis." In: *Mechanical Systems and Signal Processing* 154, p. 107583. ISSN: 0888-3270. DOI: https://doi.org/10.1016/j.ymssp.2020.107583.

Manshour, Pouya, M Reza Rahimi Tabar, and Joachim Peinke (Aug. 2015). "Fully developed turbulence in the view of horizontal visibility graphs." In: *Journal of Statistical Mechanics: Theory and Experiment* 2015.8, P08031. DOI: https://doi.org/10.1088/1742-5468/2015/08/p08031.

Marletto, Gerardo (2019). "Who will drive the transition to self-driving? A socio-technical analysis of the future impact of automated vehicles." In: *Technological Forecasting and Social Change* 139, pp. 221–234. ISSN: 0040-1625. DOI: https://doi.org/10.1016/j.techfore.2018.10.023.

Mayes, I. W. and W. G. R. Davies (Jan. 1984). "Analysis of the Response of a Multi-Rotor-Bearing System Containing a Transverse Crack in a Rotor." In: *Journal of Vibration, Acoustics, Stress, and Reliability in Design* 106.1, pp. 139–145. ISSN: 0739-3717. DOI: https://doi.org/10.1115/1.3269142.

McMillan, David and Graham W. Ault (2007). "Quantification of Condition Monitoring Benefit for Offshore Wind Turbines." In: *Wind Engineering* 31.4, pp. 267–285. DOI: https://doi.org/10.1260/030952407783123060.

Mehrotra, Kishan G., Chilukuri K. Mohan, and HuaMing Huang (2017). "Distance and Density Based Approaches." In: *Anomaly Detection Principles and Algorithms*. Cham: Springer International Publishing, pp. 97–117. ISBN: 978-3-319-67526-8. DOI: https://doi.org/10.1007/978-3-319-67526-8_6.

Meyer, Martin and Otto Mildenberger (2002). "Einführung." In: *Grundlagen der Informationstechnik: Signale, Systeme und Filter*. Ed.

by Otto Mildenberger. Wiesbaden: Vieweg+Teubner Verlag, pp. 1–15. ISBN: 978-3-322-91582-5. DOI: https://doi.org/10.1007/978-3-322-91582-5_1.

Mitschke, Manfred and Henning Wallentowitz (2014a). "Einführung, Schwingungsanregung, regellose Schwingungen." In: *Dynamik der Kraftfahrzeuge*. Wiesbaden: Springer Fachmedien Wiesbaden, pp. 301–347. ISBN: 978-3-658-05068-9. DOI: https://doi.org/10.1007/978-3-658-05068-9_11.

— (2014b). "Motorerregte Fahrzeugschwingungen." In: *Dynamik der Kraftfahrzeuge*. Wiesbaden: Springer Fachmedien Wiesbaden, pp. 561–599. ISBN: 978-3-658-05068-9. DOI: https://doi.org/10.1007/978-3-658-05068-9_18.

Mobley, R. Keith (1998). "Condition based maintenance." In: *Handbook of Condition Monitoring: Techniques and Methodology*. Ed. by Aled. Davies. Dordrecht: Springer Netherlands, pp. 35–53. ISBN: 978-94-011-4924-2. DOI: https://doi.org/10.1007/978-94-011-4924-2_2.

Mockenhaupt, Andreas (2021). *Digitalisierung und Künstliche Intelligenz in der Produktion*. Springer. ISBN: 978-3-658-32772-9. DOI: https://doi.org/10.1007/978-3-658-32773-6.

Mohammadi, Ali, Abdesslem Djerdir, Nadia Yousfi Steiner, David Bouquain, and Davood Khaburi (2015). "Diagnosis of PEMFC for automotive application." In: *2015 5th International Youth Conference on Energy (IYCE)*, pp. 1–6. DOI: https://doi.org/10.1109/IYCE.2015.7180793.

Mohammadi, Reza and Qing He (2022). "A deep reinforcement learning approach for rail renewal and maintenance planning." In: *Reliability Engineering & System Safety* 225, p. 108615. ISSN: 0951-8320. DOI: https://doi.org/10.1016/j.ress.2022.108615.

Moskowitz, Martin A (2002). *A Course in Complex Analysis in One Variable*. WORLD SCIENTIFIC. DOI: https://doi.org/10.1142/4836.

Mouatamir, Abderrahim (Mar. 2018). "Decision Support System for Condition Monitoring Technologies." English. PhD thesis. Netherlands: University of Twente. ISBN: 978-90-365-4519-8. DOI: https://doi.org/10.3990/1.9789036545198.

Muldoon, S.E., M. Kowalczyk, and J. Shen (2002). "Vehicle fault diagnostics using a sensor fusion approach." In: *SENSORS, 2002 IEEE*. Vol. 2, 1591–1596 vol.2. DOI: https://doi.org/10.1109/ICSENS.2002.1037361.

Müller, Meinard (2015). "Fourier Analysis of Signals." In: *Fundamentals of Music Processing: Audio, Analysis, Algorithms, Applications*. Cham: Springer International Publishing, pp. 39–114. ISBN: 978-3-319-21945-5. DOI: https://doi.org/10.1007/978-3-319-21945-5_2.

Neusser, Klaus (2009). "Schätzung von ARMA-Modellen." In: *Zeitreihenanalyse in den Wirtschaftswissenschaften*. Wiesbaden:

Vieweg+Teubner, pp. 79–97. ISBN: 978-3-8348-9564-6. DOI: https://doi.org/10.1007/978-3-8348-9564-6_6.

Ng, Andrew (2011). "Sparse autoencoder." In: *CS294A Lecture notes* 72.2011, pp. 1–19.

Nguyen, H.D., K.P. Tran, S. Thomassey, and M. Hamad (2021). "Forecasting and Anomaly Detection approaches using LSTM and LSTM Autoencoder techniques with the applications in supply chain management." In: *International Journal of Information Management* 57, p. 102282. ISSN: 0268-4012. DOI: https://doi.org/10.1016/j.ijinfomgt.2020.102282.

O'Shaughnessy, Douglas (2000). "Speech Perception." In: *Speech Communications: Human and Machine*, pp. 141–172. DOI: https://doi.org/10.1109/9780470546475.ch5.

Obst, Heike-Ursurla, Christian Hardt, and Bernd Fuhrmann (2018). *Damping of Structure-Borne Noise in Automobiles*. SZ Scala GmbH. ISBN: 978-3-86236-116-8.

Oppenheim, Alan V., Alan S. Willsky, and S. Hamid Nawab (1996). *Signals & Systems (2nd Ed.)* USA: Prentice-Hall, Inc. ISBN: 0138147574.

Ou, Lu and Dejie Yu (2016). "Fault diagnosis of roller bearings based on Laplacian energy feature extraction of path graphs." In: *Measurement* 91, pp. 168–176. ISSN: 0263-2241. DOI: https://doi.org/10.1016/j.measurement.2016.05.061.

Palani, S. (2022a). "Representation of Signals." In: *Signals and Systems*. Cham: Springer International Publishing, pp. 1–196. ISBN: 978-3-030-75742-7. DOI: https://doi.org/10.1007/978-3-030-75742-7_1.

— (2022b). *Signals and Systems*. Cham: Springer International Publishing. ISBN: 978-3-030-75742-7. DOI: https://doi.org/10.1007/978-3-030-75742-7_1.

Pan, Haihong, Zhiqiang Lü, Huimin Wang, Haiyan Wei, and Lin Chen (2018). "Novel battery state-of-health online estimation method using multiple health indicators and an extreme learning machine." In: *Energy* 160, pp. 466–477. ISSN: 0360-5442. DOI: https://doi.org/10.1016/j.energy.2018.06.220.

Pang, Guansong, Chunhua Shen, Longbing Cao, and Anton Van Den Hengel (2021). "Deep Learning for Anomaly Detection: A Review." In: *ACM Comput. Surv.* 54.2. ISSN: 0360-0300. DOI: https://doi.org/10.1145/3439950.

Park, Kun Il (2018). "Stochastic Process." In: *Fundamentals of Probability and Stochastic Processes with Applications to Communications*. Cham: Springer International Publishing, pp. 135–184. ISBN: 978-3-319-68075-0. DOI: https://doi.org/10.1007/978-3-319-68075-0_6.

Pawellek, Günther (2016). *Integrierte Instandhaltung und Ersatzteillogistik*. Springer Vieweg Berlin, Heidelberg. ISBN: 978-3-662-48666-5. DOI: https://doi.org/10.1007/978-3-662-48667-2.

Peters, Benjamin, Murat Yildirim, Nagi Gebraeel, and Kamran Paynabar (2020). "Severity-based diagnosis for vehicular electric systems with multiple, interacting fault modes." In: *Reliability Engineering & System Safety* 195, p. 106605. ISSN: 0951-8320. DOI: https://doi.org/10.1016/j.ress.2019.106605.

Pichler, Melanie, Nora Krenmayr, Etienne Schneider, and Ulrich Brand (2021). "EU industrial policy: Between modernization and transformation of the automotive industry." In: *Environmental Innovation and Societal Transitions* 38, pp. 140–152. ISSN: 2210-4224. DOI: https://doi.org/10.1016/j.eist.2020.12.002.

Pletschen, Bernd (2010). "Akustikgestaltung in der Fahrzeugentwicklung." In: *Sound-Engineering im Automobilbereich: Methoden zur Messung und Auswertung von Geräuschen und Schwingungen*. Ed. by Klaus Genuit. Berlin, Heidelberg: Springer Berlin Heidelberg, pp. 89–108. ISBN: 978-3-642-01415-4. DOI: https://doi.org/10.1007/978-3-642-01415-4_3.

Preusche, Christian (Aug. 2018). "Clusterbasierte Zustandsbewertung von technischen Systemen zur Unterstützung der prädiktiven Instandhaltung." de. PhD thesis. Darmstadt: Technische Universität. URL: http://tuprints.ulb.tu-darmstadt.de/7720/.

Proakis, John G. and Dimitris K. Manolakis (2006). *Digital Signal Processing (4th Edition)*. USA: Prentice-Hall, Inc. ISBN: 978-0-13-187374-2.

Rajamani, Rajesh (2006). "Lateral and Longitudinal Tire Forces." In: *Vehicle Dynamics and Control*. Boston, MA: Springer US, pp. 387–432. ISBN: 978-0-387-28823-9. DOI: https://doi.org/10.1007/0-387-28823-6_13.

Ramaswamy, Sridhar, Rajeev Rastogi, and Kyuseok Shim (2000). "Efficient algorithms for mining outliers from large data sets." In: *SIGMOD '00: Proceedings of the 2000 ACM SIGMOD international conference on Management of data*. Dallas, Texas, United States: ACM, pp. 427–438. ISBN: 1-58113-217-4. DOI: https://doi.acm.org/10.1145/342009.335437.

Randall, Robert Bond (2021). "Basic Signal Processing Techniques." In: *Vibration–based Condition Monitoring*. John Wiley & Sons, Ltd. Chap. 3, pp. 63–121. ISBN: 9781119477631. DOI: https://doi.org/10.1002/9781119477631.ch3.

Rao, Singiresu S. (2018). *Mechanical Vibrations*. 6th ed. Pearson. ISBN: 978-1-292-17860-8.

Reif, Konrad (2012). "Sensormessprinzipien." In: *Sensoren im Kraftfahrzeug*. Ed. by Konrad Reif. Wiesbaden: Vieweg+Teubner Verlag, pp. 34–119. ISBN: 978-3-8348-2208-6. DOI: https://doi.org/10.1007/978-3-8348-2208-6_2.

Rifai, Salah, Pascal Vincent, Xavier Muller, Xavier Glorot, and Yoshua Bengio (2011). "Contractive Auto-Encoders: Explicit Invariance during Feature Extraction." In: *Proceedings of the 28th International Conference on International Conference on Machine Learning*. ICML'11. Bellevue, Washington, USA: Omnipress, 833–840. ISBN: 9781450306195. DOI: https://doi.org/10.5555/3104482.3104587.

Ringnér, Markus (2008). "What is principal component analysis?" In: *Nature Biotechnology* 26.3, pp. 303–304. ISSN: 1546-1696. DOI: https://doi.org/10.1038/nbt0308-303.

Rishel, Tracy D. and Cem Canel (2006). "Using a maintenance contribution model to predict the impact of maintenance on profitability." In: *Journal of Information and Optimization Sciences* 27.1, pp. 21–34. DOI: 10.1080/02522667.2006.10699676.

Ro, Yuna and Youngwook Ha (2019). "A Factor Analysis of Consumer Expectations for Autonomous Cars." In: *Journal of Computer Information Systems* 59.1, pp. 52–60. DOI: https://doi.org/10.1080/08874417.2017.1295791.

Rojas, Raúl (1996). "The Backpropagation Algorithm." In: *Neural Networks: A Systematic Introduction*. Berlin, Heidelberg: Springer Berlin Heidelberg, pp. 149–182. ISBN: 978-3-642-61068-4. DOI: https://doi.org/10.1007/978-3-642-61068-4_7.

Rong, Lei and Pengjian Shang (Apr. 2018). "Topological entropy and geometric entropy and their application to the horizontal visibility graph for financial time series." In: *Nonlinear Dynamics* 92.1, pp. 41–58. ISSN: 1573-269X. DOI: https://doi.org/10.1007/s11071-018-4120-6.

Rosenblatt, Frank et al. (1962). *Principles of neurodynamics: Perceptrons and the theory of brain mechanisms*. Vol. 55. Spartan books Washington, DC.

Rosner, Bernard (1983). "Percentage Points for a Generalized ESD Many-Outlier Procedure." In: *Technometrics* 25.2, pp. 165–172. DOI: https://doi.org/10.1080/00401706.1983.10487848.

Routray, Aurobinda, Aparna Rajaguru, and Satnam Singh (2010). "Data reduction and clustering techniques for fault detection and diagnosis in automotives." In: *2010 IEEE International Conference on Automation Science and Engineering*, pp. 326–331. DOI: https://doi.org/10.1109/COASE.2010.5584324.

Roy, Sayanjit Singha, Soumya Chatterjee, Saptarshi Roy, Pradip Bamane, Ashish Paramane, U. Mohan Rao, and Muhammad Tariq Nazir (2022). "Accurate Detection of Bearing Faults Using Difference Visibility Graph and Bi-Directional Long Short-Term Memory Network Classifier." In: *IEEE Transactions on Industry Applications* 58.4, pp. 4542–4551. DOI: https://doi.org/10.1109/TIA.2022.3167658.

Ryll, Frank and Jens Götze (2010). "Methoden und Werkzeuge zur Instandhaltung technischer Systeme." In: *Instandhaltung technischer Systeme: Methoden und Werkzeuge zur Gewährleistung eines sicheren und wirtschaftlichen Anlagenbetriebs*. Ed. by Michael Schenk. Berlin, Heidelberg: Springer Berlin Heidelberg, pp. 103–229. ISBN: 978-3-642-03949-2. DOI: https://doi.org/10.1007/978-3-642-03949-2_3.

Sánchez, René-Vinicio, Pablo Lucero, Rafael E. Vásquez, Mariela Cerrada, Jean-Carlo Macancela, and Diego Cabrera (2018). "Feature ranking for multi-fault diagnosis of rotating machinery by using random forest and KNN." In: *Journal of Intelligent & Fuzzy Systems* 34. 6, pp. 3463–3473. ISSN: 1875-8967. DOI: https://doi.org/10.3233/JIFS-169526.

Sandler, Mark, Andrew Howard, Menglong Zhu, Andrey Zhmoginov, and Liang-Chieh Chen (2018). *MobileNetV2: Inverted Residuals and Linear Bottlenecks*. DOI: https://doi.org/10.48550/ARXIV.1801.04381.

Sankavaram, Chaitanya, Bharath Pattipati, Krishna Pattipati, Yilu Zhang, Mark Howell, and Mutasim Salman (2012). "Data-driven fault diagnosis in a hybrid electric vehicle regenerative braking system." In: *2012 IEEE Aerospace Conference*, pp. 1–11. DOI: 10.1109/AERO.2012.6187368.

Santos, Carlos Henrique dos and José Arnaldo Barra Montevechi (2022). "Digital Twins Architecture." In: *Digital Twins: Basics and Applications*. Ed. by Zhihan Lv and Elena Fersman. Cham: Springer International Publishing, pp. 1–12. ISBN: 978-3-031-11401-4. DOI: https://doi.org/10.1007/978-3-031-11401-4_2.

Sauer, Wolfgang, Klaus Kramer, and Metin Ersoy (2017). "Fahrkomfort." In: *Fahrwerkhandbuch: Grundlagen – Fahrdynamik – Fahrverhalten– Komponenten – Elektronische Systeme – Fahrerassistenz – Autonomes Fahren– Perspektiven*. Ed. by Metin Ersoy and Stefan Gies. Wiesbaden: Springer Fachmedien Wiesbaden, pp. 207–243. ISBN: 978-3-658-15468-4. DOI: https://doi.org/10.1007/978-3-658-15468-4_4.

Scheithauer, Rainer (1998). "Einleitung." In: *Signale und Systeme*. Wiesbaden: Vieweg+Teubner Verlag, pp. 1–5. ISBN: 978-3-322-99517-9. DOI: https://doi.org/10.1007/978-3-322-99517-9_1.

Schmidl, Sebastian, Phillip Wenig, and Thorsten Papenbrock (2022). "Anomaly Detection in Time Series: A Comprehensive Evaluation." In: *Proc. VLDB Endow.*, 1779–1797. ISSN: 2150-8097. DOI: https://doi.org/10.14778/3538598.3538602.

Schmidt, Jonas (2022). "Tire Pressure Monitoring using Weighted Horizontal Visibility Graphs." In: *2022 International Conference on Control, Automation and Diagnosis (ICCAD)*, pp. 1–6. DOI: https://doi.org/10.1109/ICCAD55197.2022.9853892.

Schmidt, Jonas, Michael Hertkorn, and Martin Damian Trochowski (2021). "Computer-implemented method for the calculation of convolutional networks." Pat. DE 10 2020 202 871 A1.

Schmidt, Jonas, Kai-Uwe Kühnberger, Dennis Pape, and Tobias Pobandt (2023). "Detecting Loose Wheel Bolts of a Vehicle Using Accelerometers in the Chassis." In: *Pattern Recognition and Image Analysis*. Cham: Springer Nature Switzerland, pp. 665–679. ISBN: 978-3-031-36616-1. DOI: https://doi.org/10.1007/978-3-031-36616-1_53.

Schmidt, Jonas and Daniel Köhne (2023). "A simple scalable linear time algorithm for horizontal visibility graphs." In: *Physica A: Statistical Mechanics and its Applications* 616, p. 128601. ISSN: 0378-4371. DOI: https://doi.org/10.1016/j.physa.2023.128601.

Schölkopf, Bernhard, Robert Williamson, Alex Smola, John Shawe-Taylor, and John Platt (1999). "Support Vector Method for Novelty Detection." In: *Proceedings of the 12th International Conference on Neural Information Processing Systems*. NIPS'99. Denver, CO: MIT Press, 582–588. DOI: https://doi.org/10.5555/3009657.3009740.

Schönewolf, Carolin (2020). "Vergangenheit und Zukünfte des autonomen Fahrens – eine Transformation?" In: *Vereindeutigung von Technikzukünften: Von der tradierenden Disruption autonomer Automobilität*. Wiesbaden: Springer Fachmedien Wiesbaden, pp. 7–51. ISBN: 978-3-658-32803-0. DOI: https://doi.org/10.1007/978-3-658-32803-0_2.

Schröder, Werner (2010). *Ganzheitliches Instandhaltungsmanagement*. Gabler Verlag Wiesbaden. ISBN: 978-3-8349-2038-6. DOI: https://doi.org/10.1007/978-3-8349-8481-45.

Seeck, Andre et al. (2021). "Anforderungen, Zielkonflikte, Grundlagen." In: *Vieweg Handbuch Kraftfahrzeugtechnik*. Ed. by Stefan Pischinger and Ulrich Seiffert. Wiesbaden: Springer Fachmedien Wiesbaden, pp. 15–123. ISBN: 978-3-658-25557-2. DOI: https://doi.org/10.1007/978-3-658-25557-2_2.

Seera, Manjeevan, Chee Peng Lim, Saeid Nahavandi, and Chu Kiong Loo (2014). "Condition monitoring of induction motors: A review and an application of an ensemble of hybrid intelligent models." In: *Expert Systems with Applications* 41.10, pp. 4891–4903. ISSN: 0957-4174. DOI: https://doi.org/10.1016/j.eswa.2014.02.028.

Serrat, Olivier (2012). "World Sustainable Development Timeline." In.

Shafi, Uferah, Asad Safi, Ahmad Raza Shahid, Sheikh Ziauddin, and Muhammad Qaiser Saleem (Jan. 2018). "Vehicle Remote Health Monitoring and Prognostic Maintenance System." In: *Journal of Advanced Transportation* 2018. ISSN: 0197-6729. DOI: https://doi.org/10.1155/2018/8061514.

Sharma, Anurag and Dharmendra Sharma (2011). "Clonal Selection Algorithm for Classification." In: *Artificial Immune Systems*. Ed. by

Pietro Liò, Giuseppe Nicosia, and Thomas Stibor. Berlin, Heidelberg: Springer Berlin Heidelberg, pp. 361–370. ISBN: 978-3-642-22371-6. DOI: https://doi.org/10.1007/978-3-642-22371-6_31.

Shewhart, W.A. (1931). *Economic Control of Quality of Manufactured Product*. Books from Bell Telephone Laboratories. D. Van Nostrand Company, Incorporated. ISBN: 9780598557667.

Shrieve, P. and J. Hill (1998). "Commercial applications of vibration monitoring." In: *Handbook of Condition Monitoring: Techniques and Methodology*. Ed. by A. Davies. Dordrecht: Springer Netherlands, pp. 354–374. ISBN: 978-94-011-4924-2. DOI: https://doi.org/10.1007/978-94-011-4924-2_14.

Shrivastava, Amit and Sulochana Wadhwani (2013). "Development of fault detection system for ball bearing of induction motor using vibration signal." In: *International Journal Of Scientific Research*.

Siegel, Joshua E., Yongbin Sun, and Sanjay Sarma (2018). "Automotive Diagnostics as a Service: An Artificially Intelligent Mobile Application for Tire Condition Assessment." In: *Artificial Intelligence and Mobile Services – AIMS 2018*. Ed. by Marco Aiello, Yujiu Yang, Yuexian Zou, and Liang-Jie Zhang. Cham: Springer International Publishing, pp. 172–184. ISBN: 978-3-319-94361-9. DOI: https://doi.org/10.1007/978-3-319-94361-9_13.

Siegel, Joshua (2018). "Smartphone-Based Vehicular Tire Pressure and Condition Monitoring." In: *Proceedings of SAI Intelligent Systems Conference (IntelliSys) 2016*. Ed. by Yaxin Bi. Cham: Springer International Publishing, pp. 805–824. ISBN: 978-3-319-56994-9. DOI: https://doi.org/10.1007/978-3-319-56994-9_56.

Simsir, Mehmet, Raif Bayir, and Yılmaz Uyaroğlu (Dec. 2015). "Real-Time Monitoring and Fault Diagnosis of a Low Power Hub Motor Using Feedforward Neural Network." In: *Computational Intelligence and Neuroscience* 2016, p. 7129376. ISSN: 1687-5265. DOI: https://doi.org/10.1155/2016/7129376.

Singh, Pushpendra, Amit Singhal, Binish Fatimah, Anubha Gupta, and Shiv Dutt Joshi (2022). "Proper Definitions of Dirichlet Conditions and Convergence of Fourier Representations [Lecture Notes]." In: *IEEE Signal Processing Magazine* 39.5, pp. 77–84. DOI: https://doi.org/10.1109/MSP.2022.3172620.

Smith, Julius O. (2007). *Mathematics of the Discrete Fourier Transform (DFT) with Audio Applications, Second Edition*. W3K Publishing. ISBN: 978-0-9745607-4-8.

Smith, Wade A. and Robert B. Randall (2015). "Rolling element bearing diagnostics using the Case Western Reserve University data: A benchmark study." In: *Mechanical Systems and Signal Processing* 64-65, pp. 100–131. ISSN: 0888-3270. DOI: https://doi.org/10.1016/j.ymssp.2015.04.021.

Socoró, Joan Claudi, Francesc Alías, and Rosa Ma Alsina-Pagès (2017). "An Anomalous Noise Events Detector for Dynamic Road Traf-

fic Noise Mapping in Real-Life Urban and Suburban Environments." In: *Sensors* 17.10. ISSN: 1424-8220. DOI: https://doi.org/10.3390/s17102323.

Stratmann, Jens (2015). *Mit ZF zur Vision Zero! Das Video vom ZF Global Press Event 2017*. URL: https://www.rad-ab.com/2017/07/18/mit-zf-zur-vision-zero-das-video-vom-zf-global-press-event-2017/ (visited on 07/08/2023).

Strogatz, Steven H. (Mar. 2001). "Exploring complex networks." In: *Nature* 410.6825, pp. 268–276. ISSN: 1476-4687. DOI: https://doi.org/10.1038/35065725.

Strunz, Matthias (2012). *Instandhaltung*. Springer Berlin, Heidelberg. ISBN: 978-3-642-27389-6. DOI: https://doi.org/10.1007/978-3-642-27390-2.

Stéphane, Mallat (2009). *A Wavelet Tour of Signal Processing (Third Edition)*. Third Edition. Boston: Academic Press. ISBN: 978-0-12-374370-1. DOI: https://doi.org/10.1016/B978-0-12-374370-1.X0001-8.

Su, Ya, Youjian Zhao, Chenhao Niu, Rong Liu, Wei Sun, and Dan Pei (2019). "Robust Anomaly Detection for Multivariate Time Series through Stochastic Recurrent Neural Network." In: *Proceedings of the 25th ACM SIGKDD International Conference on Knowledge Discovery & Data Mining*. KDD '19. Anchorage, AK, USA: Association for Computing Machinery, 2828–2837. ISBN: 9781450362016. DOI: https://doi.org/10.1145/3292500.3330672.

Supriya, Supriya, Siuly Siuly, Hua Wang, Jinli Cao, and Yanchun Zhang (2016). "Weighted Visibility Graph With Complex Network Features in the Detection of Epilepsy." In: *IEEE Access* 4, pp. 6554–6566. DOI: https://doi.org/10.1109/ACCESS.2016.2612242.

Sutton, R.S. and A.G. Barto (1998). "Reinforcement Learning: An Introduction." In: *IEEE Transactions on Neural Networks* 9.5, pp. 1054–1054. DOI: https://doi.org/10.1109/TNN.1998.712192.

Suwanda, R, Z Syahputra, and E M Zamzami (2020). "Analysis of Euclidean Distance and Manhattan Distance in the K-Means Algorithm for Variations Number of Centroid K." In: *Journal of Physics: Conference Series* 1566.1, p. 012058. DOI: https://dx.doi.org/10.1088/1742-6596/1566/1/012058.

Szczucka-Lasota, Bożena, Joanna Kamińska, and Iwona Krzyżewska (2019). "Influence of tire pressure on fuel consumption in trucks with installed tire pressure monitoring system (TPMS)." In: *Zeszyty Naukowe. Transport/Politechnika Śląska* 103, pp. 167–181. DOI: https://doi.org/10.20858/sjsutst.2019.103.13.

Tagawa, Takaaki, Yukihiro Tadokoro, and Takehisa Yairi (Nov. 2015). "Structured Denoising Autoencoder for Fault Detection and Analysis." In: *Proceedings of the Sixth Asian Conference on Machine Learning*. Ed. by Dinh Phung and

Hang Li. Vol. 39. Proceedings of Machine Learning Research. Nha Trang City, Vietnam: PMLR, pp. 96–111. URL: https://proceedings.mlr.press/v39/tagawa14.html.

Tang, Jian, Zhixiang Chen, Ada Wai-chee Fu, and David W. Cheung (2002). "Enhancing Effectiveness of Outlier Detections for Low Density Patterns." In: *Advances in Knowledge Discovery and Data Mining*. Ed. by Ming-Syan Chen, Philip S. Yu, and Bing Liu. Berlin, Heidelberg: Springer Berlin Heidelberg, pp. 535–548. ISBN: 978-3-540-47887-4. DOI: https://doi.org/10.1007/3-540-47887-6_53.

Tappe, Stefan (2013). "Absolutstetige Verteilungen und Zufallsvariablen." In: *Einführung in die Wahrscheinlichkeitstheorie*. Berlin, Heidelberg: Springer Berlin Heidelberg, pp. 47–67. ISBN: 978-3-642-37544-6. DOI: 10.1007/978-3-642-37544-6_4. URL: https://doi.org/10.1007/978-3-642-37544-6_4.

Theissler, Andreas (2017). "Detecting known and unknown faults in automotive systems using ensemble-based anomaly detection." In: *Knowledge-Based Systems* 123, pp. 163–173. ISSN: 0950-7051. DOI: https://doi.org/10.1016/j.knosys.2017.02.023.

Theissler, Andreas, Judith Pérez-Velázquez, Marcel Kettelgerdes, and Gordon Elger (2021). "Predictive maintenance enabled by machine learning: Use cases and challenges in the automotive industry." In: *Reliability engineering & system safety* 215, p. 107864. DOI: https://doi.org/10.1016/j.ress.2021.107864.

Tinga, Tiedo (2013). *Principles of loads and failure mechanisms. Applications in maintenance, reliability and design.* English. Springer Series in Reliability Engineering. Springer. ISBN: 978-1-4471-4916-3. DOI: https://doi.org/10.1007/978-1-4471-4917-0.

Tinga, Tiedo and Richard Loendersloot (2019). "Physical Model-Based Prognostics and Health Monitoring to Enable Predictive Maintenance." In: *Predictive Maintenance in Dynamic Systems: Advanced Methods, Decision Support Tools and Real-World Applications*. Ed. by Edwin Lughofer and Moamar Sayed-Mouchaweh. Cham: Springer International Publishing, pp. 313–353. ISBN: 978-3-030-05645-2. DOI: https://doi.org/10.1007/978-3-030-05645-2_11.

Tranquillo, Joseph V. (2014). "Time Domain Analysis." In: *Biomedical Signals and Systems*. Cham: Springer International Publishing, pp. 149–161. ISBN: 978-3-031-01659-2. DOI: https://doi.org/10.1007/978-3-031-01659-2_10.

UNEP (2015). *Paris Agreement*. URL: https://wedocs.unep.org/20.500.11822/20830.

Vasan, Vinod, Naveen Venkatesh Sridharan, Anoop Prabhakaranpillai Sreelatha, and Sugumaran Vaithiyanathan (2023). "Tire Condition Monitoring Using Transfer Learning-Based Deep Neural Network Approach." In: *Sensors* 23.4. ISSN: 1424-8220. DOI: https://doi.org/10.3390/s23042177.

Victor, Trent, Kristofer Kusano, Tilia Gode, Ruoshu Chen, and Matthew Schwall (2023). "Safety Performance of the Waymo Rider-Only Automated Driving System at One Million Miles." In: URL: https://storage.googleapis.com/waymo-uploads/files/documents/safety/Safety%20Performance%20of%20Waymo%20RO%20at%201M%20miles.pdf.

Vincent, Pascal, Hugo Larochelle, Yoshua Bengio, and Pierre-Antoine Manzagol (2008). "Extracting and Composing Robust Features with Denoising Autoencoders." In: *Proceedings of the 25th International Conference on Machine Learning*. ICML '08. Helsinki, Finland: Association for Computing Machinery, 1096–1103. DOI: https://doi.org/10.1145/1390156.1390294.

Voskuijl, Mark, Michel J.L. van Tooren, and Daniel J. Walker (2015). "Condition-based flight control for helicopters: An extension to condition-based maintenance." In: *Aerospace Science and Technology* 42, pp. 322–333. ISSN: 1270-9638. DOI: https://doi.org/10.1016/j.ast.2015.01.026.

Wallentowitz, Henning (2005). *Vertikal- / Querdynamik von Kraftfahrzeugen: Federungssysteme, Fahrverhalten, Lenkung, Radaufhängung; Vorlesungsumdruck Fahrzeugtechnik II*. 7th ed. Forschungsgesellschaft Kraftfahrwesen Aachen mbH. ISBN: 3-925 194-35-5.

Wang, Guang and Shen Yin (2014). "Data-driven fault diagnosis for an automobile suspension system by using a clustering based method." In: *Journal of the Franklin Institute* 351.6, pp. 3231–3244. ISSN: 0016-0032. DOI: https://doi.org/10.1016/j.jfranklin.2014.03.004.

Wang, Meng-Hui, Kuei-Hsiang Chao, Wen-Tsai Sung, and Guan-Jie Huang (2010). "Using ENN-1 for fault recognition of automotive engine." In: *Expert Systems with Applications* 37.4, pp. 2943–2947. ISSN: 0957-4174. DOI: https://doi.org/10.1016/j.eswa.2009.09.041.

Wang, Yuxuan, Pascal Getreuer, Thad Hughes, Richard F. Lyon, and Rif A. Saurous (2017). "Trainable frontend for robust and far-field keyword spotting." In: *2017 IEEE International Conference on Acoustics, Speech and Signal Processing (ICASSP)*, pp. 5670–5674. DOI: https://doi.org//10.1109/ICASSP.2017.7953242.

Watzka, B., St. Scheler, and Th. Wilhelm (2012). "Beschleunigungssensoren." In: *Praxis der Naturwissenschaften - Physik in der Schule* 61.7, pp. 25–33. ISSN: 0177-8374; 1617-5689.

Weber, Manfred (2012). "Piezoelektrische Beschleunigungsaufnehmer - Theorie und Anwendung." In: *Metra Mess-und Frequenztechnik in Radebeul e. K.*

Weglarczyk, Stanislaw (2018). "Kernel density estimation and its application." In: *ITM Web Conf.* 23, p. 00037. DOI: https://doi.org/10.1051/itmconf/20182300037.

Werbos, P.J. (1990). "Backpropagation through time: what it does and how to do it." In: *Proceedings of the IEEE* 78.10, pp. 1550–1560. DOI: https://doi.org/10.1109/5.58337.

Wienrich, Jan (2023). *Autonomous Driving: The Steps to Self-Driving Vehicles*. URL: https://www.zf.com/mobile/en/technologies/autonomous_driving/stories/6_levels_of_automated_driving.html (visited on 07/08/2023).

Wilhelm, Ulf, Susanne Ebel, and Alexander Weitzel (2015). "Funktionale Sicherheit und ISO 26262." In: *Handbuch Fahrerassistenzsysteme: Grundlagen, Komponenten und Systeme für aktive Sicherheit und Komfort*. Ed. by Hermann Winner, Stephan Hakuli, Felix Lotz, and Christina Singer. Wiesbaden: Springer Fachmedien Wiesbaden, pp. 85–103. ISBN: 978-3-658-05734-3. DOI: https://doi.org/10.1007/978-3-658-05734-3_6.

Wodecki, Jacek, Piotr Kruczek, Anna Bartkowiak, Radoslaw Zimroz, and Agnieszka Wyłomańska (2019). "Novel method of informative frequency band selection for vibration signal using Nonnegative Matrix Factorization of spectrogram matrix." In: *Mechanical Systems and Signal Processing* 130, pp. 585–596. ISSN: 0888-3270. DOI: https://doi.org/10.1016/j.ymssp.2019.05.020.

Wolf, Peter, Artur Mrowca, Tam Thanh Nguyen, Bernard Bäker, and Stephan Günnemann (2018). "Pre-ignition Detection Using Deep Neural Networks: A Step Towards Data-driven Automotive Diagnostics." In: *2018 21st International Conference on Intelligent Transportation Systems (ITSC)*, pp. 176–183. DOI: https://doi.org/10.1109/ITSC.2018.8569908.

Wong, Pak Kin, Jianhua Zhong, Zhixin Yang, and Chi Man Vong (2016). "Sparse Bayesian extreme learning committee machine for engine simultaneous fault diagnosis." In: *Neurocomputing* 174, pp. 331–343. ISSN: 0925-2312. DOI: https://doi.org/10.1016/j.neucom.2015.02.097.

Wu, Jian-Da and Jun-Ming Kuo (2010). "Fault conditions classification of automotive generator using an adaptive neuro-fuzzy inference system." In: *Expert Systems with Applications* 37.12, pp. 7901–7907. ISSN: 0957-4174. DOI: https://doi.org/10.1016/j.eswa.2010.04.046.

Wyk, Franco van, Yiyang Wang, Anahita Khojandi, and Neda Masoud (2020). "Real-Time Sensor Anomaly Detection and Identification in Automated Vehicles." In: *IEEE Transactions on Intelligent Transportation Systems* 21.3, pp. 1264–1276. DOI: https://doi.org/10.1109/TITS.2019.2906038.

Xie, Guoqi, Yawen Zhang, Renfa Li, Kenli Li, and Keqin Li (2023). *Functional Safety for Embedded Systems*. CRC Press. DOI: https://doi.org/10.1201/9781003391517.

Yang, Ruixin, Rui Xiong, Hongwen He, and Zeyu Chen (2018). "A fractional-order model-based battery external short circuit fault

diagnosis approach for all-climate electric vehicles application." In: *Journal of Cleaner Production* 187, pp. 950–959. ISSN: 0959-6526. DOI: https://doi.org/10.1016/j.jclepro.2018.03.259.

Yang, Yue, Jianbo Wang, Huijie Yang, and Jingshi Mang (2009). "Visibility graph approach to exchange rate series." In: *Physica A: Statistical Mechanics and its Applications* 388.20, pp. 4431–4437. ISSN: 0378-4371. DOI: https://doi.org/10.1016/j.physa.2009.07.016.

Yela, Delia Fano, Dan Stowell, and Mark Sandler (2019). "Spectral Visibility Graphs: Application to Similarity of Harmonic Signals." In: *2019 27th European Signal Processing Conference (EUSIPCO)*, pp. 1–5. DOI: https://doi.org/10.23919/EUSIPCO.2019.8903055.

Yin, Shen and Zenghui Huang (2015). "Performance Monitoring for Vehicle Suspension System via Fuzzy Positivistic C-Means Clustering Based on Accelerometer Measurements." In: *IEEE/ASME Transactions on Mechatronics* 20.5, pp. 2613–2620. DOI: https://doi.org/10.1109/TMECH.2014.2358674.

You, Gae-Won, Sangdo Park, and Dukjin Oh (2017). "Diagnosis of Electric Vehicle Batteries Using Recurrent Neural Networks." In: *IEEE Transactions on Industrial Electronics* 64.6, pp. 4885–4893. DOI: 10.1109/TIE.2017.2674593.

Yurtsever, Ekim, Jacob Lambert, Alexander Carballo, and Kazuya Takeda (2020). "A Survey of Autonomous Driving: Common Practices and Emerging Technologies." In: *IEEE Access* 8, pp. 58443–58469. DOI: https://doi.org/10.1109/ACCESS.2020.2983149.

Zehelein, Thomas, Thomas Hemmert-Pottmann, and Markus Lienkamp (2020). "Diagnosing Automotive Damper Defects Using Convolutional Neural Networks and Electronic Stability Control Sensor Signals." In: *Journal of Sensor and Actuator Networks* 9.1. ISSN: 2224-2708. DOI: https://doi.org/10.3390/jsan9010008.

Zeller, Peter (2012a). "Berechnung und Simulation." In: *Handbuch Fahrzeugakustik: Grundlagen, Auslegung, Berechnung, Versuch*. Ed. by Peter Zeller. Wiesbaden: Vieweg+Teubner Verlag, pp. 336–355. ISBN: 978-3-8348-8657-6. DOI: https://doi.org/10.1007/978-3-8348-8657-6_15.

— (2012b). "Schwingungsphänomene im Kraftfahrzeug." In: *Handbuch Fahrzeugakustik: Grundlagen, Auslegung, Berechnung, Versuch*. Ed. by Peter Zeller. Wiesbaden: Vieweg+Teubner Verlag, pp. 68–115. ISBN: 978-3-8348-8657-6. DOI: https://doi.org/10.1007/978-3-8348-8657-6_5.

Zhang, Zhe, Yong Qin, Limin Jia, and Xin'an Chen (Nov. 2018). "Visibility Graph Feature Model of Vibration Signals: A Novel Bearing Fault Diagnosis Approach." In: *MATERIALS* 11.11. DOI: https://doi.org/10.3390/ma11112262.

Zhu, Guohun, Yan Li, and Peng Paul Wen (2012). "An Efficient Visibility Graph Similarity Algorithm and Its Application on Sleep

Stages Classification." In: *Brain Informatics*. Ed. by Fabio Massimo Zanzotto, Shusaku Tsumoto, Niels Taatgen, and Yiyu Yao. Berlin, Heidelberg: Springer Berlin Heidelberg, pp. 185–195. ISBN: 978-3-642-35139-6. DOI: https://doi.org/10.1007/978-3-642-35139-6_18.

Zhu, Guohun, Yan Li, and Peng (Paul) Wen (2014). "Epileptic seizure detection in EEGs signals using a fast weighted horizontal visibility algorithm." In: *Computer Methods and Programs in Biomedicine* 115.2, pp. 64–75. ISSN: 0169-2607. DOI: https://doi.org/10.1016/j.cmpb.2014.04.001.

Zhu, Guohun, Yan Li, Peng Paul Wen, and Shuaifang Wang (Sept. 2014). "Analysis of alcoholic EEG signals based on horizontal visibility graph entropy." en. In: *Brain Inform* 1.1-4, pp. 19–25.

Zollanvari, Amin (2023). "Recurrent Neural Networks." In: *Machine Learning with Python: Theory and Implementation*. Cham: Springer International Publishing, pp. 415–433. ISBN: 978-3-031-33342-2. DOI: https://doi.org/10.1007/978-3-031-33342-2_15.

Zuo, Jian, Hong Lv, Daming Zhou, Qiong Xue, Liming Jin, Wei Zhou, Daijun Yang, and Cunman Zhang (2021). "Deep learning based prognostic framework towards proton exchange membrane fuel cell for automotive application." In: *Applied Energy* 281, p. 115937. ISSN: 0306-2619. DOI: https://doi.org/10.1016/j.apenergy.2020.115937.

EU Vehicle Data Initiative (2022). *Access to vehicle data, functions and resources*. URL: https://ec.europa.eu/info/law/better-regulation/have-your-say/initiatives/13180-Access-to-vehicle-data-functions-and-resources_en (visited on 04/11/2023).

ORAD Committee (2021). *Taxonomy and Definitions for Terms Related to Driving Automation Systems for On-Road Motor Vehicles*. DOI: https://doi.org/10.4271/J3016_202104.

Reg. (EU) 2019/2144 (2019). *On type-approval requirements for motor vehicles and their trailers, and systems, components and separate technical units intended for such vehicles, as regards their general safety and the protection of vehicle occupants and vulnerable road users*. URL: https://eur-lex.europa.eu/legal-content/EN/TXT/?uri=OJ:L:2019:325:TOC (visited on 03/26/2023).

Reg. (EU) 2023/851 (2023). *Regulation (EU) 2023/851 of the European Parliament and of the Council of 19 April 2023 amending Regulation (EU) 2019/631 as regards strengthening the CO2 emission performance standards for new passenger cars and new light commercial vehicles in line with the Union's increased climate ambition (Text with EEA relevance)*. URL: http://data.europa.eu/eli/reg/2023/851/oj.

Reg. No 64 UN/ECE (Nov. 2010). *Uniform provisions concerning the approval of vehicles with regard to their equipment which may include: a temporary-use spare unit, run-flat tyres and/or a run-flat system, and/or*

a tyre pressure monitoring system. URL: https://eur-lex.europa.eu/legal-content/EN/TXT/?uri=OJ:L:2010:310:TOC (visited on 03/26/2023).

Statistisches Bundesamt (2022). *Ursachen von Unfällen mit Personenschaden*. URL: https://www.destatis.de/DE/Themen/\\Gesellschaft-Umwelt/Verkehrsunfaelle/Tabellen/ursachen-personenschaden1.html (visited on 04/12/2022).

— (2023). *Pressemitteilung Nr. 090 vom 9. März 2023*. URL: https://www.destatis.de/DE/Presse/Pressemitteilungen/2023/03/PD23_090_43312.html (visited on 04/03/2023).

TE Connectivity (2017). *Choosing the right type of accelerometer*. URL: https://www.mouser.com/pdfdocs/choosing-the-right-accelerometer-white-paper.pdf (visited on 05/06/2023).

Erklärung über die Eigenständigkeit der erbrachten wissenschaftlichen Leistung

Ich erkläre hiermit, dass ich die vorliegende Arbeit ohne unzulässige Hilfe Dritter und ohne Benutzung anderer als der angegebenen Hilfsmittel angefertigt habe. Die aus anderen Quellen direkt oder indirekt übernommenen Daten und Konzepte sind unter Angabe der Quelle gekennzeichnet.

Bei der Auswahl und Auswertung folgenden Materials haben mir die nachstehend aufgeführten Personen in der jeweils beschriebenen Weise entgeltlich/ unentgeltlich geholfen.

1. Die Veröffentlichung I wurde gemeinsam mit Daniel Köhne konzipiert und verfasst. Martina Juhnke-Kubitzke hat die Arbeit betreut, mit uns diskutiert und das Manuskript überarbeitet.

2. Bei der Veröffentlichung II ist Johannes Bernhard Erstautor. Diese wurde gemeinsam mit Mark Schutera konzipiert und verfasst. Johannes Bernhard hat den verwendeten Algorithmus entwickelt und implementiert. Die Datenvorverarbeitung und Merkmalsextraktion wurden von mir programmiert.

3. Die Daten für die Veröffentlichungen III und IV wurden im Rahmen eines Projekts der ZF Friedrichshafen AG gemeinsam mit Dennis Pape aufgenommen. Die Veröffentlichungen wurden von Kai-Uwe Kühnberger betreut und mit ihm diskutiert. Die Veröffentlichung III wurde von ihm, Dennis Pape und Tobias Pobandt überarbeitet.

4. Die Veröffentlichung V wurde von Daniel Köhne mitkonzipiert, überarbeitet und diskutiert. Außerdem hat er die Beweise für die Laufzeiten und die Korrektheit der Algorithmen verfasst. Martina Juhnke-Kubitzke hat die Veröffentlichung überarbeitet.

5. Das Patent I wurde gemeinsam während eines Projektes der ZF Friedrichshafen AG mit Michael Hertkorn und Martin Damian Trochowski konzipiert und verfasst.

6. Die Veröffentlichung im Appendix wurde von mir allein verfasst. Die in Python implementierten Algorithmen basieren auf der gemeinsamen Arbeit mit Daniel Köhne aus der Veröffentlichung V.

7. Alle weiteren Kapitel der Dissertation sind eigenständig verfasst worden. Die Inhalte sind in Absprache mit meinem Betreuer erstellt worden und sein Feedback wurde berücksichtigt. Mithilfe von Grammarly wurden sprachliche Formulierungen überarbeitet.

Weitere Personen waren an der inhaltlichen materiellen Erstellung der vorliegenden Arbeit nicht beteiligt. Insbesondere habe ich hierfür nicht die entgeltliche Hilfe von Vermittlungs- bzw. Beratungsdiensten (Promotionsberater oder andere Personen) in Anspruch genommen. Niemand hat von mir unmittelbar oder mittelbar geldwerte

Leistungen für Arbeiten erhalten, die im Zusammenhang mit dem Inhalt der vorgelegten Dissertation stehen.

Die Arbeit wurde bisher weder im In- noch im Ausland in gleicher oder ähnlicher Form einer anderen Prüfungsbehörde vorgelegt.

....
(Ort. Datum) (Unterschrift)

COLOPHON

This document was typeset using the typographical look-and-feel `classicthesis` developed by André Miede. The style was inspired by Robert Bringhurst's seminal book on typography "*The Elements of Typographic Style*". `classicthesis` is available for both LaTeX and LyX:

https://bitbucket.org/amiede/classicthesis/

Happy users of `classicthesis` usually send a real postcard to the author, a collection of postcards received so far is featured here:

http://postcards.miede.de/